5399

C 82
H
SCH

• CANADIAN HYDROLOGY SYMPOSIUM 82
• ASSOCIATE COMMITTEE ON HYDROLOGY
NATIONAL RESEARCH COUNCIL OF CANADA
• JUNE 14-16, 1982
FREDERICTON, NEW BRUNSWICK

• SYMPOSIUM CANADIEN D'HYDROLOGIE: 82
• COMITÉ ASSOCIÉ D'HYDROLOGIE
CONSEIL NATIONAL DE RECHERCHES CANADA
• LES 14 ET 16 JUIN 1982
FREDERICTON, NOUVEAU-BRUNSWICK

MEASUREMENT OF SOIL WATER CONTENT USING TIME DOMAIN REFLECTOMETRY[1]

G.C. Topp[1] and J.L. Davis[2]

ABSTRACT

Time domain reflectometry (TDR) which measures the propagation velocity of a voltage step has been used to determine the dielectric constant of soil. The relationship between dielectric constant and water content was established from TDR measurements on coaxial transmission lines filled with soil. TDR applied to parallel wire transmission lines in a soil column gave a precise measure ($\pm 0.02\ m^3m^{-3}$) of the average water content over the total length of line even when the water was unevenly distributed.

In a corn field repeated measurements at the same locations on permanently installed parallel wire transmission lines were highly correlated, one with another, over the season. Comparisons of water contents by TDR with those from gravimetric samples gave standard deviations of differences of $\pm 0.02\ m^3m^{-3}$ when measured locations were the same but increased to ± 0.06 when measured location were different. Horizontally installed parallel wire transmission lines spanning greater horitonzal are gave less variable results than vertical lines near the surface. Data from transmission lines with impedance discontinuities gave water content profiles from a single measurement but the analyse of the readings were more complex than for the lines without impedance discontinuities. Although a battery-powered cable tester was satisfactory, instrumentation under development will eliminate calculations and give water content directly.

1 Land Resource Research Institute, Agriculture Canada, Ottawa Ontario. K1A 0C6. LRRI Contribution No. 82-46

2 EarthTech Research Corporation, 6655 Amberton Dr., Baltimore Md., U.S.A. 21227.

9210150327 920916
PDR WASTE
WM-11 PDR

Enclosure 3
8.3.1.2.2.1

INTRODUCTION

The unsaturated soil zone plays a critical role in the hydrological cycle regardless of whether the vegetative cover is forest, grassland, or cultivated crops. Lennox and Parsons (1975) identified the lack of adequate instrumentation and measurement techniques as a factor limiting research on the transfer processes across the upper and lower boundary of the unsaturated soil. Soil water content is probably the most sought after measurement. As yet no single technique meets all or even most requirements. The gravimetric method of sampling and drying is direct, simple and precise. The sampling procedure, however, is disruptive of the measured location and additional measurements of soil density are required to get water contents on a volume basis. The other widely used technique, based on the moderation of fast neutrons by the water molecule, is reliable and accurate. It requires, however, site calibration and two instruments for shallow and deep measurements. The neutron meters involve the use of radioactive sources which require special care and precautions.

In recent years numerous laboratory studies have shown that the dielectric constant of soil is primarily related to its water content (Thomas 1966; Lundien 1971; Hoekstra and Delaney 1974; Selig and Mansukhani 1975; Okrasinski et al. 1978; Topp et al. 1980). A simple and reliable measurement of dielectric constant in the frequency range 1MHz to 1GHz would be a practical and effective measure of soil water content. Many of the methods available at the present time for determination of dielectric constant are not appropriate for use in the field (Selig and Mansukhani 1975). The results from capacitance techniques (Thomas 1966; Kuraz 1972; Selig and Mansukhani 1975; Woodschall 1978; McKim et al. 1980) depend upon specific electrode configuration and detailed calibration. By contrast, the time-domain reflectometry (TDR) approach is very promising for measurements of water content <u>in situ</u>.

In this paper we discuss our progress toward the application of TDR to the measurement of soil water content. This method makes use of the uniquely high dielectric constant of liquid water compared to the other materials in soil. Parallel wire transmission lines of various designs have been used with a portable cable tester for measurements in the field at depths to 1 m. The principles and the procedures are briefly described. The advantages and disadvantages of the different parallel wire transmission line configurations are discussed.

THE PRINCIPLES OF TIME-DOMAIN REFLECTOMETRY

The TDR technique as applied to the measurement of the electrical properties of soils was described by Davis and Chudobiak (1975), Davis and Annan (1977), Chudobiak et al.

propagates down the instrument transmission line through the receiver, B, to the transmission line filled with soil, C to D. All the signal is reflected at D, the end of the transmission line. The receiver used an electronic sampling technique to put out on the display an audio frequency facsimile of the radio frequency signal. The displayed signal was either photographed or recorded on an x-y plotter. The travel time of the step in the soil was obtained by measuring the distance C to D along the time axis in plots similar to that in Fig. 1. Eq. 3 was used to calculate the apparent dielectric constant.

LABORATORY EXPERIMENTS

Applying the TDR technique to coaxial transmission lines filled with soil Topp et al. (1980) have measured in detail the relationship between apparent dielectric constant and volumetric water content (Fig. 2). Although the soils they studied had a wide range of textures (9 to 66% clay) the relationship between dielectric constant and water content was essentially singular. In that phase of the work it was shown that bulk density, temperature and/or salt content had no measurable effect on the dielectric constant-water content relationship. The data from the four mineral soils were fitted empirically with a third degree polynomial equation. The error of estimate for water

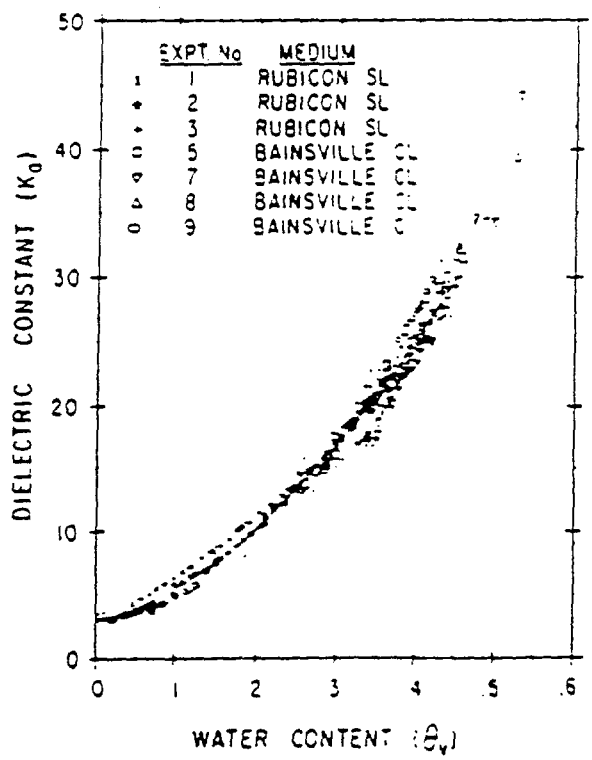

Figure 2. The relationship between dielectric constant and water content measured by Topp et al. (1980).

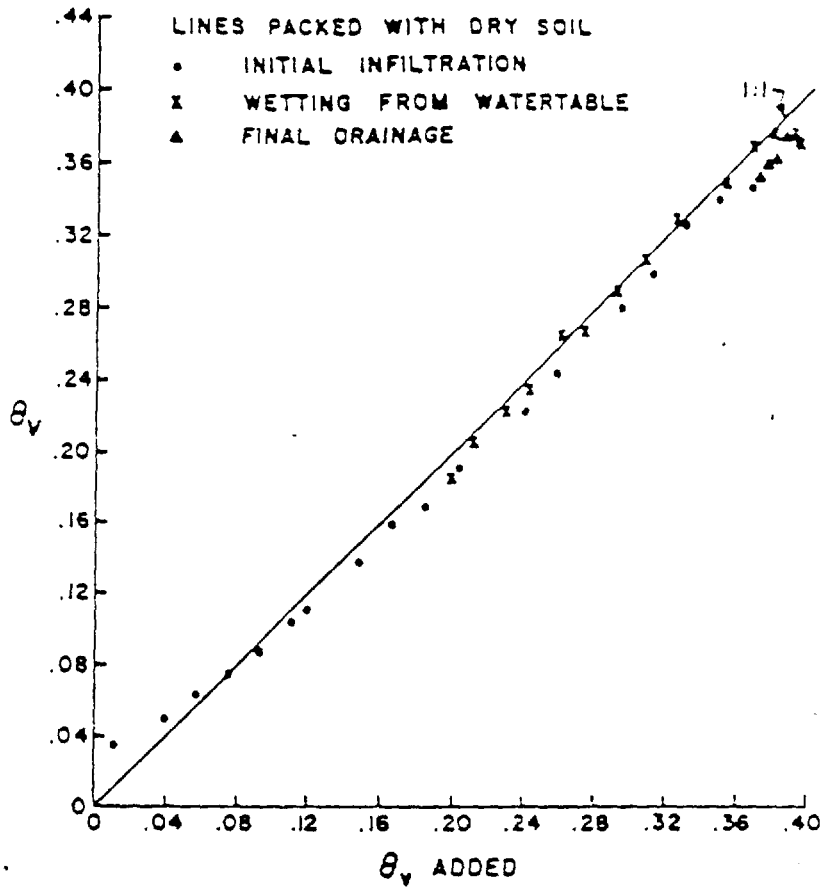

Figure 3. A comparison of TDR measured water content, θ_v, with that added or removed from a soil column, θ_v added (Topp et al. 1982b).

September 19. Three sites with differing soil and landscape characteristics were chosen. The major site, #1, which was more intensively instrumented than the other two was on a flat location of the Dalhousie soil association with a clay loam texture. The second site was a similar soil but in a depressional area. The third site of the Manotick soil association had about 0.85 m sandy loam soil underlain by clay.

Parallel pair transmission lines were installed in triplicate with both horizontal and vertical orientation in the soil. Those installed vertically at site #1 were of two types, those with and without electrical impedance discontinuities. These vertical lines were located within and along the corn rows (Fig. 4). The use of lines with impedance discontinuities to obtain water

content profiles was discussed by Topp et al. (1982b). Such lines used at site #1 had the region of the discontinuity filled with plastic material of high dielectric constant as depicted by the heavier lines in Fig. 4.

The line without discontinuities (i.e. continuous lines) consisted of pairs of rods 12.7 mm in diameter, separated by 50 mm. The soil between and surrounding the rods served as the dielectric of the transmission lines. The lengths of lines used were 0.25, 0.50, 0.75 and 1.00 m. Triplicate sets of these were installed at all three sites. A portable hand probe (Fig. 4) was used for measurement of 0 to 0.125 m. This probe was inserted in a new location for each measurement each day.

The third type of transmission line tested at site #1 was of the parallel pair type installed horizontally in the soil from the side of a soil pit (Fig. 4). These transmission lines each consisted of a pair of 1.6 mm diameter stainless steel rods separated by 50 mm. The lengths of these lines were 0.40 m and they were installed at depths of 0.065, 0.125, 0.185, 0.375, 0.625, 0.875 and 1.00 m in the soil.

The installation procedure for the vertical transmission lines was similar to that used by Topp and Davis (1981) and Topp et al. (1982 a and b) where the rods of 12.7 mm diameter were pushed into pilot holes 10 mm in diameter. The horizontal lines were pushed through a guide and directly into the face of the soil pit at the selected depths, perpendicular to the direction of the corn rows (Fig. 4). A 3 m length of coaxial cable was connected to each of the soil transmission lines so that the soil pit could be back-filled and the cables extend above the soil surface for connection to the TDR unit. Connections of the TDR unit to vertical lines and the hand probe were by means of a "balun" board at the end of a coaxial cable. The balun, a small pulse transformer, minimized impedance difference on going from the unbalanced coaxial line of the TDR unit to the balanced parallel lines in the soil.

The TDR measurements were made at weekly to half weekly intervals depending on weather conditions. Measurements were made more frequently when rain occurred. All TDR measurements were made with a portable, battery operated TDR cable tester (Tektronix model 1502). The determinations of travel times were made from photographs of the TDR traces. Eqs. 3 and 4 were used to calculate volumetric water contents. Soil samples for gravimetric determination of water content, converted to a volume basis, were taken at selected times during the growing season and compared to the TDR values. The neutron moderation technique was compared with TDR. Only limited comparisons were available because the neutron meter broke down during the season. After the final TDR reading on the vertical transmission lines, soil samples (20 mm diam.) were taken from directly between the rods

Graphs of the data from the other lines and the other sites had patterns very similar to that shown in Fig. 5. It appeared that on any day the deviation observed had a large contribution which was location dependent. We reasoned that since each location was subjected to similar rainfall and evapotranspiration conditions the water content values from comparable depth intervals at any site should be highly correlated with each other over the season. Correlation coefficients for the data taken from pairs of comparable lines were very highly correlated i.e. there was< 1% probability that the data were uncorrelated. For example, correlation coefficients, r, in Fig. 5 are cosiderably >0.78%, the values at which there is a 1% probability that the data sets are uncorrelated. Similar strong correlations were found when data from the different types of transmission lines at site #1 were compared.

From measurements, made in triplicate, each day the standard deviation varied quite widely, especially for those taken in the upper 0.25 m. The lowest daily standard deviation was generally $<0.01\ m^3m^{-3}$ and the highest values ranged up to 0.08 m^3m^{-3} in the 0-0.25 m. For depths greater than 0.25 m the maximum standard deviation was always $<0.06\ m^3m^{-3}$. The average of the daily standard deviations for the season were $<0.04\ m^3m^{-3}$ for the upper 0.25 m and $<0.03\ m^3m^{-3}$ for depths greater than 0.25 m. Throughout, the data from the horizontal lines had smaller daily standard deviations than for the vertical lines. These deviations did not appear to show the same depth dependence as that for the vertical lines. This presumably resulted from the fact that horizontal lines (0.4 m in length) spanned a greater horizontal cross-section than the vertical lines (0.028 m^2 vs 0.002 m^2), giving better integration of the spatial variability.

The above results are indicative of the reproducibility or precision achieved in this study where variation arose both from spatial variability and instrument precision. In general these can not be separated in a field study. Comparisons of water contents measured from samples (gravimetrically) with those from TDR will indicate the accuracy of the TDR.

The gravimetric and TDR measured water contents sampled different soil during the season in order that the gravimetric sampling did not disturb the soil measured by TDR. At the end of the season, however, the soil measured by the TDR was sampled for gravimetric water content and bulk density. A paired t statistical test showed no significant difference between the TDR measured water contents and those sampled gravimetrically during the season. Good agreement was also found between the end of season TDR measurements and the gravimetric samples at sites #1 and #2. For site #3 the TDR, on average, gave readings which were 0.027 $m^3\ m^{-3}$ higher than those from the gravimetric samples. There was some evidence that the discrepancy resulted from excess water which had collected at the top of the

31, and at the end of the season (one of the wettest dates) for sites #1. In general, the TDR horizontal and vertical line compare well with each other and with the gravimetric samples. Near the surface the horizontal TDR lines gave water contents which tended to be high. These lines averaged the water content from midway between corn rows to the corn row. The vertical TDR lines and gravimetric samples were within the corn row. Thus the observed differences may reflect differences in rainfall distribution under the corn canopy on September 18, or in distribution of root extractions of water on July 31. The different types and orientations of transmission lines used at site #1 all gave reliable measurement of water content. In the next section consideration will be given to choosing transmission lines for specific applications.

Figs. 8 and 9 show a TDR measured profile for July 31 and profiles resulting from both TDR and gravimetric samples of September 18 and 19 for sites #2 and #3, respectively. There is good agreement between gravimetric and TDR measured data of these profiles except for the one pair of points at 0.18 m in Fig.9. The differences between measurements on the driest date, July 31, and those on September 18 and 19, show that only the top 0.5 m of soil actually dried during this season at sites #2 and #3. Fig. 7 indicates that some drying had occurred at 1 m deep at site #1.

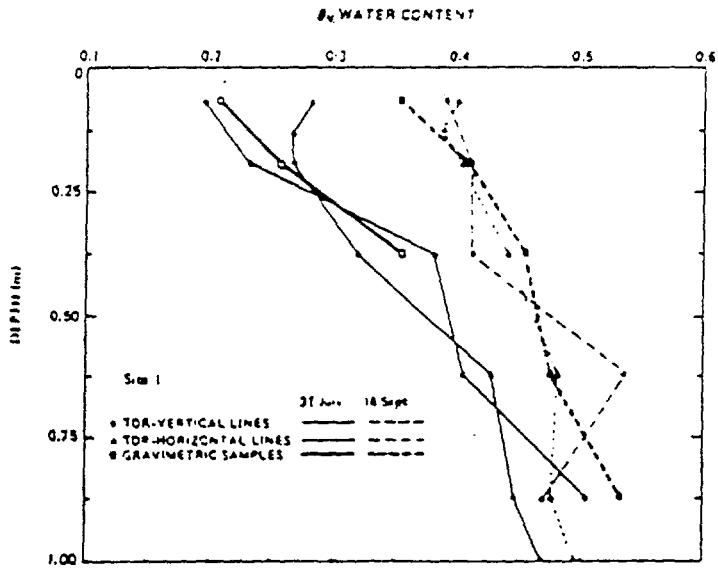

Figure 7. Water content profiles at site #1 comparing the data from horizontal and vertical TDR lines with those from gravimetric sampling on two dates.

The current field study has demonstrated the applicability of the TDR technique to measure field water contents. Equivalent results were obtained using gravimetric sampling or the TDR technique and the TDR has the advantage that it is not disruptive of the site after installation of the transmission lines. Although the current study used 1.6 and 12.7 mm diameter rods for the horizontal and vertical transmission lines, we have later found it was unnecessary to use pilot holes for the vertical installations. Accordingly, we are now using 3 mm or 6 mm diam. rods in pairs for the transmission lines. The 3 mm diam. rods are used for lines up to 0.5 m long and 6 mm diam. rods are used for lengths >0.5 m. We have found the direct insertion of the transmission lines causes little disturbance to soil. It is possible to have flexibility of orientation and length of transmission lines so that TDR measurements can be tailored to many specific applications. For example, an hydrologist wishing to know the water content in the top metre of soil would install vertical transmission lines of length 1 m to give one value from each single reading. The number of replicates would be determined by the variability found at the location of measurement and by the desired precision.

Fig. 10 shows examples of TDR responses which were obtained from the different types of transmission lines used at site #1.

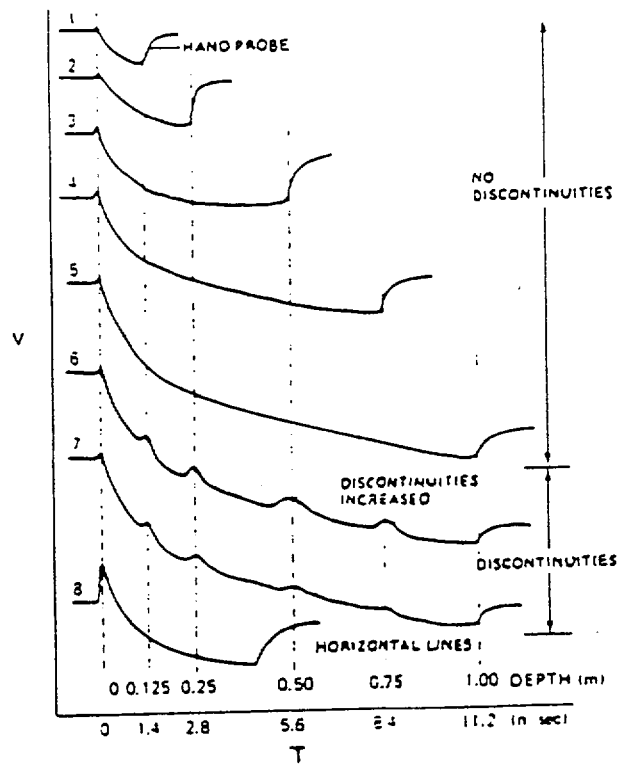

Figure 10. Typical TDR traces from which travel times are determined for the calculation of various water contents using Eqs. 3 and 4.

and frost tubes for use in monitoring frost penetration in the field. Futher observations during spring melt (Hayhoe et al. 1981a) determined the depth to the thaw front while showing the accumulation of water above the frozen layer.

CONCLUSIONS

In earlier laboratory studies Topp et al. (1980) had shown that the dielectric constant of soil as measured by TDR was primarily dependent on its water content. In later laboratory experiments Topp et al. (1982 a, b) found that TDR applied to a variety of parallel wire transmission lines gave accurately the average water content of the soil column. The current study has demonstrated that with a battery powered instrument the TDR technique is an accurate method of measuring soil water content in the field. The accuracy was found to be comparable to that from gravimetric samples. In both cases the limit of accuracy appeared to be dependent upon the variability of the soil. When both methods sampled the same soil, as occurred at the end of the season, standard deviations of differences were as low as 0.02 $m^3 m^{-3}$. When TDR and gravimetric samples measured non coincident samples the standard deviation increased to 0.06. Both horizontally and vertically installed lines gave satisfactory measurements of water content. The horizontally installed lines, measuring over a larger horizontal cross-sectional area, showed less variation than vertically placed lines measuring near the surface. The variety of transmission line configurations which have been evaluated provide considerable flexibility in choice of transmission lines to provide the desired water content information.

ACKNOWLEDGEMENTS

Grateful appreciation is expressed to W.D. Zebchuk, L.M. Dwyer and K.C. Wires for their assistance in data collection and/or analysis. Discussions with A.P. Annan are acknowledged.

Selig, E.T. and Mansukhani, S. (1975): Relationship of soil moisture to the dielectric property. Journal Geotechnical Engineering Division, Proceedings ASCE 101:GT8:755-770.

Thomas, A.M. (1966): In situ measurement of moisture in soil and similar substances by 'fringe' capacitance. Journal Scientific Instruments. 43:21-27.

Topp, G.C. and Davis, J.L. (1981): Detecting infiltration of water through the soil cracks by time-domain reflectometry. Geoderma 26:13-23.

Topp, G.C., Davis, J.L. and Annan, A.P. (1980): Electromagnetic determination of soil water content; measurement in coaxial transmission lines. Water Resources Research. 16: 574-582.

Topp, G.C., Davis, J.L. and Annan, A.P. (1982a): Electromagnetic determination of soil water content using TDR: I Applications to wetting fronts and steep gradients. Soil Science Society of America Journal. (in press).

Topp, G.C., Davis, J.L. and Annan, A.P. (1982b): Electromagnetic determination of soil water content using TDR: II Evaluation of installation and configuration of parallel transmission lines. Soil Science Society of America Journal. (in press).

Wobschall, D. (1978): A frequency shift dielectric soil moisture sensor. IEEE Transactions on Geoscience Electronics GE-16: 112-118.

Carlene

APR 0 1 1991
version
T.B. 4/11/91

DRAFT

PRECIPITATION ESTIMATION IN MOUNTAINOUS TERRAIN USING MULTIVARIATE GEOSTATISTICS: 1. STRUCTURAL ANALYSIS

DIRECTOR APPROVED COPY

- Greg Tenne
ASSISTANT
STAFF HYDROLOGIST FOR REPORTS, RESTON

SIM - BSP
6-20-91

By Joseph A. Hevesi[1], Jonathan D. Istok[2] and Alan L. Flint[3]

[1]Geologist, Raytheon Services Nevada, Las Vegas, Nevada
[2]Associate Professor, Dept. of Civil Engineering, Oregon State University, Corvallis, OR
[3]Hydrologist, U.S. Geological Survey, Mercury, Nevada

Quick Scan review this from first stand is out of my league!!

I trust your cont. reviewers would have considered any "fatal flaws" —

Technical Journal for

JOURNAL OF APPLIED METEOROLOGY

Enclosure 3
8.3.1.2.2.1

DIRECTOR APPROVED
COPY

(FOR REVIEW PURPOSES ONLY)

Table of Contents

	Page
Title Page	iv
List of Tables	v
List of Figures	vi
Abstract	1
Introduction	2
Study Area	4
Geographic and Physiographic Setting	4
Climate	5
Elevation - Precipitation Correlation	6
Geostatistical Theory	7
Methods	10
Precipitation Data	10
Elevation Data	10
Preliminary Statistical Analysis	11
Sample Variograms	12
Model Fitting	13
Cross-Validation Procedure	14

DIRECTOR APPROVED
COPY

Page

Results and Discussion---------- 16

Precipitation Data Base---------- 16

Preliminary Statistical Analysis---------- 17

Sample Direct-variogram for TAAP---------- 19

Sample Direct-variogram for Elevation---------- 20

Sample Cross-variogram for Elevation and TAAP---------- 21

Model Fitting and Cross-validation---------- 22

TAAP Direct-variogram Model---------- 22

Elevation Direct-variogram Model---------- 23

Positive Definite Condition---------- 25

Sliding Neighborhood Search Radius for Elevation---------- 27

TAAP - Elevation Cross-variogram Model---------- 27

Comparison of Cokriging with Alternate Estimation Methods---------- 30

Summary and Conclusions---------- 31

References---------- 35

DIRECTOR APPROVED
COPY

PRECIPITATION ESTIMATION IN MOUNTAINOUS TERRAIN USING MULTIVARIATE GEOSTATISTICS: 1. STRUCTURAL ANALYSIS

Joseph A. Hevesi
Raytheon Services Nevada
Las Vegas, Nevada

Jonathan D. Istok
Associate Professor
Department of Civil Engineering
Oregon State University
Corvallis, Oregon

Alan L. Flint
U. S. Geological Survey
Mercury, Nevada

April 3, 1991

DIREC.

LIST OF TABLES

		Page
Table 1	Equations defining positive definite variogram models.	38
Table 2	Descriptive statistics for AAP, TAAP, and elevation.	39
Table 3	Precipitation data used for geostatistical analysis.	40
Table 4	Combinations of structures and parameters, and range of resulting cross-validation statistics for alternate direct-variogram models for TAAP.	42
Table 5	Structures, parameters, and cross-validation statistics for fitted variogram models.	43
Table 6	Cross-validation results for alternate estimation methods.	44

RECTOR APPROVED
COPY

LIST OF FIGURES

		Page
Figure 1	Location of study area and precipitation stations.	45
Figure 2	Topographic map of UARW showing boundary of sampling grid for elevation.	46
Figure 3	Standard error for AAP as a function of length of record for 64 precipitation stations.	47
Figure 4	Regression equations for AAP as a function of station elevation.	48
Figure 5	Sample direct-variogram and fitted model for TAAP.	49
Figure 6	Sample direct-variogram and fitted model for elevation.	50
Figure 7	Sample direct-variogram and fitted model for elevation (expanded scale).	51
Figure 8	Sample cross-variogram and fitted model for TAAP and elevation.	52
Figure 9	Effect of neighborhood search radius on cross-validation statistics for fitted, direct-variogram model for TAAP.	53
Figure 10	Effect of neighborhood search radius on cross-validation statistics for fitted, direct-variogram model for elevation.	54
Figure 11 a,b,c	Effect of neighborhood search radius for elevation on cross-validation statistics: a) percent average estimation error, (PAEE), b) relative mean squared error, (RMSE) and c) standardized mean squared error (SMSE) for alternate cross-variogram model for TAAP and elevation.	55

PRECIPITATION ESTIMATION IN MOUNTAINOUS TERRAIN USING MULTIVARIATE GEOSTATISTICS: 1. STRUCTURAL ANALYSIS

ABSTRACT

Values of Average Annual Precipitation (AAP) are desired for hydrologic studies within a watershed containing Yucca Mountain, Nevada, a potential site for a high-level nuclear-waste repository. Reliable values of AAP are not yet available for most areas within this watershed because of a sparsity of precipitation measurements and the need to obtain measurements over a sufficient length of time. To estimate AAP over the entire watershed, historical precipitation data and station elevations were obtained from a network of stations in southern Nevada and southeastern California. Multivariate geostatistics (cokriging) was selected as an estimation method because of a significant ($p=0.05$) correlation of $r = 0.75$ between the natural log of AAP and station elevation. A sample direct-variogram for the transformed variable, $TAAP=\ln((AAP)*1000)$, was fitted with an isotropic, spherical model defined by a small nugget value of 5,000, a range of 190,000 ft, and a sill value equal to the sample variance of 163,151. Elevations for 1,531 additional locations were obtained from topographic maps to improve the accuracy of cokriged estimates. A sample direct-variogram for elevation was fitted with an isotropic model consisting of a nugget value of 5,500 and three nested transition structures: a Gaussian structure with a range of 61,000 ft, a spherical structure with a range of 70,000 ft, and a quasi-stationary, linear structure. The use of an isotropic,

stationary model for elevation was considered valid within a sliding neighborhood radius of 120,000 ft. The problem of fitting a positive definite, nonlinear model of co-regionalization to an inconsistent sample cross-variogram for TAAP and elevation was solved by a modified use of the Cauchy-Schwarz inequality. A selected cross-variogram model consisted of two nested structures: a Gaussian structure with a range of 61,000 ft and a spherical structure with a range of 190,000 ft. Cross-validation was used for model selection and for comparing the geostatistical model with 6 alternate estimation methods. Multivariate geostatistics provided the best cross-validation results.

1. Introduction

Precipitation data are required for many hydrologic analyses. Values of average annual precipitation (AAP) can be important for water-balance calculations, estimating recharge boundary conditions for ground-water flow models, and defining current climatic conditions. One of the fundamental problems of hydrology is to estimate precipitation at an unmonitored site using data from surrounding precipitation stations. Obtaining reliable estimates is particularly difficult when the areal coverage provided by the surrounding stations is sparse or when precipitation characteristics vary greatly with location. This situation frequently occurs in mountainous terrain when few stations are available and orographic effects can be large. An example of such an area is Yucca Mountain, Nevada, a potential site for a high-level, nuclear-waste repository. Reliable values of AAP are not yet available from the stations at Yucca Mountain because of

short lengths of record (less than 4 years). In addition, there is a sparsity of stations at many locations that may be important for hydrologic studies concerning the potential repository. Values of AAP can be estimated at these locations using a regional network of stations in southern Nevada and southeastern California with longer lengths of record (14 to 53 years).

Tabios and Salas (1985) compared several methods for estimating AAP and concluded that geostatistical methods (including ordinary and universal kriging) were superior to Thiessen polygon, polynomial interpolation, and inverse-distance weighting methods. If a sufficient sample size and spatial distribution of data are available for defining a representative model, geostatistical methods can provide unbiased estimates with minimized estimation variances and ~~has~~ have been widely used to estimate climatological data, including AAP (Dingman et al., 1988). Cokriging is a multivariate geostatistical method that uses the spatial correlation between two or more variables to reduce estimation variances when one of the variables is undersampled (David, 1977). The magnitude of variance reduction depends on the correlation between the variables and on the data spatial configuration. Selection of cokriging as an estimation method for this study is based on the [observed] calculated/measured -or- delete correlation between AAP and elevation for southern Nevada (Quiring, 1983; French, 1986).

The two articles in this series present an application of multivariate geostatistics to the problem of estimating AAP for a study area defined by a watershed containing Yucca Mountain. This article describes the characterization and modeling of the spatial correlations and cross-correlation for AAP and elevation, and the use of cross-validation

to evaluate model performance. The second article describes the use of the geostatistical models to develop isohyetal maps of AAP for the watershed. The overall objective is to ascertain if a multivariate geostatistical approach can be used to improve estimation accuracy by reducing estimation variances within the study area. An application of multivariate geostatistics that uses elevation to estimate AAP has not previously been reported.

2. Study Area

a. Geographic and Physiographic Setting

Yucca Mountain is located in the Great Basin Physiographic Province in southern Nevada, along the western border of the Nevada Test Site (NTS) (Fig. 1). The conceptual perimeter drift boundary of a potential nuclear-waste repository underlies an area of approximately 2 square miles beneath the southern extent of Yucca Mountain. The study area for an isohyetal mapping of AAP is defined by a watershed containing Yucca Mountain, referred to as the Upper Amargosa River Watershed (UARW). The UARW is an area of approximately 2,600 square miles centered on the potential repository site (Figs. 1, 2). The general direction of drainage within the UARW is from north to south, and flow in all drainages is sporadic. The UARW is a subbasin of Death Valley, which is a closed basin.

Physiography within the UARW varies from the near horizontal depositional

surfaces of the Amargosa Desert to the rugged escarpments and steep slopes formed by fault scarps and erosional surfaces in the surrounding mountain ranges (Fig. 2). Elevations in the UARW range from 2,000 ft in the Amargosa Desert to 7,694 ft on Pahute Mesa. Local relief (defined here as the change in elevation over a distance of 50,000 ft) within the UARW ranges from near zero in the Amargosa Desert to 4,000 ft in the Spring and Funeral Mountains. Local relief in the vicinity of Yucca Mountain ranges from 1,000 to 3,000 ft. The highest elevation of the Yucca Mountain massif is 6,703 feet (Chocolate Mountain). Elevations within the area overlying the conceptual perimeter drift boundary range from 3,980 to 4,940 ft.

b. Climate

The UARW is located along the transition zone between the Mojave Desert to the south and the Great Basin Desert to the north (McMahon, 1985). The climate for this region is classified as a midlatitude-desert, and AAP is less than 300 mm in most locations. Winter (October to March) precipitation primarily results from frontal storm systems traveling eastward from the Pacific Ocean. Summer precipitation primarily results from localized convective-type storms; possible sources of moisture are the Gulf of Mexico to the southeast and the Gulf of California to the south. After analyzing measurements of AAP from 63 southern Nevada and southeastern California precipitation stations, French (1983) concluded that the combined effects of the Sierra Nevada rain shadow and the circulation of moisture from the Gulf of Mexico causes a

trend of increasing precipitation from west to east across southern Nevada. This trend results in a "moisture deficit" zone in the west and a "moisture excess" zone in the east, relative to a central "transition" zone. The NTS and the eastern half of the UARW are within the transition zone. The western half of the UARW is within the deficit zone. Yucca Mountain is located along the gradational boundary between the transition and deficit zones.

c. Elevation - Precipitation Correlation

Precipitation tends to increase with an increase in elevation in southern Nevada because of the orographic effect of mountainous terrain and to the virgis effect, which is the depletion by evaporation of the falling rain (Jones, 1981). Quiring (1983) calculated a correlation coefficient (r) of 0.90 between AAP and elevation for 11 stations on the NTS. French (1986) examined the correlation between AAP and elevation for 12 stations on the NTS with 10 or more years of complete record, and computed r values of 0.92 between AAP and elevation, and 0.87 between log(AAP) and elevation. Change in vegetation type and increase in vegetation density with elevation is indirect evidence of increased precipitation with increased elevation. Pinyon pine and Juniper are prevalent above elevations of approximately 6,000 ft. Mountain mahogany, pinyon pine, and juniper occur on Telescope Peak in the Panamint Range (Fig. 2). Within the UARW, juniper occurs on Pahute Mesa, Timber Mountain, Shoshone Mountain, the Grapevine Mountains, the Spring Mountains, and on the higher elevations of the Yucca Mountain

massif.

3. Geostatistical Theory

The term geostatistics refers to a collection of statistical methods for describing and modeling the correlation structure of regionalized variables (ReV), i.e., random variables distributed in space and/or time. The theoretical basis for these methods has been described in detail elsewhere (David, 1977; Journel and Huijbregts, 1978; Isaaks and Srivastava, 1989). Only those aspects of theory relevant to the estimation of AAP are presented here.

The set of sample values for a ReV is considered to be a single realization of a random function. In this study, the two random functions of interest, $Z_i(x)$ and $Z_j(x)$, correspond to AAP and elevation. The spatial correlation structure for a pair of random functions is defined by the variogram:

$$\gamma_{ij}(h) = \frac{1}{2} E \{[Z_i(x+h)-Z_i(x)][Z_j(x+h)-Z_j(x)]\} \quad , \tag{1}$$

where E is the expectation operator and x and $(x + h)$ define locations separated by the vector h. If i = j, Eq. 1 defines the direct-variogram for Z_i. If i ≠ j, Eq. 1 defines the cross-variogram for Z_i and Z_j. In this study, Eq. 1 is used to define a direct-variogram for AAP, a direct-variogram for elevation, and a cross-variogram for AAP and elevation.

Because the available data represent only one realization of the random functions, estimating the direct- and cross-variograms is not possible unless certain simplifying

assumptions are made. One simplifying assumption is that the expectations of Z_i and Z_j are stationary, i.e., $E[Z_i(x)] = m_i$ and $E[Z_j(x)] = m_j$, where m_i and m_j are constants within a circular neighborhood of the point to be estimated. It is also assumed that the variograms defined by Eq. 1 are stationary. These two assumptions constitute the intrinsic hypothesis and permit the calculation of sample variograms (see Methods) that can be used to estimate the direct- and cross-variograms for AAP and elevation. Mathematical models can be selected to represent the spatial structure displayed by the sample variograms.

Variogram models must be positive definite. For a single ReV, this condition can be met by selecting allowable model functions such as the spherical, Gaussian, and linear functions defined in Table 1. A multivariate model for two ReVs (AAP and elevation) consists of 1 cross-variogram and 2 direct-variograms, and an additional requirement for the positive definite condition is that the Cauchy-Schwarz inequality is satisfied for all values of h (Journel and Huijbregts, 1978):

$$\gamma_{ij}(h) \leq \sqrt{\gamma_{ii}(h)\gamma_{jj}(h)} \quad , \tag{2}$$

where $\gamma_{ij}(h)$ is the cross-variogram model for AAP and elevation, and $\gamma_{ii}(h)$ and $\gamma_{jj}(h)$ are the direct-variogram models for AAP and elevation.

The linear estimator for AAP at an unsampled location, x_o, consists of a weighted combination of the available AAP and elevation data:

$$Z_i^*(x_o) = \sum_{k=1}^{n_i} \lambda_{ik} z_i(x_k) + \sum_{l=1}^{n_j} \lambda_{jl} z_j(x_l) \quad , \tag{3}$$

where $Z_i^*(x_o)$ is the estimate for AAP at x_o, λ_{ik} is the weight assigned to the measured value of AAP, z_i, at location x_k (x_k, k = 1, n_i are the locations of the precipitation stations), and λ_{jl} is the weight assigned to the measured value of elevation, z_j, at location x_l (x_l, l = 1, n_j are the locations of points with known elevation).

The weights in Eq. 3 are obtained by minimizing the estimation variance:

$$Var\ \{Z_i^*(x_o) - Z_i(x_o)\} \quad , \tag{4}$$

with the constraint that the estimate be unbiased i.e.,

$$E\ \{Z_i^*(x_o) - Z_i(x_o)\} = 0 \quad . \tag{5}$$

The result is a system of linear equations, the cokriging system (Yates and Warrick, 1987):

$$\begin{aligned}
&\sum_{k=1}^{n_i} \lambda_{ik}\gamma_{ii}(x_m,x_k) + \sum_{l=1}^{n_j} \lambda_{jl}\gamma_{ij}(x_m,x_l) + \mu_i = \gamma_{ii}(x_o,x_m), \quad m = 1,\ n_i \\
&\sum_{k=1}^{n_i} \lambda_{ik}\gamma_{ij}(x_m,x_k) + \sum_{l=1}^{n_j} \lambda_{jl}\gamma_{jj}(x_m,x_l) + \mu_j = \gamma_{ij}(x_o,x_m), \quad m = 1,\ n_j \\
&\sum_{k=1}^{n_i} \lambda_{ik} = 1 \\
&\sum_{k=1}^{n_j} \lambda_{jk} = 0 \quad ,
\end{aligned} \tag{6}$$

where μ_i and μ_j are Lagrange multipliers. The minimized estimation variance at the unsampled location x_o, $\sigma^2(x_o)$ is:

$$\sigma^2(x_o) = \mu_i - \sum_{k=1}^{n_i} \lambda_{ik}\gamma_{ii}(x_k,x_o) + \sum_{l=1}^{n_j} \lambda_{jl}\gamma_{ij}(x_l,x_o) \quad . \tag{7}$$

When $n_j = 0$, Eqs. 6 and 7 define the kriging estimate and estimation variance for regionalized variable i (AAP), otherwise Eqs. 6 and 7 define the cokriging estimate and estimation variance for AAP.

4. Methods

a. Precipitation Data

Records of AAP and station elevation were obtained from French (1983, 1986, 1987) for 62 precipitation stations in southern Nevada and southeastern California, and from the unpublished records for two precipitation stations on Yucca Mountain. Many of the stations had been moved during their period of record, and corrections were made by French using a double mass analysis. Descriptive statistics for the 64 AAP values are listed in Table 2. Eighteen stations were located within the UARW. The length of record ranged from 2 to 53 years. The maximum and minimum values of AAP were 544 mm for an elevation of 7,165 ft in the Spring Mountains and 69 mm for an elevation of -168 ft in Death Valley.

b. Elevation Data

An additional 1,531 ground elevations were manually recorded from 1:250,000

scale topographic maps (Caliente, Death Valley, Goldfield, and Las Vegas). The data were recorded at locations on a square grid with a regular spacing of 10,000 ft. The grid was centered on the UARW (Fig. 2) and extended approximately 50,000 ft beyond the watershed boundary to reduce extrapolation and edge effects on estimates of AAP made near the boundary (Renard and Yancey, 1984; Journel and Huijbregts, 1978). A total of 747 grid locations were within the UARW. Inspection of contour maps prepared from the elevation sample indicated that the sample accurately represented major physiographic features within the UARW (e.g., the northeast to southwest alignment of Basin and Range physiography). Descriptive statistics for the elevation sample are listed in Table 2.

Ideally, the areal extent of the sampled domain for AAP and elevation should be identical to ensure consistency in the analysis of the spatial correlations and cross-correlations. However, two factors prevented the use of an elevation grid with the same areal extent as the precipitation stations: 1) the sample size for elevation with the selected grid spacing of 10,000 ft would have been too large to allow for practical computing time using the available facilities, and 2) major changes could be identified in the characteristics of the physiography within southern Nevada and southeastern California, which causes the structure of spatial variability for elevation on this scale to be nonstationary (see the discussion of the sample direct-variogram for elevation).

c. Preliminary Statistical Analysis

To estimate the minimum length of record necessary for reliable AAP values, standard errors for the 64 available measurements of AAP were compared with the number of years of record for each station. Standard errors were calculated for each station using:

$$SE = \sqrt{\sigma^2/N} \quad , \tag{8}$$

where SE = the standard error, σ^2 = the variance of annual precipitation, and N = the number of years of record.

The sample distributions for AAP and elevation were tested for normality by inspection of histograms and normal probability plots. Sample means and variances were calculated for use in fitting models to the direct-variograms and for use in calculating cross-validation statistics and limits of model validity. Sample covariances and correlation coefficients were calculated for use in fitting models to the sample cross-variogram.

d. Sample Variograms

Sample variograms were computed using (e.g., Journel and Huijbregts, 1978):

$$\gamma_{ij}^{*} = \frac{1}{2n_i} \sum_{k=1}^{n_i} [z_i(x_k+h)-z_i(x_k)][z_j(x_k+h)-z_j(x_k)] \quad , \tag{9}$$

where z_i and z_j are the measured values of AAP and elevation, and n_i is the number of

sample pairs separated by vector h. In this form, Eq. 9 is used to calculate the sample cross-variogram. Sample direct-variograms for AAP and elevation were calculated using Eq. 9 by setting $z_i = z_j$. Calculations were made using the computer program VARIO (Cooper et al., 1988).

e. Model Fitting

A set of alternate direct- and cross-variogram models were fitted to the sample variograms with the criteria that each model be positive definite. The equations used for variogram models are defined in Table 1. Cross-variogram model parameters were selected with the additional criteria of satisfying the Cauchy-Schwarz inequality (Eq. 2). In this study, combining the small AAP sample with the large elevation sample prevented the use of a linear model of co-regionalization (Journel and Huijbregts, 1978), which is required for the usual procedure of testing the positive definite condition with the Cauchy-Schwarz inequality. A new procedure was developed using the function PDC (for positive definite condition):

$$\mathrm{PDC} = \sqrt{\gamma_{ii}(h)\gamma_{jj}(h)} \quad , \tag{10}$$

where $\gamma_{ii}(h)$ and $\gamma_{jj}(h)$ are the model direct-variograms for AAP and elevation. By plotting a graph of the proposed model with the PDC curve defined by Eq. 10, it was possible to visually test fitted cross-variogram models . Models were considered to be

positive definite if the value of $\gamma_{ij}(h)$ did not exceed the slope and the value of PDC for all values of h.

f. Cross-Validation Procedure

Cross-validation statistics were used to help select direct- and cross-variogram models from a set of fitted models (Delhomme, 1979). The procedure involved deleting one sample from the dataset of one ReV, and then estimating the value of that ReV at the location of the deleted sample, using the remaining samples and the chosen variogram model(s) and parameters. The procedure was repeated until estimates were obtained for all measured values. Differences between estimated and measured values were summarized by using the cross-validation statistics: Percent Average Estimation Error (PAEE), Relative Mean Squared Error (RMSE), and Standardized Mean Squared Error (SMSE) (Cooper and Istok, 1988).

Estimates were considered unbiased if the PAEE was close to zero:

$$\text{PAEE} = \frac{100\%}{\bar{z}_i n_i} \sum_{k=1}^{n_i} [Z_i^*(x_k) - z_i(x_k)] \quad , \tag{11}$$

where $Z_i^*(x_k)$ is the estimated value of ReV Z_i at location x_k, $z_i(x_k)$ is the deleted sample value for Z_i at x_k, n_i is the total number of samples deleted, and $\bar{z}_i$ is the sample mean.

Estimates were considered accurate if the RMSE was close to zero:

$$\text{RMSE} = \frac{1}{s^2 n_i} \sum_{k=1}^{n_i} [Z_i^*(x_k) - z_i(x_k)]^2 \quad , \tag{12}$$

where s^2 is the sample variance.

The SMSE indicates the consistency of the calculated estimation variances with the observed RMSE. The SMSE is calculated as follows:

$$\text{SMSE} = \frac{1}{n_i} \sum_{k=1}^{n_i} \frac{[Z_i^*(x_k) - z_i(x_k)]^2}{\sigma_K^2(x_k)} \quad . \tag{13}$$

The estimation variances were considered consistent if SMSE was in the range $1 \pm 2(2/n_i)^{0.5}$ (Delhomme, 1979).

To investigate potential improvements in estimation accuracy using cokriging, cross-validation results for the multivariate model were compared with 6 different estimation methods that included neighborhood averaging, 3 different inverse-distance methods, and 2 regression equations. The RMSE statistic was considered the best indicator of relative performance in terms of estimation accuracy, with a minimum RMSE result indicating favorable performance. SMSE values were calculated only for kriging and cokriging estimates.

5. Results and Discussion

a. Precipitation Data Base

Standard errors for the 64 available AAP measurements were observed to be greater than 20 mm for many stations with lengths of record less than 25 years (Fig. 3). Standard errors greater than 20 mm indicated average measurement errors greater than 10 percent relative to the sample mean of 177 mm for the 64 AAP values (Table 2). French (1987), in an analysis of precipitation data for 11 NTS stations, concluded that a standard error of less than 20 mm for AAP required a length of record of at least 31 years. Only 12 of the stations available for this study had a length of record of 31 years or longer, which is too small a sample for calculating sample variograms. An adequate sample size was obtained by selecting 42 stations with lengths of record of at least 8 years. Descriptive statistics for this sample are listed in Table 2. The locations of the 42 stations are indicated in Figure 1, and a summary of the data is listed in Table 3. Standard errors for this sample ranged from 47 mm for station 215, with a length of record of 8 years, to 7 mm for station 219, with a length of record of 18 years. Station elevations ranged from 7,550 ft for station 207 in the Sheep Mountains to -168 ft for station 219 in Death Valley. The dataset included 10 stations within the boundaries of the UARW. Values of AAP for these stations ranged from 295 mm for station 84 (elevation 7,490 ft) on Pahute Mesa to 85 mm for station 224 (elevation 2,176 ft) in the Amargosa Desert. The dataset did not include the 2 stations on Yucca Mountain with

Also station 225.

lengths of record of only 2 and 4 years. Station 75, with a length of record of 16 years and an AAP value of 119 mm, was located the closest distance of approximately 50,000 ft (9.5 mi) to the potential repository site.

b. Preliminary Statistical Analysis

A significant correlation coefficient of r = 0.72 was obtained between AAP and elevation for the 42 selected stations. An improved coefficient of 0.75 was obtained between the natural log of AAP and elevation. Using the method of least squares, the nonlinear regression equation:

$$\mathrm{AAP} = \exp(4.32 + 0.00018E), \quad r^2 = 0.56 \quad , \tag{14}$$

was fit to the data, where E is the station elevation in feet and AAP is in millimeters (Fig. 4). Similar regression equations were obtained by French (1986) using data from 63 stations in southern Nevada:

$$\mathrm{AAP} = \exp(4.31 + 0.00016E), \quad r^2 = 0.48 \quad , \tag{15}$$

and using data from 12 NTS stations with 10 or more years of record:

$$\mathrm{AAP} = \exp(4.38 + 0.00019E), \quad r^2 = .76 \quad . \tag{16}$$

Equation 16 was considered applicable for estimating AAP at Yucca Mountain because of the increased reliability of the AAP measurements used to develop the equation and because the NTS stations are located closer to Yucca Mountain than many of the additional stations used to develop Eqs. 14 and 15 (Fig. 1). However, Eq. 16 may not be applicable for areas within the UARW to the west and to the south of Yucca Mountain because of the small size and areal extent of the sample consisting of the 12 NTS stations.

A comparison of the regression equations and a scatterplot of the 42 stations used to develop Eq. 14 indicated an increase in the variability of both the data and the fitted curves with increased station elevation (Fig. 4). The increased variability may be the result of: 1) the small number of stations below 2,000 ft, 2) a "rain shadow" effect caused by the location of stations on the lee slope of higher topography or adjacent to blocking ranges, 3) regional trends in AAP, such as the west to east increase hypothesized by French (1983), 4) an increase in the elevation of basins from south to north, 5) increased measurement error with increased elevation because of increasing amounts of snow, and 6) increased variability of annual precipitation with increased elevation.

Histogram and normal probability plots indicated that the values of AAP were log-normally distributed. A log-normal distribution is typical for precipitation data in arid climates (Jones, 1981). The transformation Y = ln(AAP) improved the fit of the histogram to a normal distribution, and the standardized skewness was reduced from 2.19 to 0.34 (Table 2). An additional transformation, TAAP (for transformed AAP) =

ln(AAP)•1000, was used to reduce the possibility of numerical errors during kriging and cokriging.

The elevation data were considered to be normally distributed, although the negative elevations at grid locations in Death Valley resulted in a small bimodal characteristic and a negative standardized skewness of -3.89 for the elevation sample (Table 2). Inspection of a normal probability plot showed an approximate overall fit to a normal distribution, and no attempt was made to improve this fit by a transformation.

c. Sample Direct Variogram for TAAP

Because of the small sample size for TAAP, directional variograms were computed by using wide angle and distance classes (Cooper et al., 1988), and this resulted in a loss of directional resolution. Isotropism was assumed because the analysis of spatial variability was limited to the omnidirectional sample variogram. This variogram indicated a range of spatial correlation for TAAP of about 190,000 ft (36 mi) (Fig. 5). For distances greater than 190,000 feet, the variogram approximated a constant value equal to the sample variance. Deviations about the sample variance line were considered to be fluctuations of the variogram resulting from the small sample size. The lack of slope in the overall shape of variogram for distances greater than the range of spatial correlation indicated an absence of drift in the spatial structure of TAAP, supporting the assumption of second-order stationarity.

d. Sample Direct Variogram for Elevation

The large sample size for elevation permitted the calculation of informative directional sample variograms. Sample variograms were calculated for 7 directions that ranged from 0° (east) to 180° (west) at intervals of 30°. An angle class of 45° and a distance class of 10,000 ft were used with VARIO (Cooper et al, 1988). Two sample variograms were selected to represent the observed spatial variability: the ENE-WSW sample variogram (direction 30°) that corresponded to the direction of maximum variability, and the NNW-SSE variogram (direction 120°) that corresponded to the direction of minimum variability (Fig. 2). More than 1,000 sample pairs were used to calculate most of the values defining the variograms. The value for $\gamma(h)$ for the minimum h of 3,000 ft, calculated using only 21 sample pairs, defined the spatial correlation of precipitation station elevations with adjacent grid elevations.

A comparison of the directional variograms indicated zonal anisotropism (Journel and Huijbregts, 1978) (Fig. 6). Anisotropism is caused by a general NNW-SSE alignment of Basin and Range physiographic features that includes Death Valley, the Grapevine Mountains, the Funeral Mountains, the Black Mountains, the Amargosa Desert, and the northern Spring Mountains (Fig. 2). The ENE-WSW variogram increased to more than 4 times the NNW-SSE variogram at distances of 300,000 ft because maximum spatial variability occurs in directions transverse to the alignment of Basin and Range physiography, while minimum spatial variability occurs in directions parallel to this alignment. An increase in the slope of the variograms indicated drift in

the ENE-WSW direction for distances greater than 200,000 ft and in the NNW-SSE direction for distances greater than 400,000 ft. Both drift components were identifiable in the omnidirectional variogram.

For distances less than 200,000 ft, the sample variograms were similar and the assumptions of isotropism and stationarity were considered valid. Two separate spatial structures for elevation were indicated by the decrease in the slope of the variograms at approximately 60,000 ft; a structure between 0 and 60,000 ft defining the local spatial variability of elevation within individual basins, and a structure for distances greater than 60,000 defining the regional variability of elevation between basins and ranges (Fig. 7). The separate structures were not as well defined in the NNW-SSE variogram as in the omnidirectional and ENE-WSW variograms because the NNW-SSE direction tends to parallel basins and ranges. Maintaining the assumptions of stationarity and isotropism was desirable to simplify model fitting during cross-validation, and also to maintain some consistency between the variograms in the multivariate model. Nonstationary ReV's can be modeled using geostatistics (universal kriging/cokriging techniques), but either the variogram or the form of drift is assumed to be known (Journel and Huijbregts, 1978; Clark, 1979; David, 1977).

e. Sample Cross-Variogram for Elevation and TAAP

The increase in the values of sample cross-variogram for distances from 0 to approximately 190,000 ft indicated a positive spatial cross-correlation between TAAP and

elevation (Fig. 8). For distances between 450,000 and 640,000 ft, the cross-variogram approximated the sample covariance. A negative slope in the variogram observed for distances from 220,000 to 420,000 ft was considered to be an apparent negative spatial cross-correlation between TAAP and elevation caused by the clustering of precipitation stations along a northwest to southeast alignment, parallel to the Nevada-California state boundary (Fig. 1). This direction transgresses the trend of increasing elevation from south to north, which is known to exist, and the trend of increasing AAP from west to east, hypothesized by French (1983). If more stations were available to the southwest and the northeast of the NTS, the negative slope might not be observed in the isotropic sample cross-variogram. Unfortunately, a more detailed structural analysis of the TAAP-elevation spatial cross-correlation was not possible with the available data.

f. Model Fitting and Cross-validation:

1. TAAP Direct-variogram Model

A large number of alternate models were investigated for the direct-variogram for TAAP, and many of these models had favorable cross-validation statistics. The range of parameters defining the different models, and the range of cross-validation results, are listed in Table 4. The selected model consisted of a nugget value of 5,000 and a spherical structure with C = 158,151 and a range (a) of 190,000 ft (36 mi.). The sill value (nugget + C) was defined using the TAAP sample variance of 163,151 (Table 5,

Fig. 5). The existence of a nugget structure is physically reasonable for AAP at this scale because of the many site-specific influences on precipitation measurements, such as site exposure, precipitation measurement errors, and differences in the length and the period of record for precipitation data used to compute AAP at each station. A relatively small nugget value was selected because good spatial correlation was expected for AAP over relatively small distances (less than approximately 10,000 ft).

Based on a favorable combination of cross validation results, a neighborhood search radius of 480,000 ft (91 mi) was selected with the variogram model (Fig. 9). The favorable results consisted of a minimum RMSE value of 0.71, a relatively small PAEE value of 0.45, and a SMSE value close to 1.0 (Table 5). Although 480,000 ft is much greater than the range of spatial correlation defined by the model, the use of TAAP data separated by large distances was necessary for estimating TAAP along the western and southern boundaries of the UARW because of a sparsity of precipitation stations for these areas (geostatistics does not limit the use of data for the calculation of estimates to those locations occurring within the range of spatial correlation).

2. Elevation Direct-variogram Model

The sensitivity of the cross-validation results to the parameters defining the variogram model for elevation indicated that model fitting was important for distances between 0 and approximately 60,000 ft. For distances greater than 60,000 ft, results were not sensitive to model parameters because of the efficient screening effect of the closer

grid locations; the values closest to the estimated point receive the most weight in the kriging system (Clarke, 1979; David, 1977). The sensitivity of SMSE results indicated that a close fitting of the model was required for model consistency in terms of the estimation variance, and this restricted the choice of model parameters. The RMSE and PAEE results, however, were both relatively close to 0 for a wide range of model parameters, indicating excellent model performance in terms of estimation accuracy.

A model was selected based on a favorable combination of cross-validation results (Table 5, Fig. 10). This model was defined by a nugget value of 5,500, a Gaussian structure (C = 415,000) with a range of 61,000 ft, a spherical structure (C = 185,000) with a range of 70,000 ft, and a linear structure (C = 7) with a range of 270,000 ft (Table 5, Figs. 6, 7). A nugget value was required for model validity in terms of the SMSE result. Three nested structures were necessary to provide a close fit to the sample variogram for elevation; the combination of Gaussian and spherical structures with similar ranges defined the local structure observed in the omnidirectional sample variogram, while the linear structure defined the regional structure. The range for the linear structure was the distance at which the value of the NNW-SSE sample variogram approximated the elevation sample variance.

Although the sample variograms for elevation indicated anisotropism and non-stationarity for distances greater than 200,000 ft, the three cross-validation statistics for the fitted model were not sensitive to increases in the neighborhood search radius from 10,000 to 130,000 ft (Fig. 10). Cross-validation results indicated excellent model performance even for the larger neighborhoods because of the efficient screening effect

of the grid locations. With a neighborhood search radius of 130,000 ft, the model variogram was applied to distances as large as 260,000 ft (the model is applied to data locations separated by the diameter of the neighborhood), exceeding the approximate range of quasi-stationarity (Journel and Huijbregts, 1978) indicated by the sample variogram. Selection of a neighborhood search radius for elevation is discussed in: *4. Sliding Neighborhood Search Radius for Elevation.*

3. Positive Definite Condition

Inconsistency between the spatial distributions of the elevation sample and the TAAP sample (both in the areal extent of the sample domains and the density of sample locations) caused 8 values of the sample cross-variogram to be higher than the plotted PDC curve, indicating that models fitted to the sample cross-variogram may not be positive definite (Fig. 8). Sample inconsistency, combined with the nonstationarity of elevation on a regional scale, made it difficult to use the sample cross-variogram for the purpose of defining a model.

In an effort to formulate a valid model, the three values of the sample cross-variogram between distances of 0 and 100,000 ft were considered to be representative of the spatial cross-correlation structure within the UARW, based on the observation that the smallest distances between precipitation stations generally occurred between the 15 NTS stations located within the elevation grid (Fig. 1). This assumption implies a nonstationary cross-correlation structure between TAAP and elevation on a regional

scale.

As an aid to model fitting, the function 0.75(PDC) was used as a possible spatial cross-correlation structure defined by the sample correlation coefficient of 0.75:

$$0.75(\mathrm{PDC}) = 0.75\sqrt{\gamma_{ii}(h)\gamma_{jj}(h)} \tag{17}$$

where $\gamma_{ii}(h)$ and $\gamma_{jj}(h)$ are the fitted direct-variogram models for TAAP and elevation. The plotted 0.75(PDC) curve provided a close fit to the sample cross-variogram for the 3 values between 0 and 100,000 ft (Fig. 8).

The intersection of the 0.75(PDC) curve with the range of 190,000 ft for the TAAP direct variogram model was used to define a "*pseudo-sill*". The *pseudo-sill* determined possible sill values for cross-variogram models, and was considered a modified covariance that accounted for the inconsistency between the TAAP and elevation samples. By substituting the values of the model direct-variograms into equation 17 for h = 190,000 ft, the *pseudo-sill* could be calculated:

$$\textit{Pseudo-sill} = 0.75\sqrt{\gamma_1(190{,}000)\ \gamma_2(190{,}000)} = 410{,}000 \tag{18}$$

An important assumption implicit in this reasoning is that TAAP is stationary. This assumption was considered necessary to provide a starting point for modeling the cross-variogram. However, if the true spatial variability of TAAP is nonstationary for the southern Nevada and southeastern California region, the *pseudo-sill* could represent an exaggerated correlation between TAAP and elevation.

4. Sliding Neighborhood Search Radius for Elevation

To allow cokriging using a quasi-stationary direct-variogram model for elevation restricted to a sliding neighborhood smaller than the sliding neighborhood selected for TAAP (radius = 480,000 ft), the cokriging algorithm was modified to use separate sliding neighborhood search radii for the elevation and TAAP samples. This modification was also necessary because of the inconsistent spatial distributions of the TAAP and elevation samples. The smaller neighborhood search radius defined half the maximum distance for which the cross-variogram model could be applied. During cross-validation of fitted cross-variogram model, the elevation neighborhood search radius was varied from 10,000 to 140,000 ft, at increasing intervals of 10,000 ft, while the direct-variogram model for elevation, the direct-variogram model for TAAP, and the TAAP neighborhood search radius were held constant. As the search radius for elevation was increased, the number of elevation data included in the estimation of one TAAP value also increased from a minimum of 5 using a search radius of 10,000 ft to an average value of approximately 500 using the maximum radius of 140,000 ft.

5. TAAP - Elevation Cross-variogram Model

The cross-validation results for a large number of alternate cross-variogram models indicated that a close fitting to the 0.75(PDC) curve was necessary to obtain favorable results. Models fitted below the 0.75(PDC) curve resulted in low SMSE values

because of increased estimation variances, indicating a reduced potential to minimize cokriging estimation variances relative to kriging estimation variances. Models that were fitted above the 0.75(PDC) curve resulted in high SMSE values. SMSE values exceeding the defined SMSE upper limit of 1.44 were observed for models close to failure in terms of the positive definite condition, and this was considered characteristic of models that exaggerated the TAAP - elevation spatial cross-correlation.

The cross-validation statistics for 5 similar cross-variogram models, plotted against the elevation neighborhood search radius from 0 to 140,000 ft, are shown in Figures 11a, 11b, and 11c. The 5 models were fitted to the 0.75(PDC) curve and to the three values of the sample cross-variogram between 0 and 100,000 ft. In general, cokriging cross-validation results indicated an increase in estimation accuracy relative to kriging with an increase in the neighborhood search radius for elevation. For a radius of 100,000 ft, RMSE results for all 5 models were reduced by approximately 55% relative to RMSE results for kriging (Fig. 11b). A large decrease in RMSE and SMSE values resulted with an increase in the neighborhood radius from 75,000 to 80,000 ft because of a change in the estimation method from kriging to cokriging at one location. PAEE results for most models also indicated improved estimation accuracy of cokriging relative to kriging; at a radius of 45,000 ft, the 5 models indicated an approximate 78% reduction in PAEE (Fig. 11a).

The sensitivity of cross-validation results to model changes increased with an increase in the elevation search radius. RMSE was not sensitive to model changes for search radii less than 120,000 ft, but indicated increasing sensitivity, with a reduction in

model performance, for larger radii (Fig 11b). PAEE results were more sensitive to model changes than changes in the search radius for radii greater than approximately 100,000 ft (Fig. 11a). For radii less than 80,000 ft, SMSE results for the 5 models followed similar trends, but for radii greater than 100,000 ft, SMSE followed divergent trends (Fig. 11c). For a radius of 120,000 ft, SMSE results remained close to the optimum value of 1.0 for models 2 and 3, which were fitted relatively close to the 0.75(PDC) curve, but exceeded the upper SMSE limit for models 1 and 5, which were fitted closer to the sample cross-variogram using a larger Gaussian structure (Table 5, Fig. 11c).

The use of a large neighborhood for elevation was desirable because the reduction in RMSE indicated potentially significant reductions in estimation variances within the UARW. Using a neighborhood radius of 120,000 ft, an average of 400 elevation values would be included in the calculation of each cokriged estimate of TAAP within the UARW. A large radius was also desired because unwanted edge effects can occur when small neighborhoods are used (Renard and Yancey, 1984).

Model 3 was selected because of a favorable combination of cross-validation results, consisting of a minimum RMSE of 0.32, a minimum PAEE of .05, and an SMSE value of 0.99, obtained using a search radius of 120,000 ft (Table 4, Figs 11a, 11b, 11c). The selection of the relatively large radius of 120,000 ft, which limited the application of the elevation direct-variogram model and the cross-variogram model to a maximum distances of 240,000 ft (45 mi), was based on a compromise between minimizing cokriged estimation variances and maintaining the assumptions of isotropism and quasi-

stationarity. The model was defined by a Gaussian structure with a range of 61,000 ft (C = 55,000) and a spherical structure with a range of 190,000 ft (C = 355,000). Although evidence of nested structures was lacking in the sample cross-variogram, a model with two structures was necessary to allow a close fitting to the 0.75(PDC) curve. Model 3 was selected over model 2, which had similar cross-validation results, because model 3 provided a greater potential reduction in calculated estimation variances.

g. Comparison of Cokriging with Alternate Estimation Methods

The cross-validation results for cokriging, kriging, and 6 alternate estimation methods are listed in order of RMSE performance in Table 5. In general, estimation methods using elevation had more favorable RMSE results than interpolation methods using only AAP measurements, indicating that the correlation of AAP with elevation is more important for estimating AAP than the spatial correlation of available AAP measurements. The least favorable estimation method was neighborhood averaging, with RMSE values greater than 0.90 for three different search radii. RMSE results for kriging indicated similar performance relative to the inverse distance squared method. Regression (using elevation to estimate AAP) indicated good estimation accuracy with low RMSE values of 0.46 and 0.47 for log-linear and linear regression. Cokriging was the most favorable method when larger search radii (80,000 to 120,000 ft) for elevation were used. The cokriging RMSE result of 0.32 for a search radius of 120,000 ft indicated a 64% improvement in performance relative to neighborhood averaging, a 55%

improvement relative to kriging, and a 30% improvement relative to regression.

PAEE results were not consistent with RMSE results in terms of estimation performance: the PAEE result of -3.93 for log-linear regression (Eq. 14) was unsatisfactory compared to the relatively low values for linear regression, cokriging, kriging, and neighborhood averaging. The PAEE results for the three inverse distance methods were also considered unsatisfactory. In general, kriging had the best combined cross-validation results relative to all interpolation methods not using elevation, and cokriging had the best combined results relative to all estimation methods.

5. Summary and Conclusions

Measured values of average annual precipitation (AAP) for 42 precipitation stations in the southern Nevada and southeastern California region with lengths of record of 8 to 53 years approximated a log-normal distribution. The use of stations with as few as 8 years of record was necessary to obtain a sample size of TAAP large enough for an adequate geostatistical analysis. A transformed variable, TAAP = ln(AAP)•1000, was defined for the purpose of estimating AAP, using linear geostatistics, for a watershed containing Yucca Mountain, a potential site for a high-level nuclear waste repository.

An isotropic spherical model variogram with a relatively small nugget of 5,000, a sill equal to the sample variance of 163,151, and a range of 190,000 ft (36 mi) was selected as the best representation of the spatial structure for TAAP, given the data available at the time of this study. Model selection was based on a visual fit of the

model to the sample variogram. cross-validation results, and the expected spatial structure of AAP for distances less than 10,000 ft.

A correlation coefficient of 0.75 was calculated between TAAP and elevation, and a large sample of elevation was obtained to improve estimation accuracy by using a multivariate model. Computed directional sample variograms for elevation indicated a anisotropic spatial structure for distances greater than 200,000 ft (38 mi). The axis of maximum spatial variability was orientated in the ENE-WSW direction, transverse to the dominant alignment of Basin and Range physiography. An isotropic, stationary direct-variogram model for elevation was defined using the assumption of quasi-stationarity and a neighborhood search radius of 120,000 ft (23 mi). The fitted model consisted of a nugget value of 5,500 and three nested structures: a Gaussian structure with a range of 61,000 feet, a spherical structure with a range of 70,000 feet, and an intrinsic, linear structure. The Gaussian and spherical structures defined the local spatial variability observed for elevation and the linear structure defined the regional spatial variability observed for elevation. A close fitting of the model to the sample variogram was necessary to obtain good cross-validation results.

Sample cross-variograms indicated a positive spatial cross-correlation between TAAP and elevation with a range of approximately 190,000 ft. The inconsistency of the spatial distributions between the TAAP and elevation samples, however, made it difficult to fit a positive definite model to the cross-variogram. A new method for fitting a cross-variogram model was developed using the Cauchy-Schwarz inequality and the sample correlation coefficient. The use of separate sliding neighborhood search radii for TAAP

and elevation was also necessary because of the inconsistent spatial distributions. Cross-validation results for fitted cross-variogram models were sensitive to changes in the search radius for elevation: the best results were obtained for radii between 80,000 and 120,000 ft. The fitted model, limited to a neighborhood search radius of 120,000 ft, consisted of a Gaussian structure with a range of 65,000 ft, a spherical structure with a range of 190,000 ft, and a "*pseudo-sill*" of 410,000. A cross-variogram model defined by two structures, consistent with the spatial structure defined by the variogram model for elevation, was necessary to obtain good cross-validation results.

Cokriging provided the best cross-validation results relative to regression methods that used only elevation data and interpolation methods that used only AAP data. Kriging provided the best results relative to other interpolation methods, indicating the importance of a spatial correlation model for estimating AAP. Cokriging and regression indicated improved estimation performance, in terms of reduced relative-mean-squared-error (RMSE) results, relative to all methods that did not use elevation data. It was concluded that, for the average distance separating precipitation stations in the southern Nevada and southeastern California region, the correlation between AAP and elevation is more important for estimating AAP than the spatial correlation of existing AAP measurements. This conclusion applies to most locations in a study area containing Yucca Mountain, defined as the Upper Amargosa River Watershed, where estimates of AAP are desired.

AHA! AT LAST A STATE I CAN UNDERSTAND

Acknowledgments. This work was done in cooperation with the U.S. Department of Energy, under interagency agreement DE-AI08-78ET44802.

References

Clark, I., 1979: Practical Geostatistics. Applied Science Publishers, London, U.K.

Cooper, R.M. and J.D. Istok, 1988: Geostatistics Applied to Groundwater Contamination. I: Methodology - J. Environ. Engrg., ASCE, 114(2), 270-286.

Cooper, R. M., J. D. Istok, and A. L. Flint, 1988: Three-dimensional, cross-semivariogram calculations for hydrogeological data. Ground Water, 26, 638-646.

David, M., 1977: Geostatistical Ore Reserve Estimation. Elsevier Scientific Publishing Company, New York, N.Y.

Delhomme, J. P., 1979: Spatial Variability and Uncertainty in Groundwater Flow Parameters: A Geostatistical Approach. Water Resources Research, 15, 269-280.

Dingman, S. L., D. M. Seely-Reynolds, and R. C. Reynolds III, 1988: Application of Kriging to Estimating Mean Annual Precipitation in a Region of Orographic Influence. Water Resources Bulletin, 24(2), 329-339.

French, R. H., 1983: A Preliminary Analysis of Precipitation in Southern Nevada. DOE/NV/10162-10, Water Resources Center, Desert Research Institute, Las Vegas, Nevada. 39.

French, R. H., 1986: Daily, Seasonal, and Annual Precipitation at the Nevada Test Site, Nevada. U.S. Dept. of Energy, Nevada Operations Office, #DE-AC08-85NV10384, Publication No. 45042.

French, R. H., 1987: Effects of the Length of Record on Estimates of Annual and Seasonal Precipitation at the Nevada Test Site. U.S. Dept. of Energy, Nevada Operations Office, #DE-AC08-85NV10384.

Isaaks, E. H. and R. M. Srivastava. 1989: An Introduction to Applied Geostatistics. Oxford University Press, New York.

Jones, K.R., 1981: Arid Zone Hydrology for Agricultural Development, FAO Irrigation and Drainage Paper No. 37, Food and Agriculture Organization of the United Nations, Rome.

Journel, A. G. and C. J. Huijbregts, 1978: Mining Geostatistics. Academic Press, New York, N.Y.

McMahon, J. A., 1985, Deserts, Audubon Society Nature Series, Alfred Knopf, New York, N. Y., 368 p.

Quiring, R. F., 1983: Precipitation Climatology of the Nevada Test Site. Nuclear Support Office, Las Vegas, NV.

Renard, D., and J. D. Yancey, 1984: Smoothing Discontinuities when Extrapolating Using Moving Neighborhood. Geostatistics for Natural Resources Characterization, Part II, 679-690, D. Reidel Publishing Co.

Tabios, G. Q. III., and J. D. Salas, 1985: A Comparative Analysis of Techniques for Spatial Interpolation of Precipitation. Water Resources Bulletin, 21(3), 365-380.

Yates, S.R., and A.W. Warrick, 1987: Estimating Soil Water Content Using Cokriging. Soil Sci. Soc. of Am. J., 51, 23-30.

Table 1. Equations defining positive definite variogram models.

Model Name	Model Equation
NUGGET	$\gamma(h) = C$
SPHERICAL	$\gamma(h) = C\left[\frac{1.5(h)}{a} - \frac{0.5(h^3)}{a^3}\right], \quad h < a$
	$= C, \quad h \geq a$
GAUSSIAN	$\gamma(h) = C\left[1 - \exp\left(-\frac{h^2}{b^2}\right)\right], \quad b\sqrt{3} = a^1$
LINEAR	$\gamma(h) = C(h), \quad h < a$
	$= C, \; h \geq a$

$\gamma(h)$ = variogram
C = variogram model coefficient
a = variogram model range (ft)
a^1 = practical range (ft) for gaussian model (Journel and Huijbregts, 1978)
h = magnitude of vector separating 2 locations

Table 2. Descriptive statistics for AAP, TAAP, and elevation.

Variable Name	Sample Size	Sample Minimum	Sample Mean	Sample Maximum	Sample Variance	Standardized Skewness
AAP[1] (millimeters)	64	69	177	544	6,830	5.77
AAP[2] (millimeters)	42	69	175	354	5,278	2.19
TAAP[2]	42	4,239	5,087	5,870	163,151	0.34
Elevation[1] (feet)	64	-168	4,659	7,670	3,107,320	-0.90
Elevation[2] (feet)	42	-168	4,316	7,550	2,837,470	-0.71
Elevation[3] (feet)	1,595	-250	3,932	8,400	2,466,980	-3.89

AAP = average annual precipitation
TAAP = ln(AAP) * 1000

[1] sample consisting of all available precipitation stations

[2] sample consisting of stations with lengths of record ≥ 8 years

[3] sample consisting of all available stations and 1,531 additional elevations

Table 3. Precipitation data used for geostatistical analysis. Dataset consists of 42 stations with lengths of record ≥ 8 years

Station[1] No.	Station Name	Nevada Central State Plane Coordinates Easting (ft)	Nevada Central State Plane Coordinates Northing (ft)	Station Elevation (ft)	Average Annual Precipitation (AAP) (mm)	Length of Record (yrs)	Standard Deviation of AAP (mm)
72	ROCK VALLEY	639,050	704,700	3,400	157	8	23
73	DESERT ROCK AIRPORT	688,100	681,750	3,298	157	15	17
74	MERCURY	696,738	695,045	3,770	159	13	18
75	4JA	610,605	740,840	3,422	119	16	15
76	CANE SPRINGS	663,600	751,000	4,000	208	21	21
77	WELL 5B	705,200	747,600	3,080	128	19	12
78	SHOSHONE BASIN	620,700	795,000	5,660	225	12	25
79	MID VALLEY	644,500	809,250	4,660	226	13	23
80	YUCCA	680,875	803,600	3,920	177	25	17
81	40 MN	610,600	837,100	4,820	202	18	18
82	TIPPIPAH SPRINGS 2	638,650	838,600	4,980	245	20	23
83	BJY	679,100	842,300	4,072	177	22	17
84	AREA 12 MESA	631,400	888,900	7,490	295	17	31
85	PHS FARM	682,870	895,840	4,565	193	8	22
92	LITTLE FELLER 2	602,000	858,520	5,160	229	8	36
201	ADAVEN	815,611	1,137,916	6,250	321	47	16
202	ALAMO	937,992	917,630	3,440	128	26	10
204	BOULDER CITY	1,029,489	490,470	2,525	139	50	9
205	CALIENTE	1,133,802	995,954	4,407	231	51	11
206	COLD CREEK	770,041	617,747	6,000	230	8	33
207	HIDDEN FOREST	926,689	681,385	7,550	320	9	27
209	LAS VEGAS AIRPORT	936,479	519,842	2,162	104	33	8
211	SUNRISE MANOR	960,956	554,108	1,820	106	32	8
212	OVERTON	1,156,766	652,013	1,220	91	26	13
213	PIOCHE	1,119,116	1,084,069	6,120	313	44	16
214	RED ROCK SUMMIT	828,784	534,527	6,500	270	8	36
215	ROBERTS RANCH	814,098	544,318	6,100	354	8	47

Table 3. Continued.

Station[1] No.	Station Name	Nevada Central State Plane Coordinates Easting (ft)	Northing (ft)	Station Elevation (ft)	Average Annual Precipitation (AAP) (mm)	Length of Record (yrs)	Standard Deviation of AAP (mm)
216	SEARCHLIGHT	1,009,908	338,717	3,540	185	50	14
217	BASALT	27,475	1,103,650	6,350	142	15	17
218	BEATTY	472,943	785,458	3,550	159	47	12
219	DEATH VALLEY	437,164	627,537	-168	69	18	7
220	DESERT GAME RANGE	877,736	622,642	2,920	106	42	8
221	DYER	100,904	991,059	4,975	125	31	9
222	GOLDFIELD	330,981	1,015,535	5,690	136	39	12
223	INDIAN SPRINGS	789,622	666,699	3,136	116	25	16
224	LATHROP WELLS	574,231	686,280	2,176	85	21	11
225	MINA	76,428	1,216,240	4,551	115	53	7
226	PAHRUMP	691,717	559,004	2,700	126	20	16
227	RATTLESNAKE	644,277	1,235,821	5,913	121	20	13
228	SARCOBATUS	399,514	893,154	4,020	90	14	13
229	TONOPAH AIRPORT	375,038	1,123,231	5,427	163	29	10
230	TONOPAH CITY	330,981	1,123,231	6,093	126	22	11

[1] Station numbers are the same as in French (1987, 1986, 1983)

Table 4. Combinations of structures and parameters, and range of resulting cross-validation statistics for alternate direct-variogram models for TAAP.

Model Structures	ranges for model parameters: C[1] coefficient	ranges for model parameters: a[2] (model range)	ranges for cross-validation results: percent average estimation error (PAEE)	ranges for cross-validation results: relative mean square error (RMSE)	ranges for cross-validation results: standardized mean square error (SMSE)
Nugget Linear	0 - 20,000 0.815 - 1.63	0 100,000 - 200,000	0.29 - 0.80	0.57 - 1.08	0.743 - 1.736
Nugget Spherical	0 - 30,000 133,151 - 163,151	0 100,000 - 300,000	0.28 - 0.83	0.60 - 0.99	0.680 - 1.739
Nugget Gaussian	0 - 30,000 133,151 - 163,151	0 120,000 - 210,000	0.24 - 0.78	0.58 - 0.96	0.911 - 3.824
Nugget Gaussian Spherical	0 - 30,000 65,000 - 120,000 33,151 - 93,151	0 155,000 - 190,000 155,000 - 200,000	0.32 - 0.80	0.63 - 0.89	0.869 - 1.452

[1]units are in ln(millimeters)*1000

[2]units are in feet

Table 5. Structures, parameters, and cross-validation statistics for fitted variogram models.

Model Variogram	percent average estimation errror (PAEE)	relative mean square error (RMSE)	standardized mean square error (SMSE)	model variogram Structures	model variogram C coefficient	model variogram range a (ft)	sliding neighborhood search radius (ft)
TAAP Direct-variogram	0.45	0.71	0.99	Nugget	5,000		
				Spherical	158,151	190,000	480,000
Elevation Direct-variogram	0.02	0.04	1.01	Nugget	5,500		
				Gaussian	415,000	61,000	
				Spherical	185,000	70,000	
				Linear	7	270,000	120,000
TAAP-elevation cross-variogram							
Model 1	-0.58	0.363	1.61	Gaussian	100,000	87,000	
				Spherical	309,446	190,000	120,000
Model 2	0.17	0.326	1.00	Nugget	3,880		
				Gaussian	55,000	67,000	
				Spherical	350,000	200,000	120,000
Model 3	0.06	0.321	0.99	Gaussian	55,000	61,000	
				Spherical	355,000	190,000	120,000
Model 4	-0.21	0.337	1.12	Nugget	3,880		
				Gaussian	50,000	87,000	
				Spherical	361,960	190,000	120,000
Model 5	-0.52	0.370	1.45	Gaussian	55,000	87,000	
				Spherical	366,960	190,000	120,000

Table 6. Cross-validation results for alternate estimation methods.

Estimation Method	TAAP Neighborhood Search Radius (ft)	Elevation Neighborhood Search Radius (ft)	Percent Average Estimation Error (PAEE)	Relative Mean Square Error (RMSE)	Standardized Mean Square Error (SMSE)
Neighborhood Average	400,000	-	2.32	0.90	-
	480,000	-	0.62	0.93	-
	560,000	-	0.31	0.97	-
Inverse Distance	400,000	-	4.04	0.81	-
	480,000	-	3.05	0.81	-
	560,000	-	2.64	0.85	-
Inverse Distance Squared	400,000	-	6.29	0.76	-
	480,000	-	5.72	0.74	-
	560,000	-	5.36	0.75	-
Inverse Distance Cubed	400,000	-	6.51	0.83	-
	480,000	-	6.17	0.81	-
	560,000	-	5.96	0.81	-
Kriging	400,000	-	0.75	0.78	1.05
	480,000	-	0.45	0.71	0.99
	560,000	-	0.44	0.78	1.07
Log-linear Regression	-	-	-3.93	0.46	-
Linear Regression	-	-	-0.04	0.47	-
Cokriging (model 3)	480,000	55,000	-0.26	0.56	1.16
	480,000	80,000	-0.39	0.38	1.00
	480,000	120,000	0.05	0.32	0.99

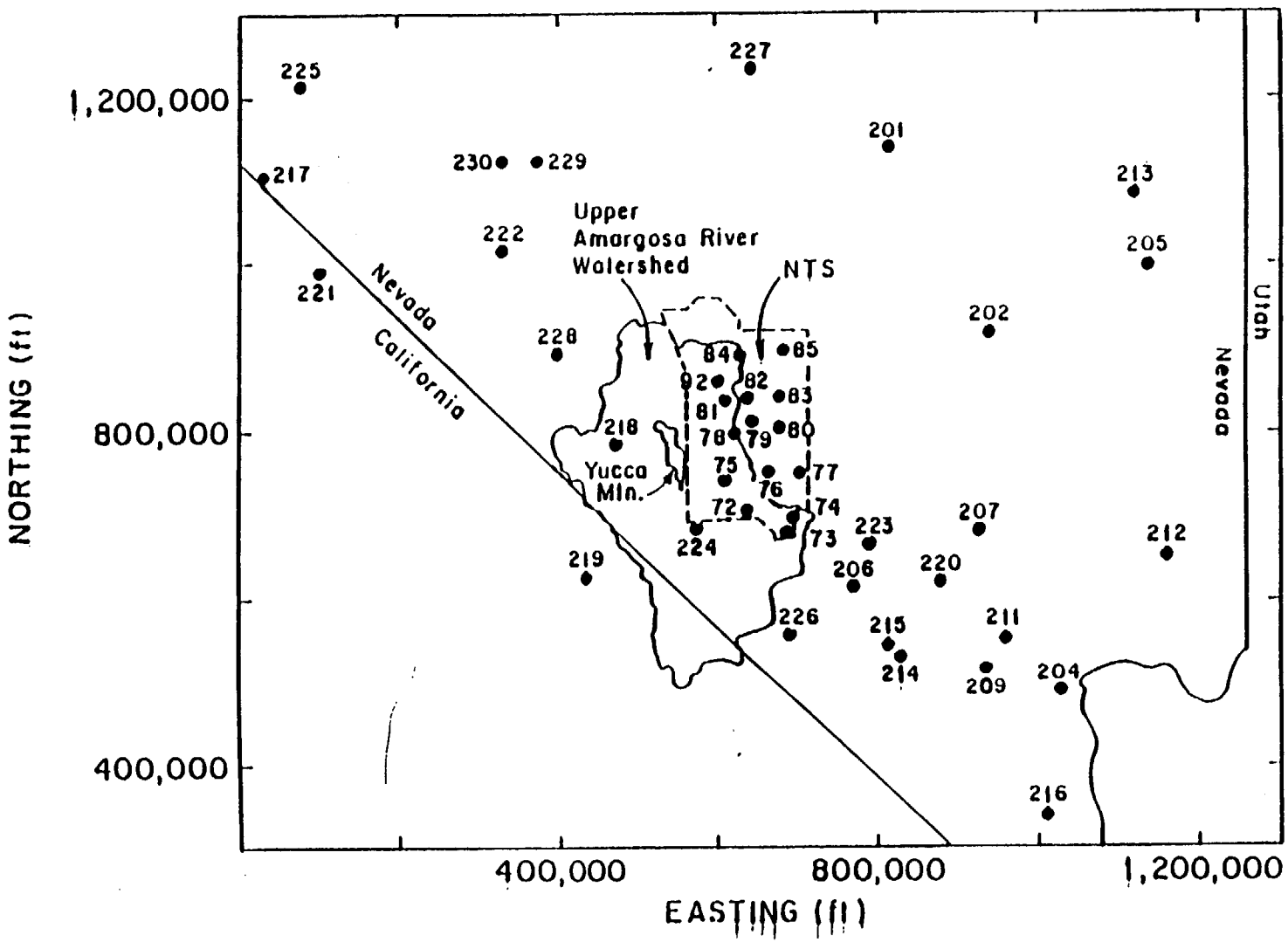
NORTHING (ft)
1,200,000
800,000
400,000
EASTING (ft)
400,000
800,000
1,200,000
Nevada
California
Utah
Nevada
Upper
Amargosa River
Watershed
NTS
Yucca
Mtn.
225
227
201
213
205
217
230
229
222
221
228
202
218
219
224
223
206
220
207
212
226
215
214
211
209
204
216
84
85
92
82
83
81
78
79
80
75
76
77
72
74
73

FIGURE 1

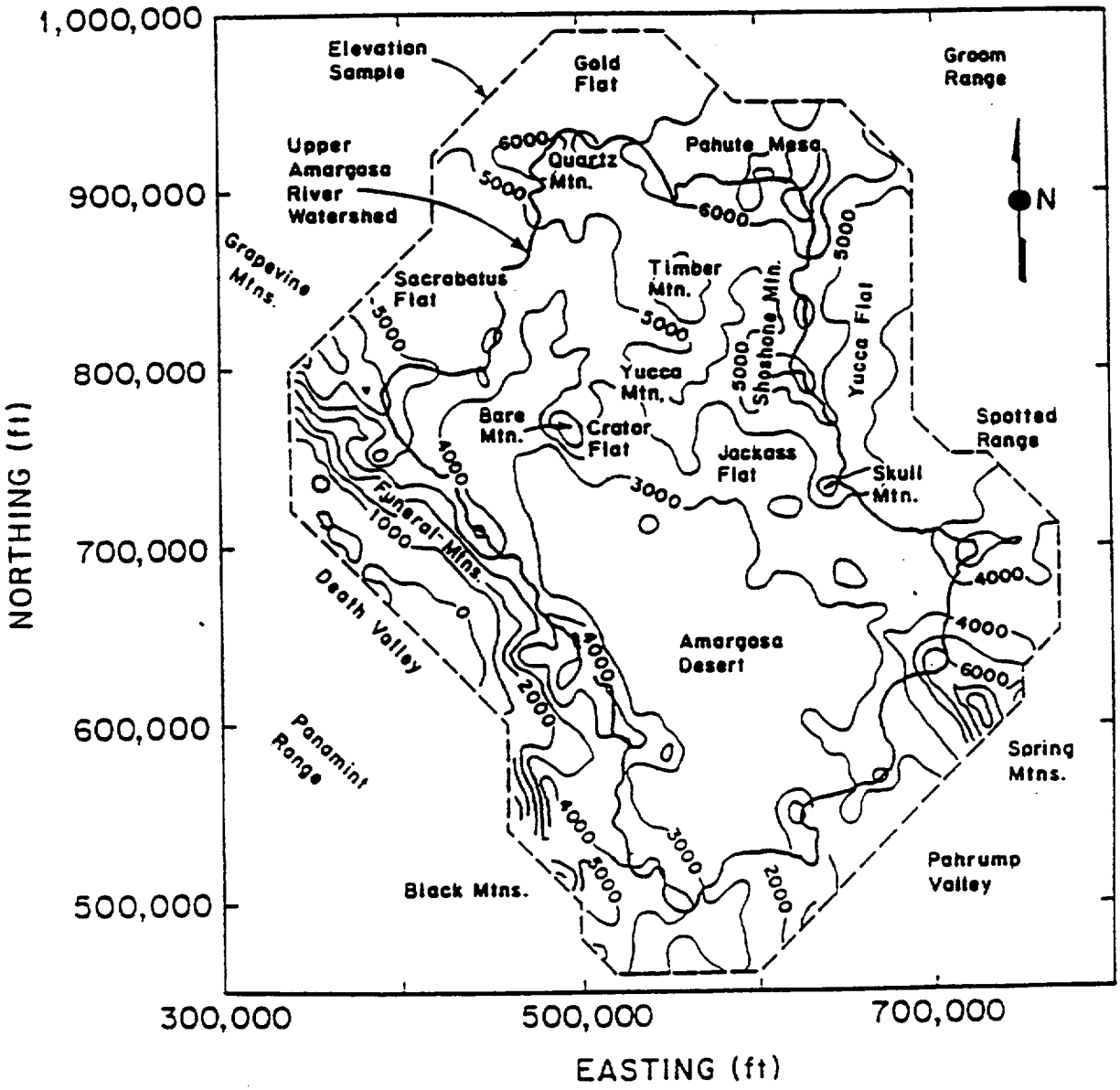

EXPLAIN THAT CONTOURS ARE IN FEET ABOVE SEA LEVEL

FIGURE 2

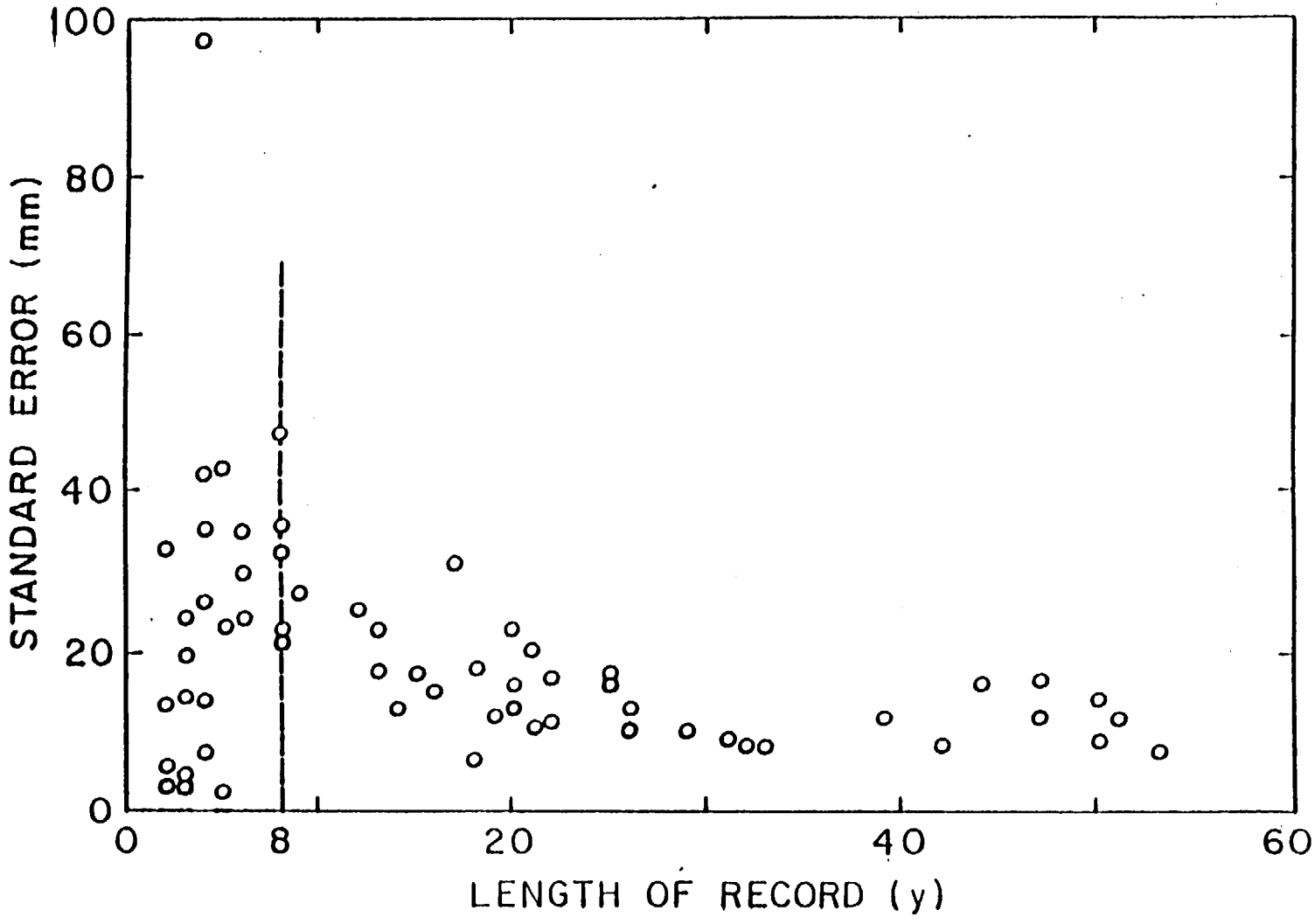
STANDARD ERROR (mm)
100
80
60
40
20
0
0
8
20
40
60
LENGTH OF RECORD (y)

FIGURE 3

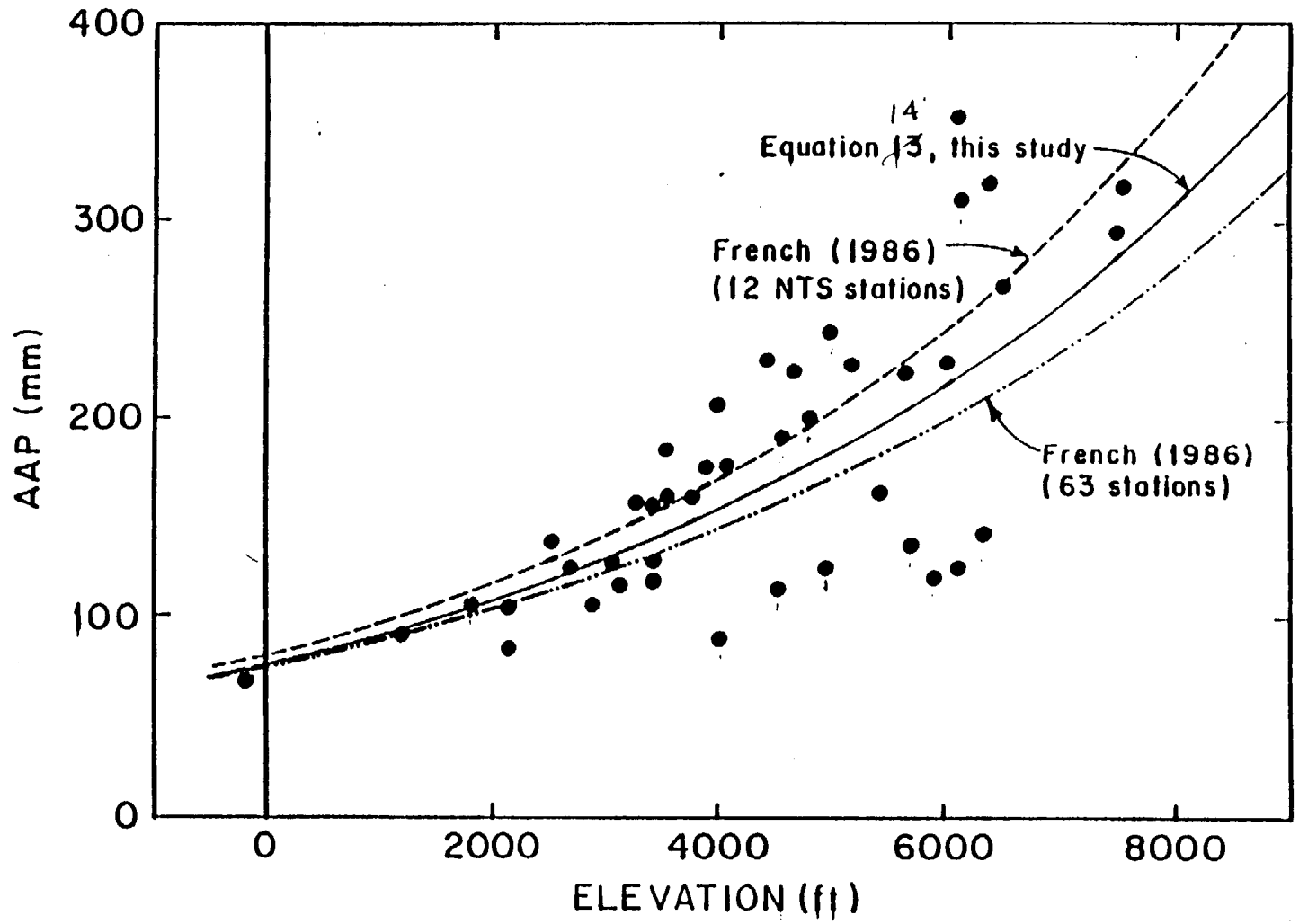
400
300
200
100
0
AAP (mm)
0
2000
4000
6000
8000
ELEVATION (ft)
Equation 14, this study
French (1986)
(12 NTS stations)
French (1986)
(63 stations)

FIGURE 4

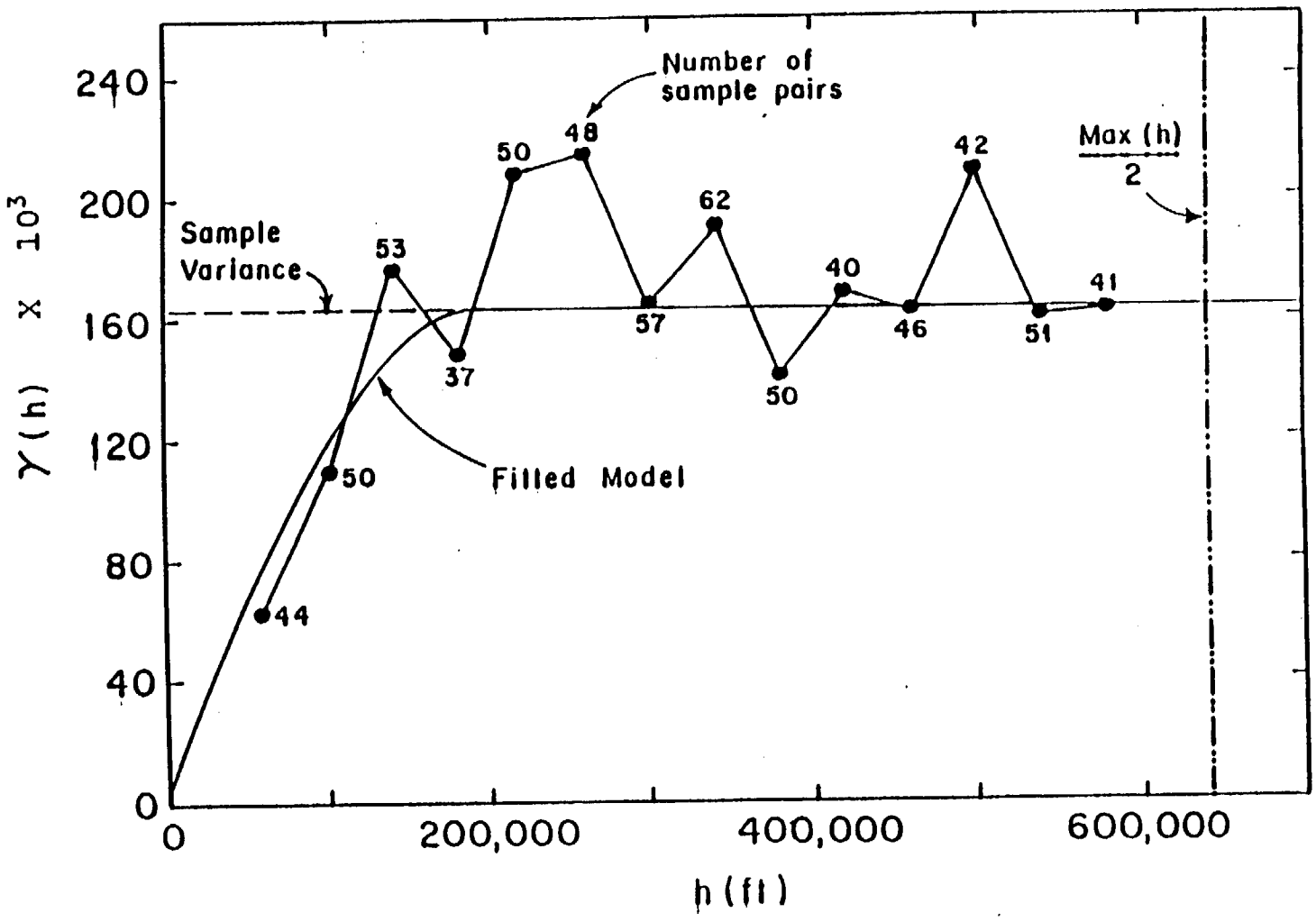
Number of sample pairs
Max (h) / 2
Sample Variance
Filled Model
γ(h) x 10³
h (ft)
0
40
80
120
160
200
240
0
200,000
400,000
600,000
44
50
53
37
50
48
57
62
50
40
46
42
51
41

FIGURE 5

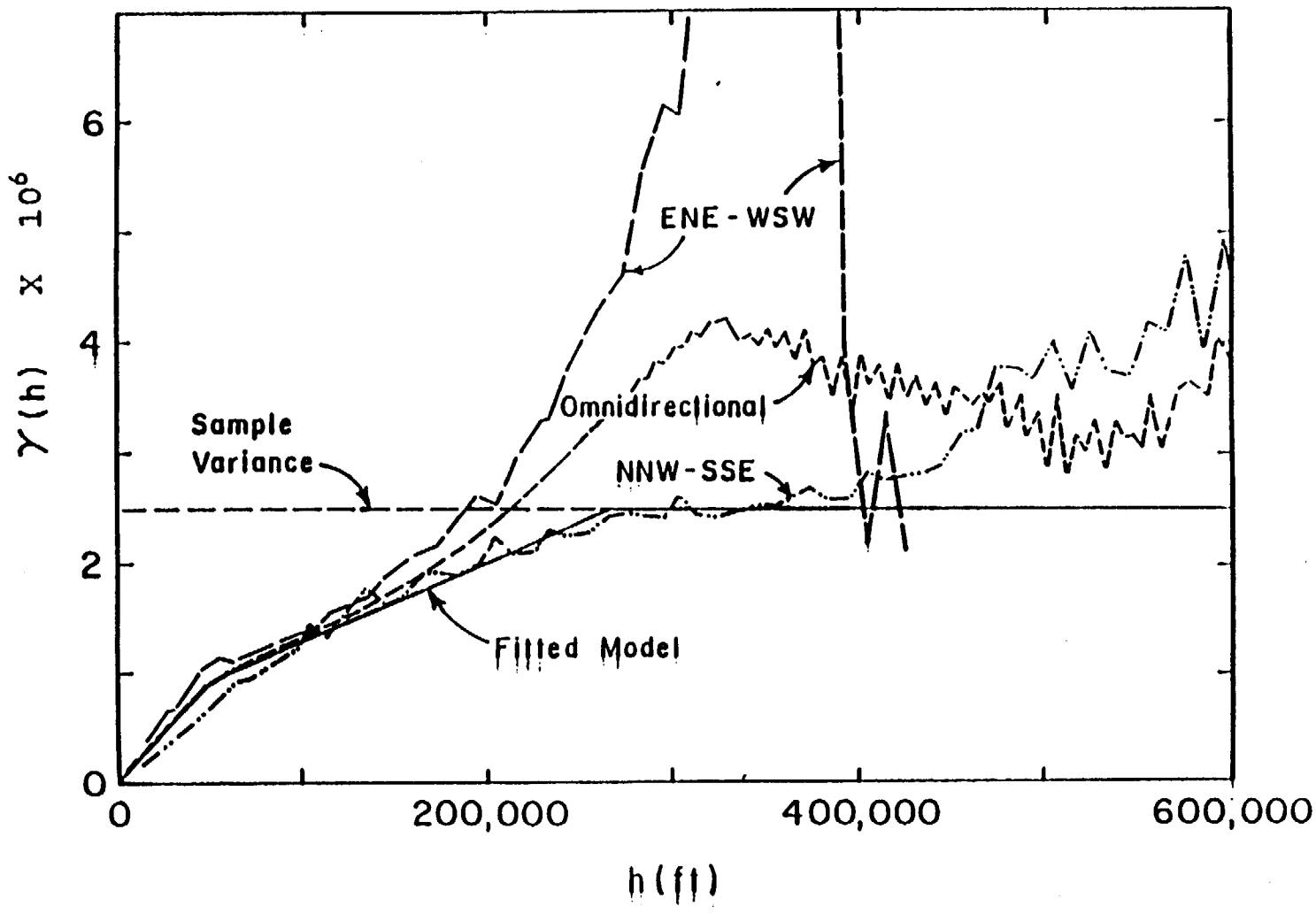
γ(h) x 10^6
6
4
2
0
0
200,000
400,000
600,000
h (ft)
ENE - WSW
Omnidirectional
NNW - SSE
Sample Variance
Fitted Model

FIGURE 6

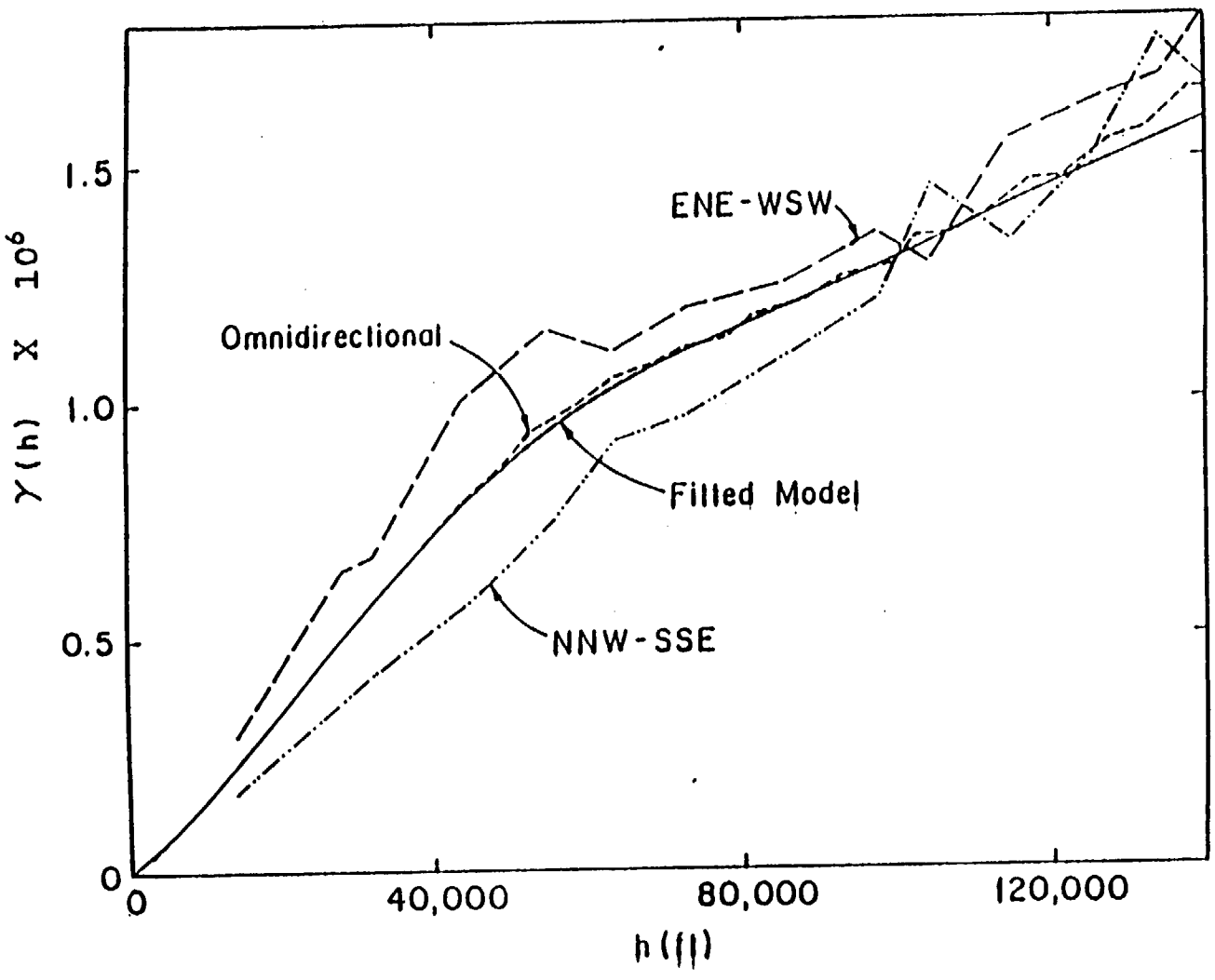
1.5
1.0
0.5
0
γ(h) X 10^6
0
40,000
80,000
120,000
h (ft)
ENE-WSW
Omnidirectional
Fitted Model
NNW-SSE

FIGURE 7

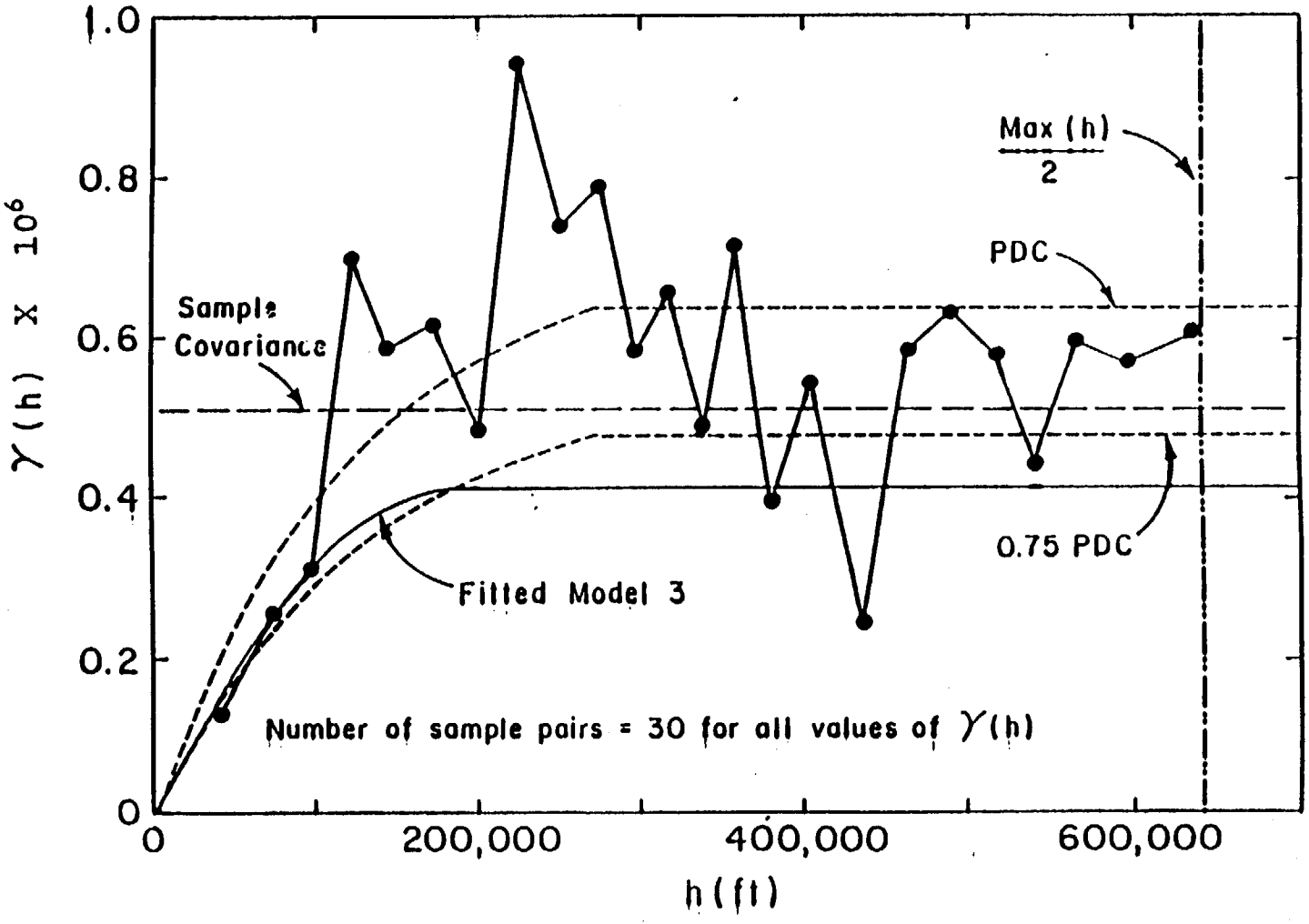
1.0
0.8
0.6
0.4
0.2
0
γ(h) X 10^6
Max (h)
2
PDC
Sample
Covariance
0.75 PDC
Fitted Model 3
Number of sample pairs = 30 for all values of γ(h)
0
200,000
400,000
600,000
h (ft)

FIGURE 8

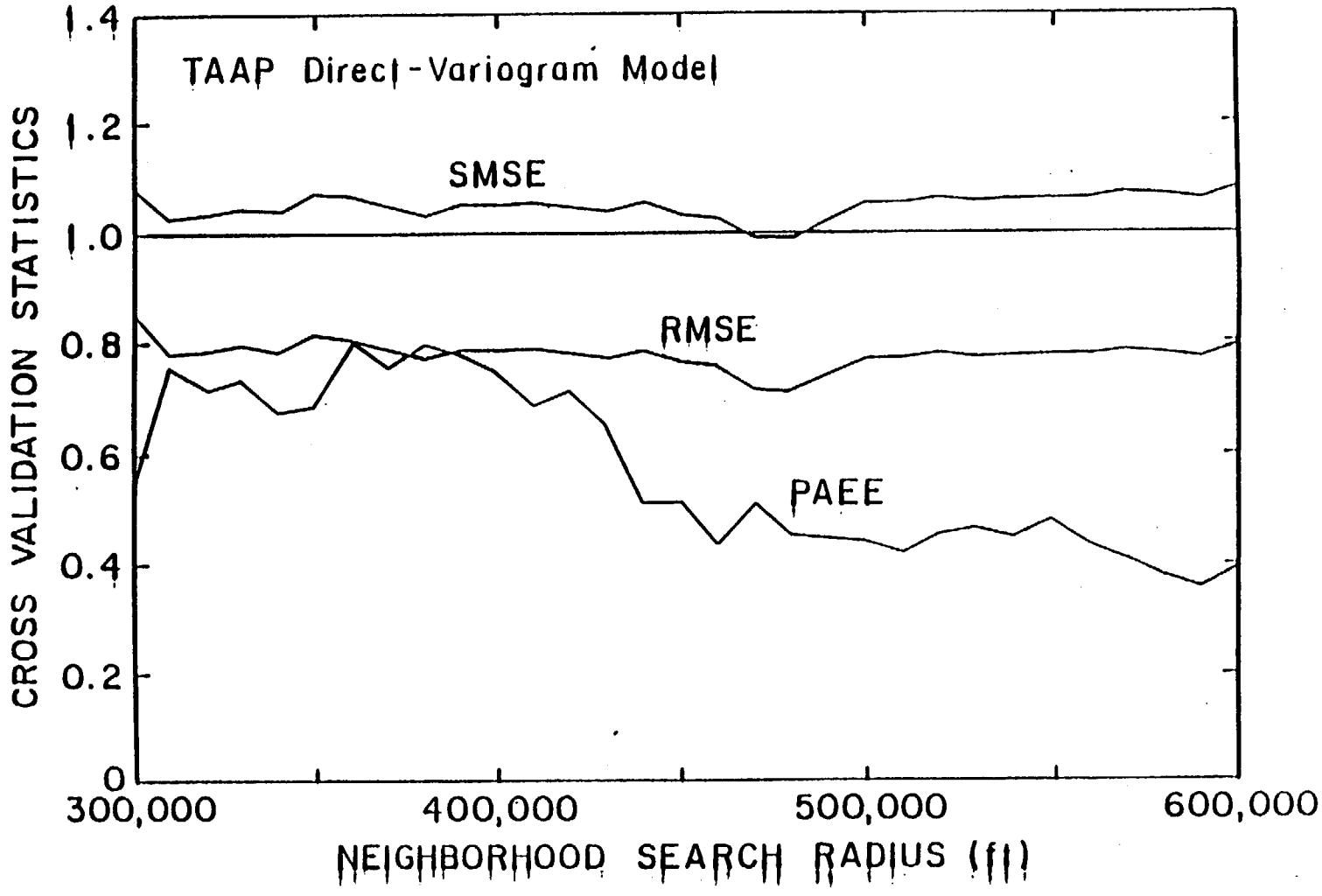
TAAP Direct-Variogram Model
SMSE
RMSE
PAEE
CROSS VALIDATION STATISTICS
1.4
1.2
1.0
0.8
0.6
0.4
0.2
0
300,000
400,000
500,000
600,000
NEIGHBORHOOD SEARCH RADIUS (ft)

FIGURE 9

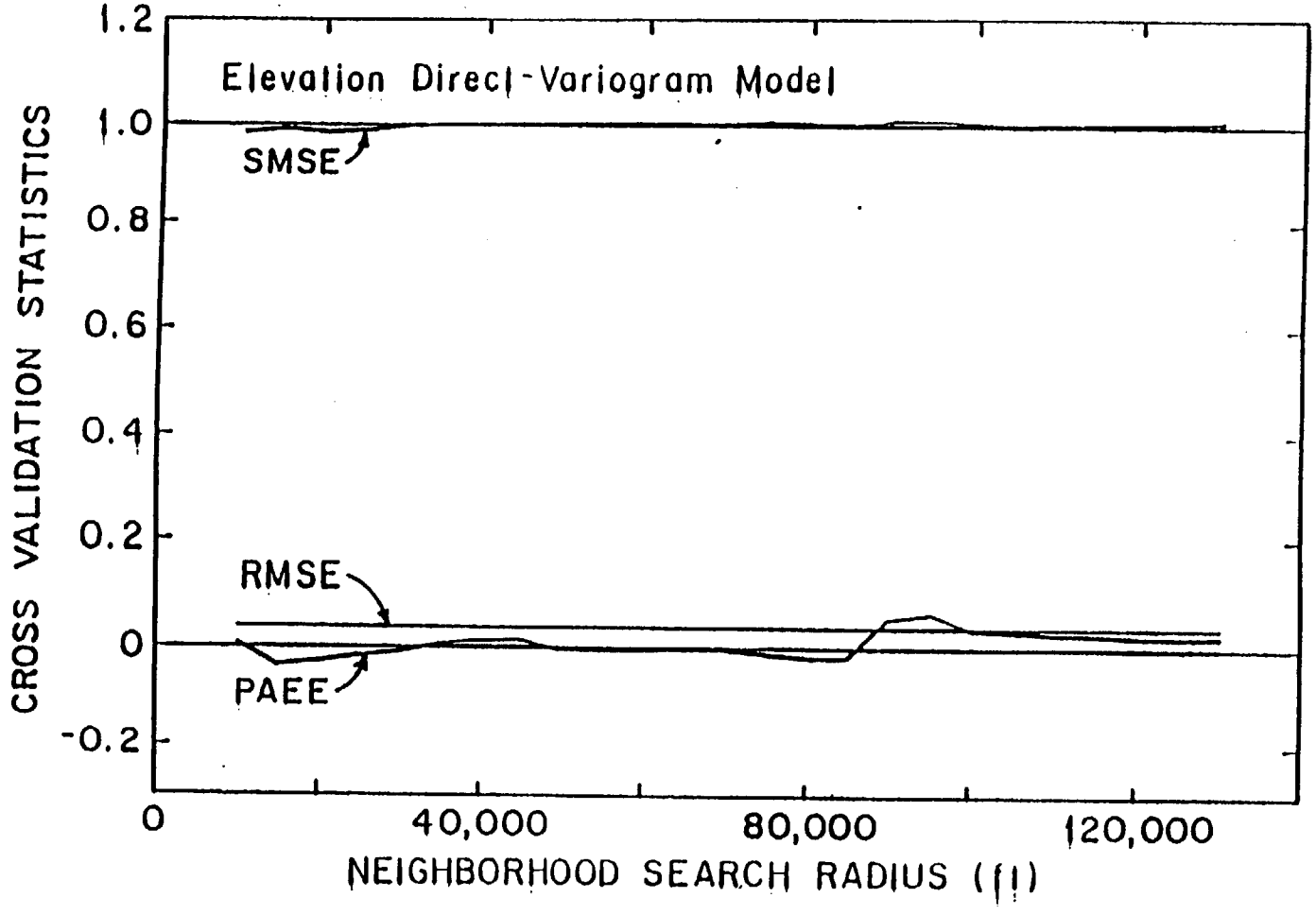
Elevation Direct-Variogram Model
SMSE
RMSE
PAEE
CROSS VALIDATION STATISTICS
1.2
1.0
0.8
0.6
0.4
0.2
0
-0.2
0
40,000
80,000
120,000
NEIGHBORHOOD SEARCH RADIUS (ft)

FIGURE 10

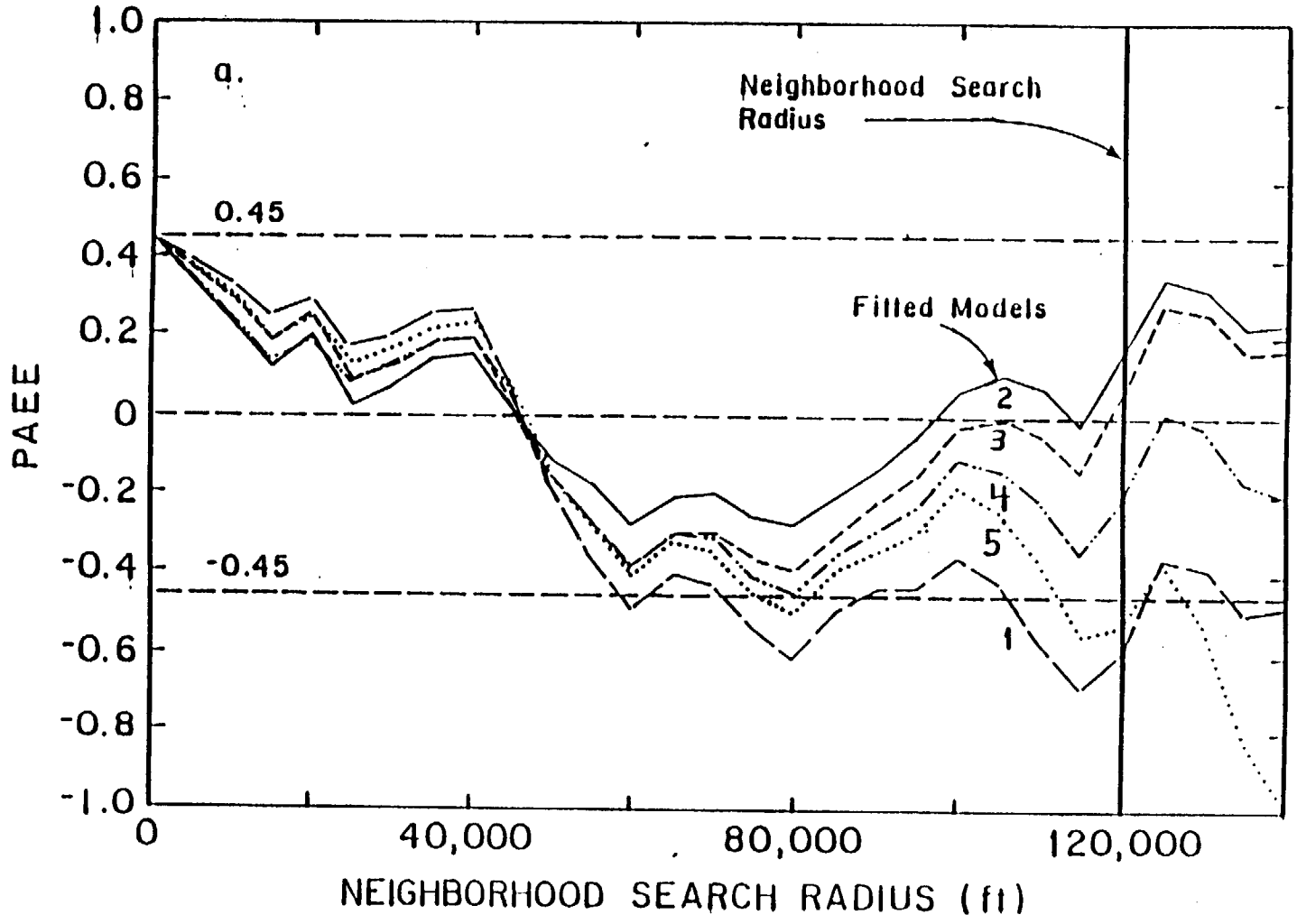
a.
Neighborhood Search Radius
Fitted Models
0.45
-0.45
2
3
4
5
1
PAEE
1.0
0.8
0.6
0.4
0.2
0
-0.2
-0.4
-0.6
-0.8
-1.0
0
40,000
80,000
120,000
NEIGHBORHOOD SEARCH RADIUS (ft)

FIGURE 11a

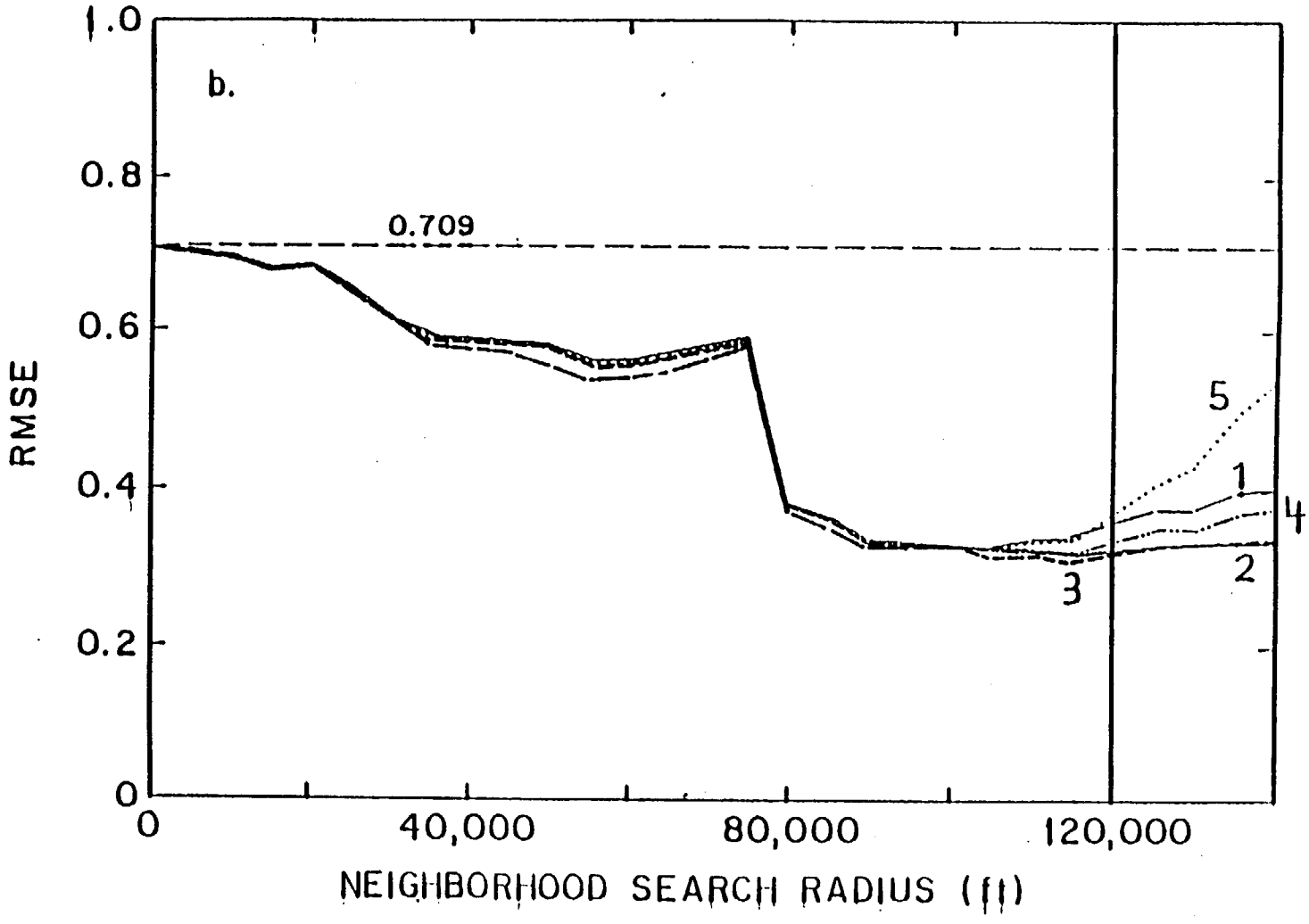
b.
0.709
RMSE
1.0
0.8
0.6
0.4
0.2
0
0
40,000
80,000
120,000
NEIGHBORHOOD SEARCH RADIUS (ft)
5
1
4
2
3

FIGURE 11b

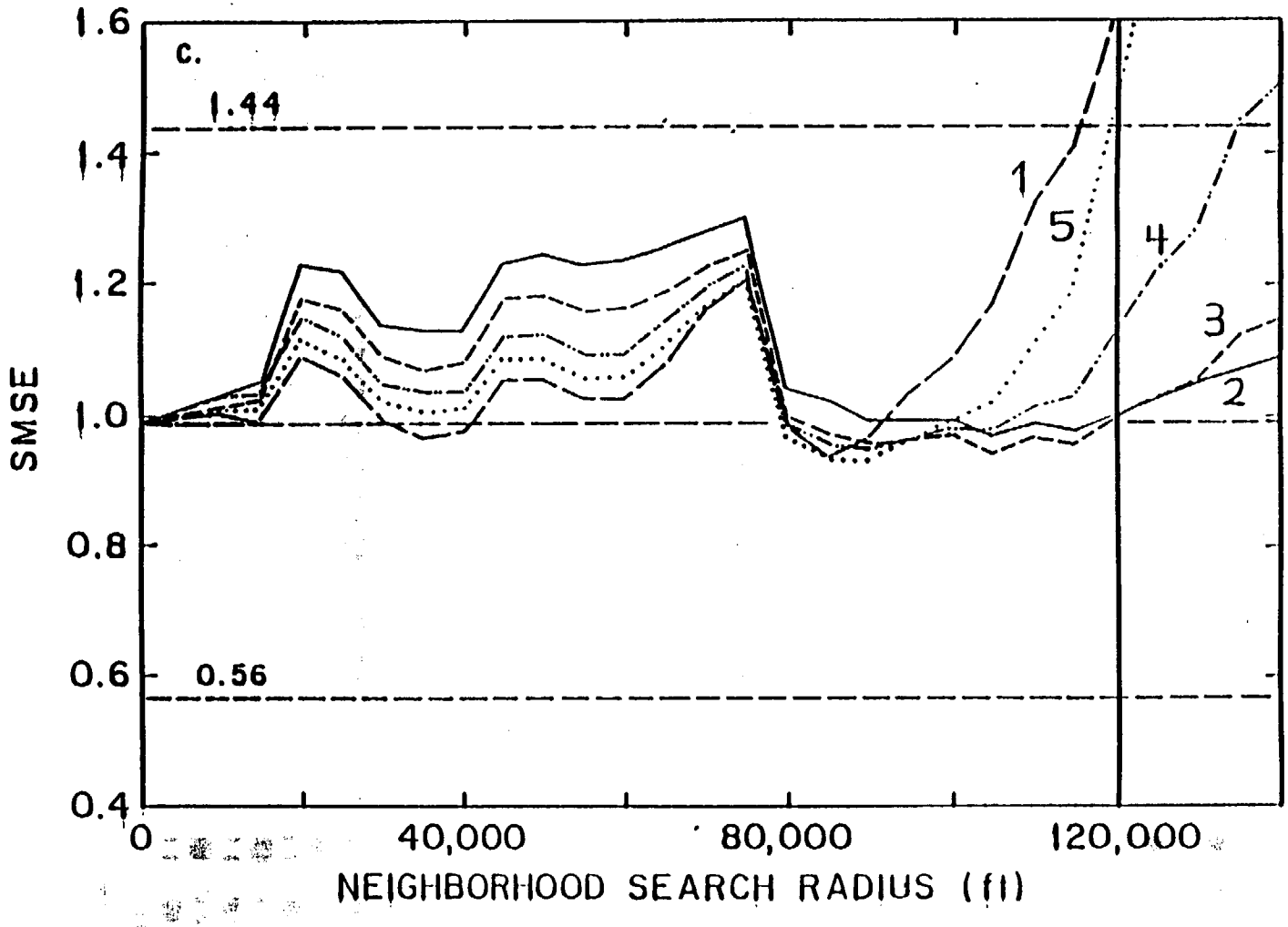
c.
1.44
0.56
1.6
1.4
1.2
1.0
0.8
0.6
0.4
SMSE
0
40,000
80,000
120,000
NEIGHBORHOOD SEARCH RADIUS (ft)
1
5
4
3
2

FIGURE 11c

content. These trends may be due to the fact that the texture-sample population is sand-dominated (Table 3), and clay occupies the interstices between sand grains. An increase in clay content would then be consistent with an increase in fine-soil bulk density, total-soil bulk density, and moisture retention.

Fine-soil bulk-density ($BD_{<2}$) shows a slight inverse relationship with slope position (VP)(r^2 = 0.30, Table 6). Although the linear correlation is poor, a graph of these two variables shows a more consistent and steeper trend in the range of about 35- to 90-percent slope position, and greater variability at the tops and bottoms of slopes (Fig. 8). The graph shows a trend of decreasing fine-soil bulk-density toward the base of the slopes. One possible mechanism causing this trend is the disruption of the soil structure by colluvial processes as the soil mass moves down the slope. The slopes in the study area are steeper in the mid to lower reaches, and the decline in soil bulk density is most rapid in these areas.

Total soil bulk-density is related positively to the volumetric rock-fragment content (r^2 = 0.62, Fig. 9). Total bulk density is a function of rock-fragment content, rock-fragment bulk density and fine-soil bulk density.

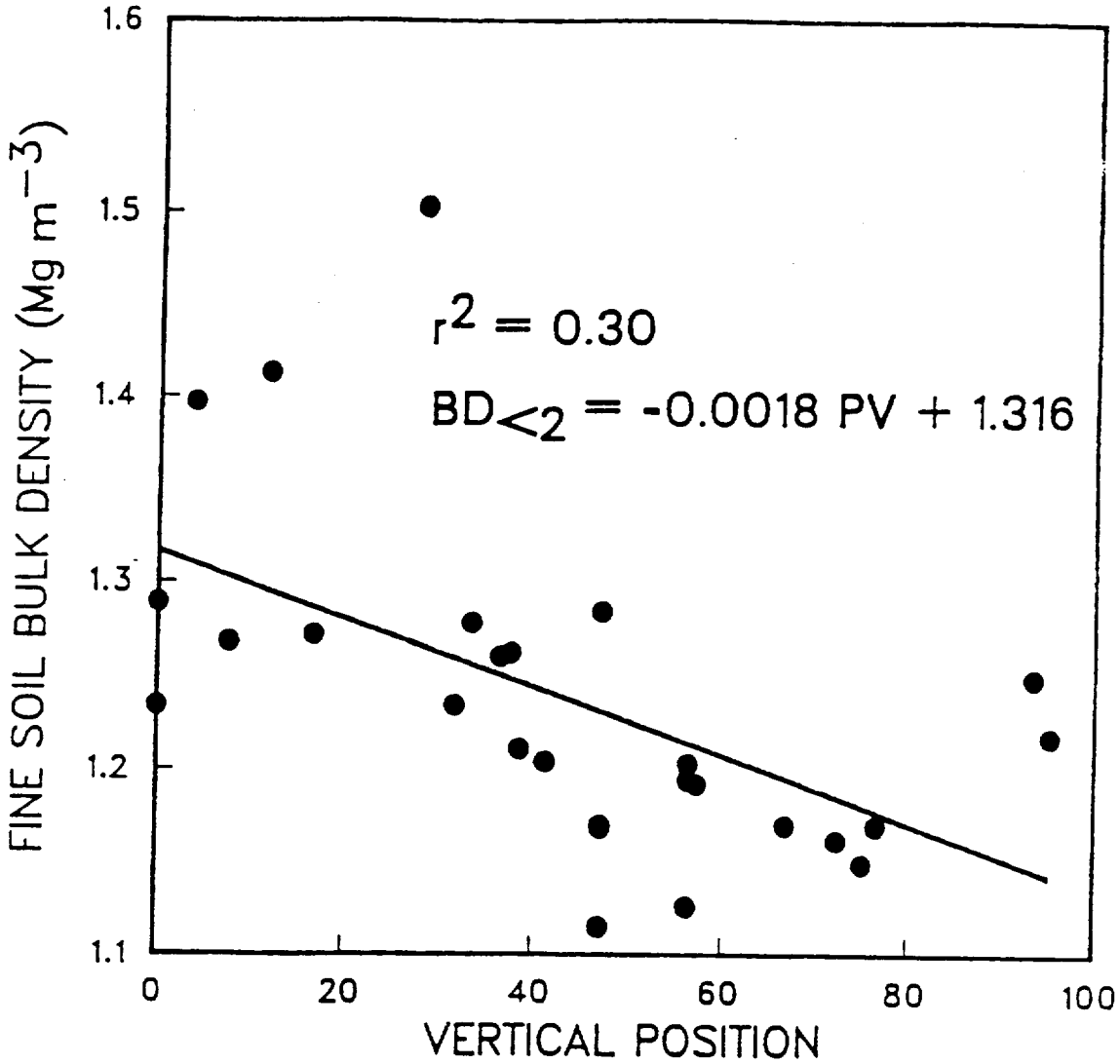

Figure 8. Linear regression of soil bulk density and vertical slope position
(0%: top of slope; 100%: base of slope)

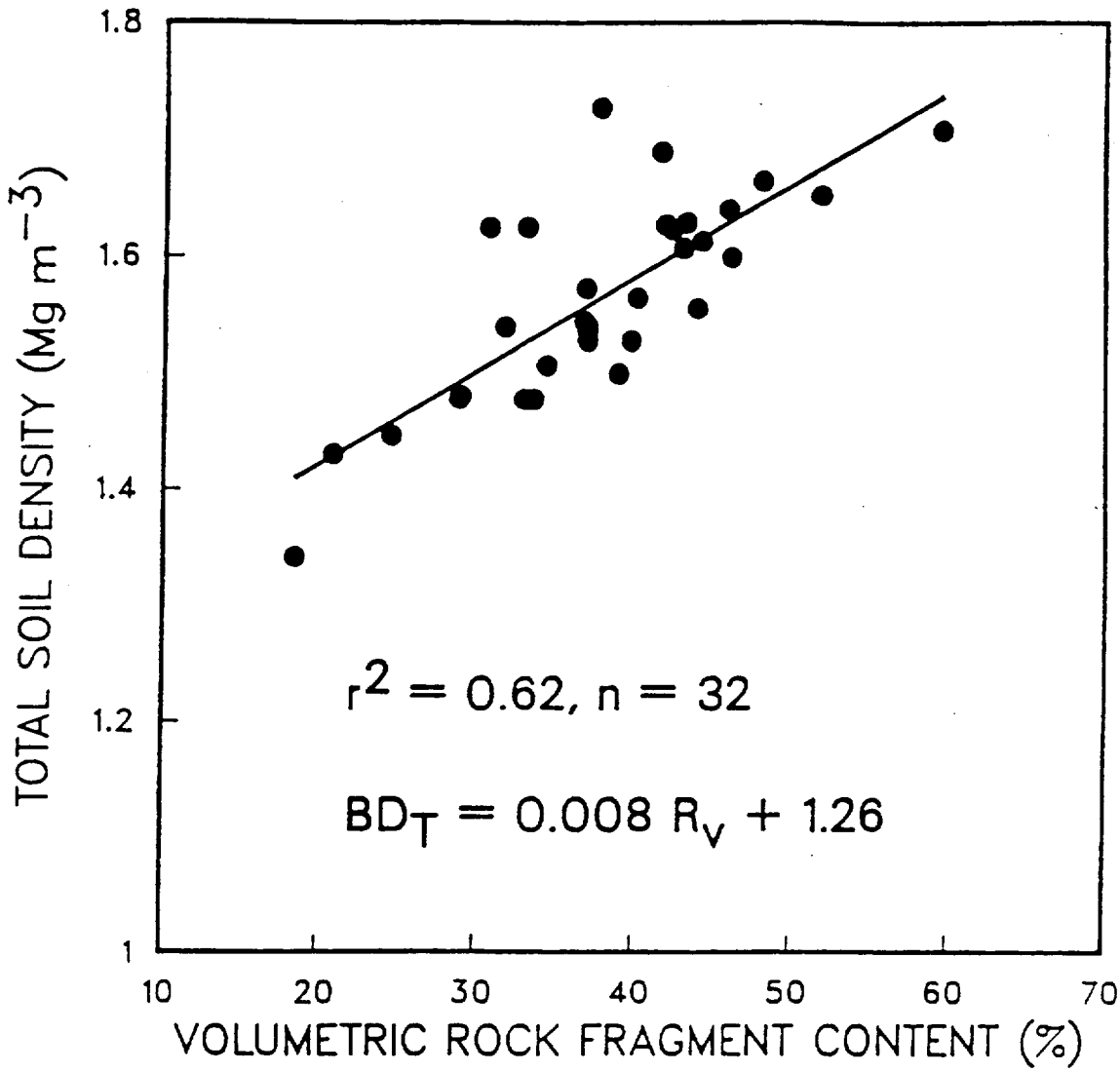

Figure 9. Field total bulk density vs. rock fragment content

Since the coefficients of variation are 22.5-, 6.1-, and 7.0-percent, respectively (Table 3), rock-fragment content affects strongly the total bulk density of the study area soils.

Physical Property Classification

Soil conditions are functions of soil-forming processes, such as weathering and translocation of materials. In contrast, factors of soil formation define the state of the soil system, and include climate, organisms, topography, parent material, and time (Birkeland, 1984). Soil properties can be predicted from a knowledge of the combination of these factors that describe a soil system.

In the Yucca Mountain study area, topography is an important factor of soil formation; topographic slope and aspect determine microclimate (insolation), and geomorphic processes (creep, earth flows, debris flows). Given the arid climate and low organic matter content (Table 3), biologic factors may be less important in soil formation, and vegetation may be more important as an indicator of soil conditions. Parent material provides the initial chemical and physical materials; therefore, bedrock units are used to catagorize data for statistical analyses. The

effects of time are relavent to the classification presented, in that similar geomorphic deposits may be of similar age.

The physical property soil classification described in the following sections is based on the relationships among soil physical properties and geomorphic and geologic conditions. It is assumed that if soil physical properties are distinctly different in large areas of the field site, these differences are due to external controls on soil development, including slope steepness, slope aspect, slope position, bedrock unit, and depositional process.

Geomorphic Groups

Soil physical property data were grouped and tested according to each of the following criteria: preliminary geomorphic map unit (15 map units); bedrock unit (4 zones of the Tiva Canyon Member, Table 2); slope steepness (0% to 10%, 10% to 40%, 40% to 70%, and >70%); slope aspect (north, east, south, west, and none); and slope position (0% to 25%, 25% to 50%, 50% to 75%, and 75% to 100%, top to base of slope). ~~Slope~~ steepness and aspect groupings were divided according to modal analyses of their frequency distributions.

Analysis of variance (AOV) was performed on the data after it was re-grouped according to each of the criteria listed above. AOV tests the null hypothesis that states that group means are equal. AOV can detect significant differences among group means; however, the group means that are different can not be specified. In each instance where the AOV null hypothesis was rejected, the data set was analyzed by the Tukey multiple comparison test to identify non-equal group means. The Tukey multiple comparison procedure (also known as the "honestly significant difference test" and the "wholly significant difference test") uses pairwise comparisons of group means and results from the AOV test to examine the differences between all possible pairs of group means (Zar, 1984). Group means are therefore assigned to populations that are distinct at a chosen level of confidence.

The Tukey analysis of the grouped data sets often yielded ambiguous results by assigning a group mean to more than one distinct population. This indicated that the Tukey test could not be used to determine accurately the statistical sample-population origin. The problem of ambiguous results indicates that the AOV test is more powerful than the multiple comparison test, and that larger statistical sample sizes would tend to result in a multiple

comparison analysis more capable of determining differences among group means (Zar, 1984).

The results of Tukey multiple comparison tests at the 95% confidence level are listed (Table 7). Ambiguous results are not included, and, in each test, no more than three populations (low, medium and high) are identified. For example, in the vertical position grouping listed in the first section of Table 7 (labeled gravel content), gravel content is found to be significantly lower on the top 25 percent of slopes, and significantly higher on the bottom half of slopes. This means that gravel content samples from the top quarter of slopes are assigned to a population with a significantly lower mean gravel content, and gravel content samples from the bottom half of slopes are assigned to a population with a significantly higher mean gravel content. Gravel content data from 25- to 50-percent vertical positions yielded ambiguous results and are not listed. In general, gravel content is higher at lower slope positions where there is a greater source area and more mass movements resulting in a greater gravel content in the soil.

Multiple comparison tests on sand content resulted in no ambiguity when grouped by vertical slope position. Sand content is lower in the 50- to 75-percent slope position

Table 7. Multiple comparison test results

Gravel Content:

Grouped By:	Group	N	Group Means (%) Low	Med.	High
Map Unit	Ridge Crest	6	31.3		
	Ridge Tops	8	32.9		
	Lower NE Facing	8			51.7
	Middle West Scarp	6			52.8
Bedrock Unit	Caprock	7	29.4		
	Upper Lithophysal	15			45.9
Slope Percent	0% to 10%	2	29.5		
	70% to 100%	3			51.2
Vertical Position	0% to 25%	20	37.6		
	75% to 100%	35			47.5
	50% to 75%	27			48.1
Aspect	None	2	29.5		
	West	19			51.3

(continued)

Table 7. (continued)

Sand Content:

Grouped By:	Group	N	Group Means (%) Low	Med.	High
Map Unit	Middle West Scarp	6	53.3		
	Ridge Crest	6			64.9
Slope Percent	40% to 70%	49	58.6		
	10% to 40%	50			62.3
Aspect	West	19	56.9		
	East	30			62.2
	South	18			62.8
Vertical Position	50% to 75%	27	57.2		
	75% to 100%	35			61.4
	25% to 50%	22			61.5
	0% to 25%	20			61.9

(continued)

Table 7. (continued)

Silt Content:

Grouped By:	Group	N	Group Means (%) Low	Med.	High
Map Unit	Ridge Crest	6	17.7		
	Middle West Scarp	6			32.7
Bedrock Unit	Caprock	7	17.5		
	Clinkstone	60			24.8
Slope Percent	10% to 40%	50	22.8		
	40% to 70%	49			27.0
Aspect	South	18	21.8		
	East	30	22.6		
	North	35			25.6
	West	19			30.2
Vertical Position	0% to 25%	20	23.0		
	75% to 100%	35	24.1		
	50% to 75%	27			27.6

Clay Content:

Grouped By:	Group	N	Group Means (%) Low	Med.	High
Map Unit	Lower West Scarp	6	10.0		
	Ridge Tops	8			17.6
	Lower NE Facing	8			18.9

(continued)

Table 7. (continued)

Fine Soil Bulk Density:

Grouped By:	Group	N	Group Means (g/cc) Low	Med.	High
Horizontal Position	50% to 75%	11	1.181		
	0% to 25%	4			1.300
	25% to 50%	8			1.304
Vertical Position	50% to 75%	6	1.175		
	0% to 25%	6			1.312

Fine-Soil Grain-Size Geometric Standard Deviation:

Grouped By:	Group	N	Group Means Low	Med.	High
Map Unit	NE Asp. Earth Flows	7	4.6		
	Ridge Crest	6			6.3
Bedrock Unit	Clinkstone	60	5.4		
	Caprock	7			6.2

(continued)

Table 7. (continued)

Cobble Count:

Grouped By:	Group	N	Group Means (%) Low	Med.	High
Map Unit	Middle West Scarp	6	9.0		
	Ridge Crest	6	10.8		
	Upper North Facing	6	10.9		
	SE Asp. Earth Flows	8	11.0		
	Eastern NE Facing	8	11.6		
	Upper NE Facing	8	11.7		
	Ridge Tops	8	12.1		
	Upper West Scarp	6			26.0

Rock Porosity:

Grouped By:	Group	N	Group Means (%) Low	Med.	High
Map Unit	Middle West Scarp	2	17.6		
	Ridge Crest	2			36.7
Bedrock Unit	Upper Cliff	3	23.2		
	Clinkstone	16	23.7		
	Upper Lithophyseal	5	27.1		
	Caprock	2			36.7
Slope Percent	40% to 70%	13	22.4		
	10% to 40%	19			26.1

(continued)

Table 7. (continued)

Rock Bulk Density:

Grouped By:	Group	N	Group Means (g/cc) Low	Med.	High
Map Unit	Ridge Crest	2	1.60		
	Middle West Scarp	2			2.04
Bedrock Unit	Caprock	2	1.60		
	Upper Lithophysael	5			1.82
	Clinkstone	16			1.89
	Upper Cliff	3			1.91
Slope Percent	10% to 40%	19	1.84		
	40% to 70%	13			1.93

Rock Particle Density:

Grouped By:	Group	N	Group Means (g/cc) Low	Med.	High
Map Unit	Lower NE Facing	2	2.46		
	NE Asp. Earth Flows	2	2.46		
	S-SE Facing	3	2.47		
	Ridge Crest	2			2.53
Bedrock Unit	Upper Cliff	3	2.48		
	Clinkstone	16	2.48		
	Caprock	2			2.53

(continued)

Table 7. (continued)

Nuclear gauge Moisture Content:

Grouped By:	Group	N	Group Means (%) Low	Med.	High
Map Unit	NE Asp. Earth Flows	7	2.05		
	Ridge Tops	8			3.34
Slope Percent	10% to 40%	50	2.6		
	70% to 100%	3	2.6		
	40% to 70%	46	2.7		
	0% to 10%	2			4.7
Aspect	South	18	2.2		
	North	35		2.9	
	None	2			4.7

Sand Cone Moisture Content:

Grouped By:	Group	N	Group Means (%) Low	Med.	High
Aspect	West	4	10.3		
	North	8			15.2

Complete sample data presented in Appendix A

group, however, all group means are close to the mean sand content for the entire data set (60.8-percent).

Many groups that are in the high category for silt content are in the low category for sand content, and, many groups that are in the low category for silt content are in the high category for sand content. The largest contrast in mean silt content is between the ridge crest, where silt may be lost by weathering and illuviation, and the middle west scarp unit, which is a non-illuviated earth-flow deposit (17.7- and 32.2-percent, respectively).

Mean clay content was resolved only among three preliminary map units; ridge tops and lower northeast-facing colluvial slopes have distinctly higher clay content than the lower west scarp pediment. This may indicate that soil on the lower west scarp pediment has been mechanically separated from the clay fraction by sheet wash, and the other two map units have not been illuviated as extensively as the other map unit soils. The high coefficient of variation from the total data set of clay contents (35.4-percent) was not resolved by any of the other groupings in this study.

Slope-position groupings yielded distinct results from fine-soil bulk-density data. With slope position measured in both the vertical and horizontal planes, groups

from the top half of slopes are assigned to a population with a higher mean fine-soil bulk-density than that of the 50- to 75-percent slope position group. The mean fine-soil bulk-density is approximately 10-percent higher for the upper half of slopes, where disruption of soil structure by mass movement is minimal, compared to that of the 50- to 75-percent group, where slopes are steeper and mass movement may be more active. The lowest slope position group (75- to 100-percent) yielded ambiguous results in both groupings. No relationship is found among other groupings of this variable.

The fine-soil geometric standard deviation is found to be higher in the stable, low-slope soils of high position: the ridge crest, which is mostly underlain by the Caprock bedrock unit. In comparison, the northeast aspect earth flows and areas underlain by the Clinkstone bedrock unit are areas of potentially more active mass movement and have lower fine-soil geometric standard deviation. Relatively lower silt content in stable, more developed soils may account for this difference.

Cobble count results show a distinctly higher group mean for the upper west scarp unit compared to seven other preliminary map units. The steep slope, active colluvial process, and source of rock fragments at the ridge crest

favor the higher surficial cobble content of the upper west scarp unit.

Rock porosity and bulk density results are shown for measurements on the 2- to 4.75-mm size fraction. Rock bulk-density results are the inverse of rock-porosity results. Slope appears to be the most important controlling factor, with a greater degree of weathering causing higher rock porosity on shallow slopes. Distinctly high rock porosity group means are shown for areas of shallow slope, and low group means for areas of steep slope. Bedrock lithology may not be an important factor, because lithophysic and non-lithophysic bedrock units have the same soil-rock porosity classification.

Rock particle density shows a pattern similar to that of rock porosity. Slightly higher rock particle density on the ridge crest may be due to weathering and the opening of pores originally sealed in the welded tuff.

Moisture content measured by the sand cone and nuclear gage methods shows slope and aspect controls, with higher mean values on north-facing slopes and slopes of 0- to 10-percent.

Final Map Classification

A final Genesis-Lithology-Qualifier (GLQ) map consisting of four map units was prepared by combining preliminary map units according to similarities based on the GLQ mapping system. The method used was a topical study in which map units were grouped by similar attributes resulting in new groups that have a maximum acceptable heterogeneity with respect to the basic GLQ criteria (Varnes, 1974). Aggregation of the 15 preliminary map units resulted in one residuum unit, one slide unit, one colluvial creep unit, and one colluvial unit including creep and talus deposits (Plate 1).

AOV and Tukey testing of the measured physical property data grouped by the four GLQ map units resulted in a more complete resolution than the test results on the 15 preliminary map units, especially with respect to texture variables. Statistical results are tabulated on Plate 1. In particular, gravel content, silt content, and cobble count data are completely resolved into groups of high or low means at the 95-percent confidence level for the entire study area. The GLQ grouping also resulted in a nearly complete statistical resolution of clay content data, with the residuum unit assigned to a high mean catagory and colluvial units assigned to a low mean category. Slide

(flow) deposits, which occupy a relatively small total area, yielded ambiguous results on mean clay content.

In general, mean gravel content is lower in residuum (mean = 33.18%) than in the other three GLQ units. Mean sand content is higher in the residuum unit than in the colluvial (creep-talus) unit, but the difference is slight (4.99%). Mean silt content is lower in the residuum unit than all others (5.74- to 7.94-%). The colluvial units have lower mean clay contents than the residuum unit (2.95%). Mean fine-soil grain-size geometric standard devation is slightly higher in the residuum unit than the slide and colluvial creep units. Rock fragment (2mm-4.75mm) porosity and bulk density show a direct inverse relationship, with high porosity and low bulk density in the residuum unit, and low porosity and high bulk density in the slide unit. Mean cobble count is higher in the colluvial creep-talus unit than all others.

All of these physical property distinctions among the GLQ map units may affect the hydrologic character and infiltration capacity of the map unit soils, however, the texture of the fine-soil component may be the most important control on hydraulic conductivity. Campbell (1985) presents an equation to estimate the saturated

hydraulic conductivity of a soil using silt and clay contents:

$$K_s = C \exp(-6.9\ m_c - 3.7\ m_s)$$

where $C = 4x10^3$ kg s m^{-3} (best fit from experimental data), and m_c and m_s are clay and silt mass fractions. Using this predictive equation, and the mean silt and clay mass fractions of the fine-soil components of the four GLQ map soils, the hydraulic conductivities listed in Table 8 are found.

Mean silt and clay contents for the colluvial creep-talus deposits yielded the lowest estimated hydraulic conductivity. This unit also shows a statistically low mean sand content (58.4%), a statistically high mean silt content (27.52%), and statistically low mean clay content (14.08) (Plate 1). The highest estimated hydraulic conductivity is found for the residuum unit, which shows a statistically high sand content (63.39%), a statistically low silt content (19.58), and a statistically high clay content (17.03). In the sand-dominated soils at the study area, it may be the relative amount of silt that determines the extent to which the interstices between sand grains are

Table 8. Estimated K-sat for surficial GLQ soils

GLQ Unit	Mean Silt Content (%)	Mean Clay Content (%)	K-sat (cm/hr)
Cgs-c(cr-ta)(0-0.9)	27.52	14.08	1.93
Sgs-c(fl)(0.2.4)	25.58	14.54	2.00
Cgs-c(cr)(0.3-1.2)	25.32	14.08	2.09
Rsg-c(wp)(0-0.6)	19.58	17.03	2.11

filled, and therefore determines the pore-size distribution that ultimately controls hydraulic conductivity.

The estimated hydraulic conductivities, although based on statistically distinct textural values, differ by insignificant amounts. Therefore, based on these estimates, the surficial soils in the study area appear to be hydrologically the same. Any contrasts in the hydrologic character of the GLQ map unit soils would then be dependent on the properties of the lower soil horizons in each map unit.

Each of the four GLQ map unit soils is observed to have different characteristics in the surface and/or subsurface soil horizons. Illuviation is evident in each map unit soil, however, the degree of illuviation may vary. Descriptions of the soil horizons present in the four GLQ

soils are presented in Table 4 and illustrated in Figure 10.

The most distinctive soil profile is that of the slide soil unit. It includes a well-cemented caliche horizon adjacent to bedrock. The caliche could act as a barrier to infiltration, however, the areal extent of this soil unit is small; it may not be important in the overall hydrologic character of Yucca Mountain soils. The soil horizons of the colluvial creep and creep-talus units are similar, except for the statistically higher mean cobble count in the creep-talus unit. The residuum soil unit shows a greater degree of illuviation than all other soil units. This is consistent with the statistically low means in gravel and silt, and statistically high mean sand content. The zone of elluviation (horizon II) may therefore have a lower hydraulic conductivity because of the deposition of fines.

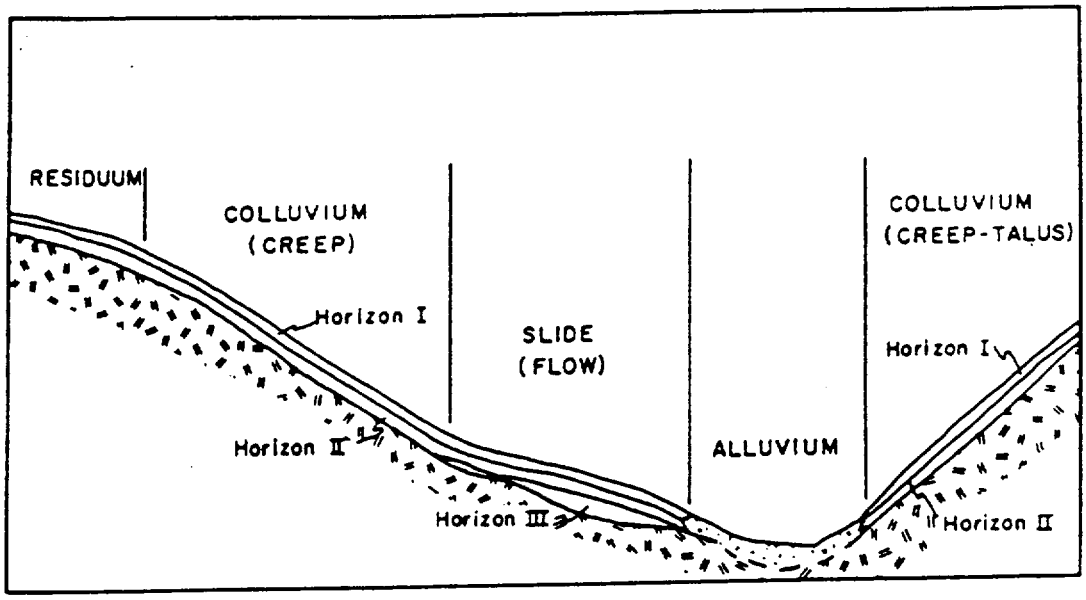

Figure 10. Schematic cross-section of GLQ soils

CONCLUSIONS AND RECOMMENDATIONS

The soils in the study area are skeletal, with the exception of the residual soils on the ridge tops. The fine-soil component of the surficial soils are sand-dominated, and the clay fraction is far more variable than the sand and silt fractions. Surficial soils are gap-graded and include large distribution modes in the gravel and fine-sand ranges.

Illuviation is evident in most areas, and is more pronounced in the residual soils where slopes are gentle. The mean clay fraction of the fine-soil component of illuviated soil horizons is approximately twice that of the surficial soils. A continuous caliche layer was found only in earth-flow deposits at slope bases. Total soil thickness ranges from 0- to 2.4-meters, and averages 74-percent thicker on north-facing slopes as compared to south-aspect slopes.

The correlation analysis of soil and geomorphic variables resulted in generally low correlation coefficients; however, several of the correlations may be important. For example, moisture content is correlated positively with fine-soil bulk density ($r^2 = 0.46$) and clay

content (r^2 = 0.18). In the sand-dominated, fine-soil component of the study area soils, the clay fraction fills interstices formed by larger soil particles, reduces pore sizes, and increases moisture retention. Moisture content, which is a simple measurement, may be related to fine-soil bulk density, clay content, and pore-size distribution.

A relationship is shown, by correlation and AOV with multiple comparison testing, between slope position and fine-soil bulk-density. Fine-soil bulk density generally decreases toward the base of slope; this relationship may be due to the disruption of soil structure by colluvial processes on steep slopes and soil-forming processes on ridge tops where slopes are more shallow.

Analysis of variance and multiple-comparison testing of physical property data shows important patterns in the geomorphic distribution of the measured variables. Testing of the data grouped by aspect shows distinctly higher silt content on south- and east-facing slopes in relation to that on north and west aspect slopes. West-facing slopes show distinctly lower sand content than east- and south-facing slopes. Aspect groupings also show distinctly lower moisture content on south-facing slopes as compared to that of north-facing slopes. Moisture content is also shown to

be lower on steep slopes, including the west-facing scarp. These patterns may be a result of lower weathering rates on the drier south- and west-facing slopes, and/or the possible influence of eolian processes on the distribution of fine sand.

Slope-position groupings resulted in distinct classifications of sand and silt contents and fine-soil bulk density. The 50- to 75-percent slope position is distinctly lower than the top half in fine-soil bulk density and distinctly lower in sand content than all other slope-position ranges. In addition, the 50- to 75-percent slope position is distinctly higher in silt content than all other slope positions. These relationships are consistant with higher fine-soil bulk density in well-graded soils.

The percent slope grouping shows that the 10- to 40-percent slope sample group has distinctly higher sand content, lower silt content, and higher rock porosity. Although moisture contents are not distinct between these sample groups, the total amount of weathering may be greater for the 10- to 40-percent group because of residence time and moisture differences during times of greater precipitation.

Results from bedrock-unit groups may reflect the effects of slope position. Bedrock unit contacts generally follow topographic contours, and the lithologies of the bedrock units are not greatly different.

Preliminary map-unit groups yielded distinct results on more physical property variables than any other grouping, however, the distinctions were usually resolved on only a few groups, and much of the study area is classified in the ambiguous catagory. Upon the aggregation of the 15 preliminary map units into four groups of similar genesis, retesting resulted in nearly complete resolution of textural variables. Because it has been shown that texture is the most important physical property related to hydrologic characteristics, the final GLQ classification may be a valid hydrologic classification of surficial soils.

An estimation of saturated hydraulic conductivity based on mean silt and clay contents of the four GLQ units shows a range of 1.93- to 2.11-cm/hr. The illuviated residuum map unit has the highest estimated hydraulic conductivity, and the colluvial creep-talus unit has the lowest estimate. These estimates are not greatly different, however, and the effects of the physical properties of the surficial soils on the infiltration

capacity of the total soil profile may be small in comparison to anticedent moisture conditions and the properties of subsurface soil horizons.

A GLQ classification of the soils in the study area resulted in four classes: a residuum (weathering profile) unit; colluvial (creep) unit; colluvial (creep-talus) unit; and a slide (flow) unit. With the grouping of surficial textural data according to the final GLQ map units, mean sand, silt, and clay content are shown to be statistically distinct in nearly every comparison among the map unit data groups. Despite the textural distinctions of surficial soils among the GLQ map units, estimated hydraulic conductivities of these soils are nearly identical; therefore, any hydrologic distinctions among the four GLQ soils should be controlled by the soil subhorizons. In each GLQ map unit, a characteristic pattern of soil horizons is observed. Because of the statistically distinct textural data and characteristic horizonation of each map unit soil, the GLQ map may be a valid hydrologic classification of Yucca Mountain soils.

The results of this study should be useful in future hydrologic studies at Yucca Mountain for the purposes of minimizing the number of field-scale infiltration experiments necessary for hydrologic characterization.

Infiltration plots could be assigned to each of the four GLQ map units, and the results combined with soil physical property data by correlation or cokriging to enhance and extend the results of "wet" tests. Other soil mapping methods, such as the Soil Conservation Service soil survey methods, should be evaluated and compared to the GLQ method in the context of the geomorphic conditions at Yucca Mountain and the objectives of the Nuclear Hydrology Program.

REFERENCES CITED

American Society for Testing and Materials, 1984, Density of soil and soil-aggregate in place by nuclear methods (shallow depth): ASTM D 2922-81, Annual Book of ASTM Standards, v. 04.08. Philadelphia, PA.

_____, 1984, Density of soil in place by the sand cone method: ASTM D 1556-82, Annual Book of ASTM Standards, v. 04.08. Philadelphia, PA.

_____, 1984, Moisture content of soil and soil-aggregate in place by nuclear methods (shallow depth): ASTM D 3017-78, Annual Book of ASTM Standards, v. 04.08. Philadelphia, PA.

_____, 1984, Standard test method for specific gravity of soils: ASTM D 854-83, Annual Book of ASTM Standards, v. 04.08. Philadelphia, PA.

_____, 1984, Standard test methods for absorption and bulk specific gravity of natural building stone: ASTM C 97-83, Annual Book of ASTM Standards, v. 04.08. Philadelphia, PA.

Arya, L. M., and Paris, J. F., 1981, A physicoempirical model to predict the soil moisture characteristic from particle-size distribution and bulk density data: Soil Sci. Soc. Am. J., v. 45, p. 1023-1030.

Avery, B. W., and Bascomb C. L., (ed.), 1974, Soil survey laboratory methods: Soil Surv. Tech. Monogr. no. 6. Harpenden Press, London.

Birkeland, P. W., 1984, Soils and geomorphology: Oxford University Press, Inc. 372 p.

Brakensiek, D. L., Engleman, R. L., and Rawls, W. J., 1981, Variation within texture classes of soil water parameters: Trans. ASAE, v. 24, p. 335-339.

Brakensiek, D.L., Rawls, W. J., and Stephenson, G.R., 1985, Determining the saturated hydraulic conductivity of a soil containing rock fragments: Soil Sci. Soc. Amer. Journal, v. 50, p. 834-835.

Campbell, G.S., 1985, Soil Physics With Basic - Transport Models for Soil-Plant Systems: Elsevier, New York, NY. 150 p.

Childs, E. C., 1940, The use of soil moisture characteristics in soil studies: Soil Science, v. 50, p. 239-252.

Childs, E. C., 1969, An introduction to the physical basis of soil water phenomena: John Wiley & Sons Ltd, New York, NY, 493 p.

Cosby, B. J., Hornberger, G. M., Clapp, R. B., and Ginn, T. R., 1984, A statistical exploration of the relationships of soil moisture characteristics to the physical properties of soils: Water Resour. Res., v. 20, no. 6, p. 682-690.

Dunn, A.J. and Mehuys, G. R., 1984, Relationship between gravel content of soils and saturated hydraulic conductivity in laboratory tests: p. 55-64 in Soil Sci. Soc. Amer. Spec. Publ. No. 13, Erosion and Productivity of Soils Containing Rock Fragments, Nichols, J. D., Brown, P. L., and Grant, W. J., (eds.)

Flint, A.L. and Childs, S., 1984a, Development and calibration of an irregular hole bulk density sampler, Soil Sci. Soc. Amer. J., v. 48, p.374-378.

Flint, A.L. and Childs, S., 1984b, Physical properties of rock fragments and their effect on available water in skeletal soils: p.91-103 in Soil Sci. Soc. Amer. Spec. Publ. No. 13, Erosion and Productivity of Soils Containing Rock Fragments, Nichols, J. D., Brown, P.L., and Grant, W. J. (eds.).

Gosh, R. K., 1980, Estimation of soil-moisture characteristics from mechanical properties of soils: Soil Science, v 130, no. 2, p. 60-63.

Gregory, S, 1978, Statistical Methods and the Geographer: Longman, New York, NY, 240 p.

Grim, R. E., 1953, Clay mineralogy: McGraw-Hill, New York, NY.

Gupta, S. C., and Larson, W. E., 1979, Estimating soil water retention characteristics from particle size distribution, organic matter percent, and bulk density: Water Resour. Res., v. 15, no. 6, p. 1633-1635.

Hammermeister, D. P., and Flint, A. L., 1987, Characterization of unsaturated zone infiltration: USGS Scientific Investigation Plan, USGS-SIP-3342G-01, RO. U.S. Geological Survey, Denver, CO. 87 p.

Hillel, D., 1982, Introduction to soil physics: Academic Press, New York, NY. 364 p.

Keaton, J. R., 1984, Genesis-Lithology-Qualifier (GLQ) system of engineering geology mapping symbols: Bulletin of the Association of Engineering Geologists, v. XXI, no. 3, p. 355-364.

McCuen, R. H., Rawls, W. J., and Brakensiek, D. L., 1981, Statistical analysis of the Brooks-Corey and the Green-Ampt parameters across soil textures: Water Resour. Res., v. 17, p. 1005-1013.

Montazer, P., and Wilson, W.E., 1984, Conceptual Hydrologic Model of Flow in the Unsaturated Zone, Yucca Mountain, Nevada: U.S. Geological Survey Water Resources Investigations Report 84-4345, U.S. GPO, Region No. 8 Denver, CO, 55 p.

P-STAT, Inc., 1986, P-STAT data management and statistical software, version 1.24, large (750 variable) size. P-STAT, Inc., Princeton, NJ.

Rawls, W. J., and Brakensiek, D. L., 1982, Estimating soil water retention from soil properties: J. Irrigat. Drain. Div. Am. Soc. Civ. Eng., v. 108, p 166-171.

Scott, R. B., and Bonk, J., 1984, Preliminary geologic map of Yucca Mountain with geologic sections, Nye County, Nevada: U.S. Geological Survey Open-File Report 84-494, scale 1:12,000.

Shirazi, M. A., and Boersma, L., A unifying analysis of soil texture: Soil Sci. Soc. Am. J., v. 48, p. 142-147.

U. S. Department of Agriculture, 1975, Soil taxonomy: USDA Handbook No. 436. U. S. Govt. Printing Office, Washington, D. C. 754 p.

U.S. Department of Agriculture Soil Conservation Service, 1986, Advance copy of pedologic map and report including part of Yucca Mountain. U.S. Department of Agriculture Soil Conservation Service, P.O. Box 4850, Reno, Nevada 89505.

U. S. Department of Agriculture Soil Conservation Service, 1981, Soil Survey Manual, 430-V-SSM: U. S. Govt. Printing Office, Washington, D. C.

Varnes, D. J., 1974, The logic of geological maps, with reference to their interpretation and use for engineering purposes. USGS Professional Paper 837, U.S. Govt. Printing Office, Washington, D.C., 48 pp.

Yates, S. R., and Warrick, A. W., 1987, Estimating soil water content using cokriging: Soil Sci. Soc. Am. J. v. 51, p. 23-30.

Zar, J. H., 1984, Biostatistical analysis: Second edition. Prentice-Hall, Inc., Englewood Cliffs, New Jersey, 718 p.

APPENDIX A

SURFICIAL SOIL DATA

EXPLANATION OF SAMPLE LABELS

Sample Label	Explanation
GLQ UNIT	Genesis-Lithology-Qualifier map unit (see Plate 1).
SAMPLE NUMBER	Sample location number (see Plate 2).
STATION	Trench sample station: C-5 = trench C, station 5 (see Plate 2).
BEDROCK UNIT	cks = Clinkstone, cul = Upper Lithophysal cuc = Upper Cliff, ccr = Caprock

EXPLANATION OF VARIABLE ABBREVIATIONS

Abbreviation	Units	Explanation
COBBLE COUNT	(%)	Percent soil surface >75 mm diameter rock.
GRAVEL	(%)	Gravimetric gravel content of <75 mm soil.
SAND	(%)	Gravimetric sand content of <2 mm soil.
SILT	(%)	Gravimetric silt content of <2 mm soil.
CLAY	(%)	Gravimetric clay content of <2 mm soil.
LT.2MM.GMGS	(mm)	Geometric mean grain size of <2 mm soil.
LT.2MM.GSTDEV		Geometric standard deviation of <2 mm soil.
ROCK.PART.DENS	(g/cc)	Rock particle density 2-4.75mm dia.
ROCK POROSITY	(%)	Rock porosity 2-4.75mm dia.
ROCK BULK DENSITY	(g/cc)	Rock bulk density 2-4.75mm dia.
BC.TOT.BD	(g/cc)	Dry bulk density of bead-cone sample.
GT.2MM.VF	(%)	Volumetric content >2mm dia., (bead-cone).
LT.2MM.BD	(g/cc)	Fine soil (<2 mm) bulk density (bead-cone).
NUC.WET.BD	(g/cc)	Nuclear gauge measured wet bulk density.
NUC.DRY.BD	(g/cc)	Nuclear gauge measured dry bulk density.
NUC.MOIST.PCT	(%)	Mass water content (nuclear gauge)
SC.MOIST.PCT	(%)	Sand-cone sample gravimetric water content.
SC.WET.BD	(g/cc)	Sand-cone sample wet bulk density.
SC.DRY.BD	(g/cc)	Sand-cone sample dry bulk density.
OM	(%)	Organic matter gravimetric content.
ASPECT		Soil surface aspect group
SLOPE.PERCENT	(%)	Soil surface slope.
VERT.POSITION	(%)	Slope position, measured in vertical.
HORIZ.POSITION	(%)	Slope position, measured in horizontal.

---------- GLQ UNIT: COLLUV..M (CREEP) ----------

GLQ UNIT	SAMPLE NUMBER	STATION	COBBLE COUNT	GRAVEL	SAND	SILT
COLLUV.(CREEP)	-	C-5	-	-	-	-
COLLUV.(CREEP)	-	D-6	-	-	-	-
COLLUV.(CREEP)	-	D-3	-	-	-	-
COLLUV.(CREEP)	-	A-8	-	-	-	-
COLLUV.(CREEP)	-	A-1	-	-	-	-
COLLUV.(CREEP)	-	A-3	-	-	-	-
COLLUV.(CREEP)	-	A-4	-	-	-	-
COLLUV.(CREEP)	-	A-6	-	-	-	-
COLLUV.(CREEP)	-	A-7	-	-	-	-
COLLUV.(CREEP)	3	-	18.75	48.08	59.58	23.28
COLLUV.(CREEP)	6	-	9.50	41.93	62.06	23.34
COLLUV.(CREEP)	10	010	12.25	43.98	58.71	29.36
COLLUV.(CREEP)	12	-	15.00	51.44	61.88	24.78
COLLUV.(CREEP)	26	-	6.75	41.95	60.59	24.59
COLLUV.(CREEP)	27	-	14.50	34.59	59.74	26.03
COLLUV.(CREEP)	28	-	9.50	47.85	61.53	22.94
COLLUV.(CREEP)	29	029	20.25	40.42	70.16	23.14
COLLUV.(CREEP)	30	030	16.00	36.95	69.78	18.32
COLLUV.(CREEP)	31	031	1.50	45.53	56.31	29.21
COLLUV.(CREEP)	32	032	12.00	43.13	53.58	30.25
COLLUV.(CREEP)	33	-	10.00	54.41	58.77	28.07
COLLUV.(CREEP)	34	-	14.75	63.37	60.37	27.89
COLLUV.(CREEP)	35	-	3.75	42.18	60.41	26.33
COLLUV.(CREEP)	36	-	10.75	46.54	59.58	24.70
COLLUV.(CREEP)	37	-	7.25	38.81	62.51	26.78
COLLUV.(CREEP)	38	-	14.00	46.48	64.44	23.47
COLLUV.(CREEP)	39	-	18.50	40.91	57.65	26.18
COLLUV.(CREEP)	40	-	12.75	52.47	61.12	23.94
COLLUV.(CREEP)	44	-	21.00	51.68	56.25	29.06
COLLUV.(CREEP)	64	-	15.25	48.88	61.80	21.77
COLLUV.(CREEP)	65	065	13.25	51.05	61.80	24.11
COLLUV.(CREEP)	66	066	26.25	48.44	63.00	21.48
COLLUV.(CREEP)	67	067	28.75	46.82	59.79	24.43
COLLUV.(CREEP)	91	-	12.00	46.79	55.89	29.14
COLLUV.(CREEP)	94	094	14.50	50.07	57.92	27.45
COLLUV.(CREEP)	95	-	8.50	46.45	50.24	30.85
COLLUV.(CREEP)	100	-	14.75	49.10	68.65	21.73
COLLUV.(CREEP)	103	-	10.00	33.62	63.34	19.48
COLLUV.(CREEP)	104	-	24.25	62.87	60.65	27.50

GLQ UNIT	SAMPLE NUMBER	STATION	CLAY	LT.2MM GMGS	LT.2MM GSTDEV	ROCK PART DENS
COLLUV.(CREEP)	-	C-5	-	-	-	-
COLLUV.(CREEP)	-	D-6	-	-	-	-
COLLUV.(CREEP)	-	D-3	-	-	-	-
COLLUV.(CREEP)	-	A-8	-	-	-	-
COLLUV.(CREEP)	-	A-1	-	-	-	-
COLLUV.(CREEP)	-	A-3	-	-	-	-
COLLUV.(CREEP)	-	A-4	-	-	-	-
COLLUV.(CREEP)	-	A-6	-	-	-	-
COLLUV.(CREEP)	-	A-7	-	-	-	-
COLLUV.(CREEP)	3	-	17.14	0.05	5.29	2.45
COLLUV.(CREEP)	6	-	14.60	0.05	5.56	-
COLLUV.(CREEP)	10	010	11.93	0.05	4.30	-
COLLUV.(CREEP)	12	-	13.34	0.05	4.81	-
COLLUV.(CREEP)	26	-	14.81	0.05	5.01	-
COLLUV.(CREEP)	27	-	14.22	0.05	4.89	-
COLLUV.(CREEP)	28	-	15.53	0.05	5.59	-
COLLUV.(CREEP)	29	029	6.71	0.08	4.44	2.53
COLLUV.(CREEP)	30	030	11.90	0.07	5.41	2.51
COLLUV.(CREEP)	31	031	14.48	0.05	4.69	-
COLLUV.(CREEP)	32	032	16.18	0.04	4.98	-
COLLUV.(CREEP)	33	-	13.16	0.05	4.96	-
COLLUV.(CREEP)	34	-	11.74	0.06	5.77	-
COLLUV.(CREEP)	35	-	13.26	0.05	4.57	2.48
COLLUV.(CREEP)	36	-	15.71	0.05	5.79	2.50
COLLUV.(CREEP)	37	-	10.71	0.06	4.76	-
COLLUV.(CREEP)	38	-	12.09	0.06	5.04	2.48
COLLUV.(CREEP)	39	-	16.17	0.05	5.77	-
COLLUV.(CREEP)	40	-	14.94	0.06	5.82	-
COLLUV.(CREEP)	44	-	14.69	0.05	5.34	2.48
COLLUV.(CREEP)	64	-	16.43	0.05	5.83	-
COLLUV.(CREEP)	65	065	14.09	0.06	5.35	2.49
COLLUV.(CREEP)	66	066	15.52	0.06	5.83	-
COLLUV.(CREEP)	67	067	15.78	0.05	5.57	-
COLLUV.(CREEP)	91	-	14.97	0.05	5.25	-
COLLUV.(CREEP)	94	094	14.62	0.05	5.31	2.47
COLLUV.(CREEP)	95	-	18.91	0.04	5.95	-
COLLUV.(CREEP)	100	-	9.63	0.07	4.24	-
COLLUV.(CREEP)	103	-	17.17	0.06	6.14	-
COLLUV.(CREEP)	104	-	11.85	0.05	4.79	-

GLQ UNIT	SAMPLE NUMBER	STATION	ROCK POROSITY	ROCK BULK DENS	BC TOT BD	GT. 2MM VF
COLLUV.(CREEP)	-	C-5	-	-	1.53	39.8
COLLUV.(CREEP)	-	D-6	-	-	1.65	51.9
COLLUV.(CREEP)	-	D-3	-	-	-	-
COLLUV.(CREEP)	-	A-8	-	-	1.54	37.0
COLLUV.(CREEP)	-	A-1	-	-	1.69	41.7
COLLUV.(CREEP)	-	A-3	-	-	-	-
COLLUV.(CREEP)	-	A-4	-	-	1.62	42.4
COLLUV.(CREEP)	-	A-6	-	-	1.73	37.8
COLLUV.(CREEP)	-	A-7	-	-	1.54	31.8
COLLUV.(CREEP)	3	-	20.38	1.95	-	-
COLLUV.(CREEP)	6	-	-	-	-	-
COLLUV.(CREEP)	10	010	-	-	1.56	44.0
COLLUV.(CREEP)	12	-	-	-	-	-
COLLUV.(CREEP)	26	-	-	-	-	-
COLLUV.(CREEP)	27	-	-	-	-	-
COLLUV.(CREEP)	28	-	-	-	-	-
COLLUV.(CREEP)	29	029	32.99	1.69	1.53	37.0
COLLUV.(CREEP)	30	030	30.87	1.73	1.34	18.5
COLLUV.(CREEP)	31	031	-	-	1.56	40.2
COLLUV.(CREEP)	32	032	-	-	1.51	34.4
COLLUV.(CREEP)	33	-	-	-	-	-
COLLUV.(CREEP)	34	-	-	-	-	-
COLLUV.(CREEP)	35	-	23.15	1.91	-	-
COLLUV.(CREEP)	36	-	28.16	1.80	-	-
COLLUV.(CREEP)	37	-	-	-	-	-
COLLUV.(CREEP)	38	-	26.39	1.83	-	-
COLLUV.(CREEP)	39	-	-	-	-	-
COLLUV.(CREEP)	40	-	-	-	-	-
COLLUV.(CREEP)	44	-	23.77	1.89	-	-
COLLUV.(CREEP)	64	-	-	-	-	-
COLLUV.(CREEP)	65	065	22.50	1.93	1.48	33.0
COLLUV.(CREEP)	66	066	-	-	1.50	39.0
COLLUV.(CREEP)	67	067	-	-	1.60	46.2
COLLUV.(CREEP)	91	-	-	-	-	-
COLLUV.(CREEP)	94	094	22.86	1.91	1.61	43.1
COLLUV.(CREEP)	95	-	-	-	-	-
COLLUV.(CREEP)	100	-	-	-	-	-
COLLUV.(CREEP)	103	-	-	-	-	-
COLLUV.(CREEP)	104	-	-	-	-	-

GLQ UNIT	SAMPLE NUMBER	STATION	LT.2MM BD	NUC WET BD	NUC DRY BD	NUC MOIST PCT
COLLUV.(CREEP)	-	C-5	1.15	-	1.36	-
COLLUV.(CREEP)	-	D-6	1.17	-	1.47	-
COLLUV.(CREEP)	-	D-3	-	-	1.43	-
COLLUV.(CREEP)	-	A-8	1.20	-	1.48	-
COLLUV.(CREEP)	-	A-1	1.40	-	1.44	-
COLLUV.(CREEP)	-	A-3	-	-	1.49	-
COLLUV.(CREEP)	-	A-4	1.27	-	1.27	-
COLLUV.(CREEP)	-	A-6	1.50	-	1.54	-
COLLUV.(CREEP)	-	A-7	1.28	-	1.58	-
COLLUV.(CREEP)	3	-	-	1.40	1.36	2.85
COLLUV.(CREEP)	6	-	-	1.40	1.37	2.60
COLLUV.(CREEP)	10	010	1.13	1.41	1.37	2.79
COLLUV.(CREEP)	12	-	-	1.48	1.45	1.91
COLLUV.(CREEP)	26	-	-	1.44	1.42	1.93
COLLUV.(CREEP)	27	-	-	1.43	1.40	1.72
COLLUV.(CREEP)	28	-	-	1.40	1.36	2.93
COLLUV.(CREEP)	29	029	1.19	1.44	1.40	3.11
COLLUV.(CREEP)	30	030	1.17	1.40	1.37	2.67
COLLUV.(CREEP)	31	031	1.20	1.40	1.36	2.66
COLLUV.(CREEP)	32	032	1.19	1.34	1.30	3.29
COLLUV.(CREEP)	33	-	-	1.43	1.40	1.91
COLLUV.(CREEP)	34	-	-	1.43	1.41	1.45
COLLUV.(CREEP)	35	-	-	1.45	1.42	1.93
COLLUV.(CREEP)	36	-	-	1.40	1.36	2.97
COLLUV.(CREEP)	37	-	-	1.46	1.41	3.26
COLLUV.(CREEP)	38	-	-	1.40	1.37	2.69
COLLUV.(CREEP)	39	-	-	1.37	1.34	2.41
COLLUV.(CREEP)	40	-	-	1.38	1.39	3.49
COLLUV.(CREEP)	44	-	-	1.37	1.34	3.14
COLLUV.(CREEP)	64	-	-	1.38	1.35	2.15
COLLUV.(CREEP)	65	065	1.17	1.48	1.45	2.07
COLLUV.(CREEP)	66	066	1.11	1.44	1.41	2.18
COLLUV.(CREEP)	67	067	1.17	1.40	1.36	2.66
COLLUV.(CREEP)	91	-	-	1.43	1.39	2.41
COLLUV.(CREEP)	94	094	1.23	1.50	1.47	2.50
COLLUV.(CREEP)	95	-	-	1.40	1.36	3.17
COLLUV.(CREEP)	100	-	-	1.36	1.32	2.99
COLLUV.(CREEP)	103	-	-	1.36	1.32	3.19
COLLUV.(CREEP)	104	-	-	1.52	1.49	2.11

GLQ UNIT	SAMPLE NUMBER	STATION	SC MOIST PCT	SC WET BD	SC DRY BD	OM
COLLUV.(CREEP)	-	C-5	10.97	1.77	1.60	0.72
COLLUV.(CREEP)	-	D-6	9.75	1.43	1.31	0.60
COLLUV.(CREEP)	-	D-3	11.77	1.49	1.33	-
COLLUV.(CREEP)	-	A-8	16.46	1.59	1.36	0.66
COLLUV.(CREEP)	-	A-1	14.04	1.93	1.69	1.00
COLLUV.(CREEP)	-	A-3	14.07	1.63	1.43	-
COLLUV.(CREEP)	-	A-4	20.97	1.33	1.10	1.28
COLLUV.(CREEP)	-	A-6	12.26	1.52	1.36	0.99
COLLUV.(CREEP)	-	A-7	14.50	1.87	1.63	0.97
COLLUV.(CREEP)	3	-	-	-	-	-
COLLUV.(CREEP)	6	-	-	-	-	-
COLLUV.(CREEP)	10	010	-	-	-	1.68
COLLUV.(CREEP)	12	-	-	-	-	-
COLLUV.(CREEP)	26	-	-	-	-	-
COLLUV.(CREEP)	27	-	-	-	-	-
COLLUV.(CREEP)	28	-	-	-	-	-
COLLUV.(CREEP)	29	029	-	-	-	0.77
COLLUV.(CREEP)	30	030	-	-	-	0.94
COLLUV.(CREEP)	31	031	-	-	-	0.46
COLLUV.(CREEP)	32	032	-	-	-	1.03
COLLUV.(CREEP)	33	-	-	-	-	-
COLLUV.(CREEP)	34	-	-	-	-	-
COLLUV.(CREEP)	35	-	-	-	-	-
COLLUV.(CREEP)	36	-	-	-	-	-
COLLUV.(CREEP)	37	-	-	-	-	-
COLLUV.(CREEP)	38	-	-	-	-	-
COLLUV.(CREEP)	39	-	-	-	-	-
COLLUV.(CREEP)	40	-	-	-	-	-
COLLUV.(CREEP)	44	-	-	-	-	-
COLLUV.(CREEP)	64	-	-	-	-	-
COLLUV.(CREEP)	65	065	-	-	-	0.63
COLLUV.(CREEP)	66	066	-	-	-	0.78
COLLUV.(CREEP)	67	067	-	-	-	1.16
COLLUV.(CREEP)	91	-	-	-	-	-
COLLUV.(CREEP)	94	094	-	-	-	0.85
COLLUV.(CREEP)	95	-	-	-	-	-
COLLUV.(CREEP)	100	-	-	-	-	-
COLLUV.(CREEP)	103	-	-	-	-	-
COLLUV.(CREEP)	104	-	-	-	-	-

GLQ UNIT	SAMPLE NUMBER	STATION	ASPECT	SLOPE PERCENT	VERT POSITION	HORIZ POSITION
COLLUV.(CREEP)	-	C-5	SOUTH	-	-	-
COLLUV.(CREEP)	-	D-6	WEST	-	-	-
COLLUV.(CREEP)	-	D-3	WEST	-	-	-
COLLUV.(CREEP)	-	A-8	EAST	25.00	16.67	28.89
COLLUV.(CREEP)	-	A-1	EAST	33.33	28.12	41.18
COLLUV.(CREEP)	-	A-3	EAST	36.36	33.33	46.15
COLLUV.(CREEP)	-	A-4	NORTH	40.00	41.18	52.34
COLLUV.(CREEP)	-	A-6	NORTH	33.33	38.46	47.89
COLLUV.(CREEP)	-	A-7	EAST	33.33	37.50	46.15
COLLUV.(CREEP)	3	-	NORTH	30.29	44.44	53.57
COLLUV.(CREEP)	6	-	NORTH	32.62	41.18	59.18
COLLUV.(CREEP)	10	010	NORTH	33.92	56.25	53.12
COLLUV.(CREEP)	12	-	EAST	42.40	53.57	57.58
COLLUV.(CREEP)	26	-	EAST	42.40	53.57	57.58
COLLUV.(CREEP)	27	-	EAST	42.40	53.57	57.58
COLLUV.(CREEP)	28	-	EAST	70.67	38.24	53.41
COLLUV.(CREEP)	29	029	NORTH	24.94	57.14	71.43
COLLUV.(CREEP)	30	030	EAST	22.32	76.47	81.08
COLLUV.(CREEP)	31	031	NORTH	33.92	56.25	53.12
COLLUV.(CREEP)	32	032	NORTH	33.92	56.25	53.12
COLLUV.(CREEP)	33	-	NORTH	42.40	33.33	33.33
COLLUV.(CREEP)	34	-	NORTH	49.88	47.37	45.12
COLLUV.(CREEP)	35	-	NORTH	37.69	76.47	75.51
COLLUV.(CREEP)	36	-	NORTH	32.62	41.18	59.18
COLLUV.(CREEP)	37	-	NORTH	32.62	41.18	59.18
COLLUV.(CREEP)	38	-	EAST	24.23	68.42	79.37
COLLUV.(CREEP)	39	-	NORTH	35.33	57.14	69.77
COLLUV.(CREEP)	40	-	NORTH	28.27	38.10	52.38
COLLUV.(CREEP)	44	-	SOUTH	40.38	80.00	82.76
COLLUV.(CREEP)	64	-	SOUTH	35.33	35.71	50.00
COLLUV.(CREEP)	65	065	SOUTH	38.55	47.06	59.09
COLLUV.(CREEP)	66	066	SOUTH	38.55	47.06	59.09
COLLUV.(CREEP)	67	067	SOUTH	38.55	47.06	59.09
COLLUV.(CREEP)	91	-	EAST	28.27	22.73	33.33
COLLUV.(CREEP)	94	094	NORTH	35.33	31.58	26.98
COLLUV.(CREEP)	95	-	NORTH	26.78	11.11	19.30
COLLUV.(CREEP)	100	-	EAST	40.38	8.51	10.00
COLLUV.(CREEP)	103	-	SOUTH	47.11	50.00	62.50
COLLUV.(CREEP)	104	-	NORTH	35.33	85.29	63.08

GLQ UNIT	SAMPLE NUMBER	STATION	BEDROCK UNIT
COLLUV.(CREEP)	-	C-5	CKS
COLLUV.(CREEP)	-	D-6	CKS
COLLUV.(CREEP)	-	D-3	CUL
COLLUV.(CREEP)	-	A-8	CKS
COLLUV.(CREEP)	-	A-1	CUL
COLLUV.(CREEP)	-	A-3	CUL
COLLUV.(CREEP)	-	A-4	CUL
COLLUV.(CREEP)	-	A-6	CUL
COLLUV.(CREEP)	-	A-7	CUL
COLLUV.(CREEP)	3	-	CKS
COLLUV.(CREEP)	6	-	CKS
COLLUV.(CREEP)	10	010	CKS
COLLUV.(CREEP)	12	-	CKS
COLLUV.(CREEP)	26	-	CKS
COLLUV.(CREEP)	27	-	CKS
COLLUV.(CREEP)	28	-	CUL
COLLUV.(CREEP)	29	029	CUL
COLLUV.(CREEP)	30	030	CUL
COLLUV.(CREEP)	31	031	CKS
COLLUV.(CREEP)	32	032	CKS
COLLUV.(CREEP)	33	-	CUL
COLLUV.(CREEP)	34	-	CUL
COLLUV.(CREEP)	35	-	CKS
COLLUV.(CREEP)	36	-	CKS
COLLUV.(CREEP)	37	-	CKS
COLLUV.(CREEP)	38	-	CUL
COLLUV.(CREEP)	39	-	CKS
COLLUV.(CREEP)	40	-	CKS
COLLUV.(CREEP)	44	-	CKS
COLLUV.(CREEP)	64	-	CKS
COLLUV.(CREEP)	65	065	CUL
COLLUV.(CREEP)	66	066	CUL
COLLUV.(CREEP)	67	067	CUL
COLLUV.(CREEP)	91	-	CUL
COLLUV.(CREEP)	94	094	CUL
COLLUV.(CREEP)	95	-	CKS
COLLUV.(CREEP)	100	-	CUL
COLLUV.(CREEP)	103	-	CUL
COLLUV.(CREEP)	104	-	CKS

---------- GLQ UNIT: SLIDE (FLOW) ----------

GLQ UNIT	SAMPLE NUMBER	STATION	COBBLE COUNT	GRAVEL	SAND	SILT
SLIDE (FLOW)	-	D-12	-	-	-	-
SLIDE (FLOW)	-	D-9	-	-	-	-
SLIDE (FLOW)	-	A-10	-	-	-	-
SLIDE (FLOW)	-	A-12	-	-	-	-
SLIDE (FLOW)	-	A-14	-	-	-	-
SLIDE (FLOW)	-	A-16	-	-	-	-
SLIDE (FLOW)	8	-	21.50	41.62	67.20	22.92
SLIDE (FLOW)	9	-	20.75	43.52	67.64	19.26
SLIDE (FLOW)	11	-	9.00	40.46	68.62	19.35
SLIDE (FLOW)	14	-	9.75	47.93	59.18	26.80
SLIDE (FLOW)	21	-	6.50	50.88	68.02	19.97
SLIDE (FLOW)	22	-	16.75	46.25	68.27	17.78
SLIDE (FLOW)	23	-	21.25	58.91	68.52	17.37
SLIDE (FLOW)	24	-	13.75	52.09	61.50	21.38
SLIDE (FLOW)	25	-	9.25	49.93	50.52	26.91
SLIDE (FLOW)	57	-	17.75	41.62	63.29	18.04
SLIDE (FLOW)	58	-	6.25	45.26	63.15	26.07
SLIDE (FLOW)	59	-	21.00	40.76	62.66	25.19
SLIDE (FLOW)	60	-	14.00	36.45	58.23	24.15
SLIDE (FLOW)	68	-	15.75	44.48	67.44	18.33
SLIDE (FLOW)	69	-	17.25	42.14	57.40	22.17
SLIDE (FLOW)	70	-	12.75	52.06	65.18	20.48
SLIDE (FLOW)	71	-	28.75	56.90	52.13	36.24
SLIDE (FLOW)	73	-	19.50	39.72	63.56	24.77
SLIDE (FLOW)	74	-	6.00	34.65	60.06	28.17
SLIDE (FLOW)	75	-	4.50	42.95	62.60	25.66
SLIDE (FLOW)	80	-	7.75	64.11	58.51	32.01
SLIDE (FLOW)	81	-	7.25	53.43	44.45	37.10
SLIDE (FLOW)	82	-	6.50	50.69	45.24	38.13
SLIDE (FLOW)	83	-	14.00	58.64	51.62	33.15
SLIDE (FLOW)	84	-	8.75	41.84	60.63	28.71
SLIDE (FLOW)	93	-	8.50	52.65	57.64	28.17
SLIDE (FLOW)	98	-	2.75	43.57	54.46	34.11
SLIDE (FLOW)	99	-	8.75	38.08	49.03	23.84

GLQ UNIT	SAMPLE NUMBER	STATION	CLAY	LT.2MM GMGS	LT.2MM GSTDEV	ROCK PART DENS
SLIDE (FLOW)	-	D-12	-	-	-	-
SLIDE (FLOW)	-	D-9	-	-	-	-
SLIDE (FLOW)	-	A-10	-	-	-	-
SLIDE (FLOW)	-	A-12	-	-	-	-
SLIDE (FLOW)	-	A-14	-	-	-	-
SLIDE (FLOW)	-	A-16	-	-	-	-
SLIDE (FLOW)	8	-	9.87	0.06	3.93	-
SLIDE (FLOW)	9	-	13.10	0.07	5.44	2.49
SLIDE (FLOW)	11	-	12.04	0.07	5.19	2.51
SLIDE (FLOW)	14	-	14.02	0.05	5.42	-
SLIDE (FLOW)	21	-	12.01	0.07	5.45	-
SLIDE (FLOW)	22	-	13.95	0.07	5.40	-
SLIDE (FLOW)	23	-	14.11	0.07	5.99	-
SLIDE (FLOW)	24	-	17.12	0.05	5.84	-
SLIDE (FLOW)	25	-	22.57	0.04	6.35	-
SLIDE (FLOW)	57	-	18.67	0.05	5.62	-
SLIDE (FLOW)	58	-	10.78	0.06	4.24	-
SLIDE (FLOW)	59	-	12.15	0.06	4.90	-
SLIDE (FLOW)	60	-	17.62	0.04	5.33	-
SLIDE (FLOW)	68	-	14.23	0.06	5.37	-
SLIDE (FLOW)	69	-	20.42	0.04	6.13	2.48
SLIDE (FLOW)	70	-	14.34	0.06	5.23	-
SLIDE (FLOW)	71	-	11.64	0.05	5.03	-
SLIDE (FLOW)	73	-	11.67	0.05	4.17	2.46
SLIDE (FLOW)	74	-	11.77	0.05	4.60	2.46
SLIDE (FLOW)	75	-	11.74	0.06	4.68	-
SLIDE (FLOW)	80	-	9.47	0.06	4.97	-
SLIDE (FLOW)	81	-	18.45	0.04	5.83	2.47
SLIDE (FLOW)	82	-	16.63	0.04	5.43	-
SLIDE (FLOW)	83	-	15.23	0.05	5.64	-
SLIDE (FLOW)	84	-	10.66	0.05	4.04	2.48
SLIDE (FLOW)	93	-	14.20	0.05	5.12	-
SLIDE (FLOW)	98	-	11.43	0.04	4.44	-
SLIDE (FLOW)	99	-	27.13	0.03	6.73	2.46

GLQ UNIT	SAMPLE NUMBER	STATION	ROCK POROSITY	ROCK BULK DENS	BC TOT BD	GT. 2MM VF
SLIDE (FLOW)	-	D-12	-	-	1.54	36.8
SLIDE (FLOW)	-	D-9	-	-	-	-
SLIDE (FLOW)	-	A-10	-	-	-	-
SLIDE (FLOW)	-	A-12	-	-	1.48	33.6
SLIDE (FLOW)	-	A-14	-	-	-	-
SLIDE (FLOW)	-	A-16	-	-	1.64	46.0
SLIDE (FLOW)	8	-	-	-	-	-
SLIDE (FLOW)	9	-	22.47	1.93	-	-
SLIDE (FLOW)	11	-	32.05	1.70	-	-
SLIDE (FLOW)	14	-	-	-	-	-
SLIDE (FLOW)	21	-	-	-	-	-
SLIDE (FLOW)	22	-	-	-	-	-
SLIDE (FLOW)	23	-	-	-	-	-
SLIDE (FLOW)	24	-	-	-	-	-
SLIDE (FLOW)	25	-	-	-	-	-
SLIDE (FLOW)	57	-	-	-	-	-
SLIDE (FLOW)	58	-	-	-	-	-
SLIDE (FLOW)	59	-	-	-	-	-
SLIDE (FLOW)	60	-	-	-	-	-
SLIDE (FLOW)	68	-	-	-	-	-
SLIDE (FLOW)	69	-	24.12	1.88	-	-
SLIDE (FLOW)	70	-	-	-	-	-
SLIDE (FLOW)	71	-	-	-	-	-
SLIDE (FLOW)	73	-	20.19	1.96	-	-
SLIDE (FLOW)	74	-	19.52	1.98	-	-
SLIDE (FLOW)	75	-	-	-	-	-
SLIDE (FLOW)	80	-	-	-	-	-
SLIDE (FLOW)	81	-	16.63	2.06	-	-
SLIDE (FLOW)	82	-	-	-	-	-
SLIDE (FLOW)	83	-	-	-	-	-
SLIDE (FLOW)	84	-	18.64	2.02	-	-
SLIDE (FLOW)	93	-	-	-	-	-
SLIDE (FLOW)	98	-	-	-	-	-
SLIDE (FLOW)	99	-	19.68	1.97	-	-

GLQ UNIT	SAMPLE NUMBER	STATION	LT.2MM BD	NUC WET BD	NUC DRY BD	NUC MOIST PCT
SLIDE (FLOW)	-	D-12	1.22	-	1.37	-
SLIDE (FLOW)	-	D-9	-	-	1.58	-
SLIDE (FLOW)	-	A-10	-	-	1.49	-
SLIDE (FLOW)	-	A-12	1.16	-	1.57	-
SLIDE (FLOW)	-	A-14	-	-	1.41	-
SLIDE (FLOW)	-	A-16	1.25	-	1.52	-
SLIDE (FLOW)	8	-	-	1.55	1.52	1.88
SLIDE (FLOW)	9	-	-	1.50	1.48	1.71
SLIDE (FLOW)	11	-	-	1.45	1.42	1.51
SLIDE (FLOW)	14	-	-	1.45	1.41	2.57
SLIDE (FLOW)	21	-	-	1.39	1.36	2.07
SLIDE (FLOW)	22	-	-	1.40	1.37	2.07
SLIDE (FLOW)	23	-	-	1.57	1.55	1.51
SLIDE (FLOW)	24	-	-	1.46	1.68	2.10
SLIDE (FLOW)	25	-	-	1.41	1.48	2.48
SLIDE (FLOW)	57	-	-	1.50	1.46	3.03
SLIDE (FLOW)	58	-	-	1.49	1.48	1.02
SLIDE (FLOW)	59	-	-	1.43	1.41	1.28
SLIDE (FLOW)	60	-	-	1.47	1.44	2.28
SLIDE (FLOW)	68	-	-	1.42	1.38	2.56
SLIDE (FLOW)	69	-	-	1.40	1.36	3.00
SLIDE (FLOW)	70	-	-	1.53	1.50	1.77
SLIDE (FLOW)	71	-	-	1.37	1.32	3.50
SLIDE (FLOW)	73	-	-	1.43	1.41	1.42
SLIDE (FLOW)	74	-	-	1.52	1.49	1.55
SLIDE (FLOW)	75	-	-	1.41	1.38	2.20
SLIDE (FLOW)	80	-	-	1.49	1.46	1.89
SLIDE (FLOW)	81	-	-	1.43	1.39	2.81
SLIDE (FLOW)	82	-	-	1.51	1.48	2.35
SLIDE (FLOW)	83	-	-	1.48	1.44	2.60
SLIDE (FLOW)	84	-	-	1.38	1.35	2.53
SLIDE (FLOW)	93	-	-	1.36	1.31	3.23
SLIDE (FLOW)	98	-	-	1.34	1.30	2.50
SLIDE (FLOW)	99	-	-	1.38	1.33	3.29

GLQ UNIT	SAMPLE NUMBER	STATION	SC MOIST PCT	SC WET BD	SC DRY BD	OM
SLIDE (FLOW)	-	D-12	7.72	1.70	1.58	1.06
SLIDE (FLOW)	-	D-9	11.97	1.63	1.45	-
SLIDE (FLOW)	-	A-10	14.22	1.57	1.38	-
SLIDE (FLOW)	-	A-12	12.62	1.64	1.46	1.20
SLIDE (FLOW)	-	A-14	12.15	1.39	1.24	-
SLIDE (FLOW)	-	A-16	-	-	-	0.98
SLIDE (FLOW)	8	-	-	-	-	-
SLIDE (FLOW)	9	-	-	-	-	-
SLIDE (FLOW)	11	-	-	-	-	-
SLIDE (FLOW)	14	-	-	-	-	-
SLIDE (FLOW)	21	-	-	-	-	-
SLIDE (FLOW)	22	-	-	-	-	-
SLIDE (FLOW)	23	-	-	-	-	-
SLIDE (FLOW)	24	-	-	-	-	-
SLIDE (FLOW)	25	-	-	-	-	-
SLIDE (FLOW)	57	-	-	-	-	-
SLIDE (FLOW)	58	-	-	-	-	-
SLIDE (FLOW)	59	-	-	-	-	-
SLIDE (FLOW)	60	-	-	-	-	-
SLIDE (FLOW)	68	-	-	-	-	-
SLIDE (FLOW)	69	-	-	-	-	-
SLIDE (FLOW)	70	-	-	-	-	-
SLIDE (FLOW)	71	-	-	-	-	-
SLIDE (FLOW)	73	-	-	-	-	-
SLIDE (FLOW)	74	-	-	-	-	-
SLIDE (FLOW)	75	-	-	-	-	-
SLIDE (FLOW)	80	-	-	-	-	-
SLIDE (FLOW)	81	-	-	-	-	-
SLIDE (FLOW)	82	-	-	-	-	-
SLIDE (FLOW)	83	-	-	-	-	-
SLIDE (FLOW)	84	-	-	-	-	-
SLIDE (FLOW)	93	-	-	-	-	-
SLIDE (FLOW)	98	-	-	-	-	-
SLIDE (FLOW)	99	-	-	-	-	-

GLQ UNIT	SAMPLE NUMBER	STATION	ASPECT	SLOPE PERCENT	VERT POSITION	HORIZ POSITION
SLIDE (FLOW)	-	D-12	WEST	15.00	3.85	11.43
SLIDE (FLOW)	-	D-9	WEST	40.00	61.11	65.57
SLIDE (FLOW)	-	A-10	EAST	-	-	-
SLIDE (FLOW)	-	A-12	EAST	14.29	7.69	10.71
SLIDE (FLOW)	-	A-14	EAST	33.33	75.00	75.76
SLIDE (FLOW)	-	A-16	EAST	33.33	95.24	92.11
SLIDE (FLOW)	8	-	EAST	36.34	88.24	79.28
SLIDE (FLOW)	9	-	SOUTH	33.92	85.11	85.71
SLIDE (FLOW)	11	-	SOUTH	42.40	84.62	75.00
SLIDE (FLOW)	14	-	WEST	47.11	73.33	66.67
SLIDE (FLOW)	21	-	SOUTH	42.40	84.62	75.00
SLIDE (FLOW)	22	-	SOUTH	42.40	84.62	75.00
SLIDE (FLOW)	23	-	SOUTH	39.91	90.48	78.90
SLIDE (FLOW)	24	-	SOUTH	47.11	84.21	75.56
SLIDE (FLOW)	25	-	SOUTH	42.40	80.00	77.27
SLIDE (FLOW)	57	-	EAST	42.40	89.66	93.58
SLIDE (FLOW)	58	-	EAST	28.27	95.71	92.86
SLIDE (FLOW)	59	-	SOUTH	33.92	87.88	82.35
SLIDE (FLOW)	60	-	SOUTH	33.92	87.50	82.69
SLIDE (FLOW)	68	-	SOUTH	28.27	83.33	76.92
SLIDE (FLOW)	69	-	SOUTH	28.27	83.33	76.92
SLIDE (FLOW)	70	-	SOUTH	28.27	83.33	76.92
SLIDE (FLOW)	71	-	EAST	47.11	53.57	71.28
SLIDE (FLOW)	73	-	EAST	28.27	95.71	92.86
SLIDE (FLOW)	74	-	EAST	28.27	95.71	92.86
SLIDE (FLOW)	75	-	EAST	53.00	87.10	83.52
SLIDE (FLOW)	80	-	WEST	47.11	73.33	66.67
SLIDE (FLOW)	81	-	WEST	47.11	73.33	66.67
SLIDE (FLOW)	82	-	WEST	47.11	69.23	63.16
SLIDE (FLOW)	83	-	WEST	47.11	57.14	31.03
SLIDE (FLOW)	84	-	NORTH	47.11	80.00	72.58
SLIDE (FLOW)	93	-	EAST	42.40	53.12	56.52
SLIDE (FLOW)	98	-	EAST	40.38	85.71	77.59
SLIDE (FLOW)	99	-	EAST	44.63	55.56	50.75

GLQ UNIT	SAMPLE NUMBER	STATION	BEDROCK UNIT
SLIDE (FLOW)	-	D-12	CKS
SLIDE (FLOW)	-	D-9	CKS
SLIDE (FLOW)	-	A-10	CKS
SLIDE (FLOW)	-	A-12	CKS
SLIDE (FLOW)	-	A-14	CKS
SLIDE (FLOW)	-	A-16	CKS
SLIDE (FLOW)	8	-	CKS
SLIDE (FLOW)	9	-	CKS
SLIDE (FLOW)	11	-	CKS
SLIDE (FLOW)	14	-	-
SLIDE (FLOW)	21	-	CKS
SLIDE (FLOW)	22	-	CKS
SLIDE (FLOW)	23	-	CKS
SLIDE (FLOW)	24	-	CKS
SLIDE (FLOW)	25	-	CKS
SLIDE (FLOW)	57	-	CKS
SLIDE (FLOW)	58	-	CKS
SLIDE (FLOW)	59	-	CKS
SLIDE (FLOW)	60	-	CKS
SLIDE (FLOW)	68	-	CKS
SLIDE (FLOW)	69	-	CKS
SLIDE (FLOW)	70	-	CKS
SLIDE (FLOW)	71	-	CKS
SLIDE (FLOW)	73	-	CKS
SLIDE (FLOW)	74	-	CKS
SLIDE (FLOW)	75	-	CKS
SLIDE (FLOW)	80	-	-
SLIDE (FLOW)	81	-	-
SLIDE (FLOW)	82	-	-
SLIDE (FLOW)	83	-	-
SLIDE (FLOW)	84	-	-
SLIDE (FLOW)	93	-	CKS
SLIDE (FLOW)	98	-	CKS
SLIDE (FLOW)	99	-	CKS

---------- GLQ UNIT: COLLUVIUM (cr-ta) ----------

GLQ UNIT	SAMPLE NUMBER	STATION	COBBLE COUNT	GRAVEL	SAND	SILT
COLLUV.(cr-ta)	-	B-11	-	-	-	-
COLLUV.(cr-ta)	-	B-15	-	-	-	-
COLLUV.(cr-ta)	-	B-9	-	-	-	-
COLLUV.(cr-ta)	2	-	13.75	42.57	60.12	24.81
COLLUV.(cr-ta)	7	-	10.00	49.90	61.30	23.07
COLLUV.(cr-ta)	13	-	46.00	48.64	64.49	25.54
COLLUV.(cr-ta)	15	-	10.50	39.19	67.18	22.96
COLLUV.(cr-ta)	41	-	15.00	65.78	59.02	24.62
COLLUV.(cr-ta)	42	-	24.00	54.55	61.44	23.89
COLLUV.(cr-ta)	43	-	24.75	58.42	53.15	23.17
COLLUV.(cr-ta)	52	-	36.00	59.31	63.52	25.67
COLLUV.(cr-ta)	53	-	29.50	52.03	60.00	24.01
COLLUV.(cr-ta)	54	-	35.75	50.89	54.14	23.46
COLLUV.(cr-ta)	55	-	24.25	52.72	59.29	25.69
COLLUV.(cr-ta)	56	-	13.50	42.79	59.95	26.24
COLLUV.(cr-ta)	72	-	26.25	38.64	55.48	28.22
COLLUV.(cr-ta)	76	-	14.25	44.82	58.02	31.65
COLLUV.(cr-ta)	77	-	14.50	49.40	63.76	29.52
COLLUV.(cr-ta)	78	-	27.25	52.52	55.43	34.65
COLLUV.(cr-ta)	79	-	24.75	49.80	55.01	31.00
COLLUV.(cr-ta)	85	-	13.75	62.91	63.38	27.72
COLLUV.(cr-ta)	86	-	15.50	50.27	61.33	31.23
COLLUV.(cr-ta)	87	-	31.75	51.78	57.56	33.11
COLLUV.(cr-ta)	88	-	31.75	48.17	61.77	27.42
COLLUV.(cr-ta)	89	-	9.25	63.25	57.91	26.37
COLLUV.(cr-ta)	90	-	22.00	42.52	55.61	29.95
COLLUV.(cr-ta)	92	-	15.50	49.18	49.42	35.85
COLLUV.(cr-ta)	96	-	36.00	56.11	56.60	24.04
COLLUV.(cr-ta)	97	-	21.75	40.70	43.48	31.73

GLQ UNIT	SAMPLE NUMBER	STATION	CLAY	LT.2MM GMGS	LT.2MM GSTDEV	ROCK PART DENS
COLLUV.(cr-ta)	-	B-11	-	-	-	-
COLLUV.(cr-ta)	-	B-15	-	-	-	-
COLLUV.(cr-ta)	-	B-9	-	-	-	-
COLLUV.(cr-ta)	2	-	15.08	0.05	5.23	-
COLLUV.(cr-ta)	7	-	15.64	0.06	6.00	-
COLLUV.(cr-ta)	13	-	9.96	0.06	4.57	-
COLLUV.(cr-ta)	15	-	9.87	0.08	5.34	-
COLLUV.(cr-ta)	41	-	16.37	0.06	6.83	-
COLLUV.(cr-ta)	42	-	14.67	0.06	6.02	-
COLLUV.(cr-ta)	43	-	23.68	0.04	7.38	-
COLLUV.(cr-ta)	52	-	10.81	0.07	5.23	2.47
COLLUV.(cr-ta)	53	-	15.98	0.05	6.12	-
COLLUV.(cr-ta)	54	-	22.40	0.04	7.47	-
COLLUV.(cr-ta)	55	-	15.02	0.05	5.79	-
COLLUV.(cr-ta)	56	-	13.81	0.05	5.13	2.50
COLLUV.(cr-ta)	72	-	16.30	0.05	5.08	-
COLLUV.(cr-ta)	76	-	10.33	0.05	4.32	-
COLLUV.(cr-ta)	77	-	6.72	0.07	4.88	-
COLLUV.(cr-ta)	78	-	9.92	0.05	4.38	2.53
COLLUV.(cr-ta)	79	-	13.98	0.05	5.68	2.51
COLLUV.(cr-ta)	85	-	8.90	0.07	4.63	-
COLLUV.(cr-ta)	86	-	7.44	0.06	4.30	2.48
COLLUV.(cr-ta)	87	-	9.33	0.06	5.01	-
COLLUV.(cr-ta)	88	-	10.80	0.06	5.08	2.47
COLLUV.(cr-ta)	89	-	15.72	0.07	7.24	-
COLLUV.(cr-ta)	90	-	14.44	0.05	5.41	-
COLLUV.(cr-ta)	92	-	14.74	0.04	5.00	-
COLLUV.(cr-ta)	96	-	19.37	0.05	6.46	2.46
COLLUV.(cr-ta)	97	-	24.79	0.03	6.14	2.47

GLQ UNIT	SAMPLE NUMBER	STATION	ROCK POROSITY	ROCK BULK DENS	BC TOT BD	GT. 2MM VF
COLLUV.(cr-ta)	-	B-11	-	-	1.54	37.0
COLLUV.(cr-ta)	-	B-15	-	-	1.57	36.9
COLLUV.(cr-ta)	-	B-9	-	-	1.63	42.0
COLLUV.(cr-ta)	2	-	-	-	-	-
COLLUV.(cr-ta)	7	-	-	-	-	-
COLLUV.(cr-ta)	13	-	-	-	-	-
COLLUV.(cr-ta)	15	-	-	-	-	-
COLLUV.(cr-ta)	41	-	-	-	-	-
COLLUV.(cr-ta)	42	-	-	-	-	-
COLLUV.(cr-ta)	43	-	-	-	-	-
COLLUV.(cr-ta)	52	-	23.60	1.88	-	-
COLLUV.(cr-ta)	53	-	-	-	-	-
COLLUV.(cr-ta)	54	-	-	-	-	-
COLLUV.(cr-ta)	55	-	-	-	-	-
COLLUV.(cr-ta)	56	-	24.27	1.89	-	-
COLLUV.(cr-ta)	72	-	-	-	-	-
COLLUV.(cr-ta)	76	-	-	-	-	-
COLLUV.(cr-ta)	77	-	-	-	-	-
COLLUV.(cr-ta)	78	-	23.62	1.93	-	-
COLLUV.(cr-ta)	79	-	24.96	1.88	-	-
COLLUV.(cr-ta)	85	-	-	-	-	-
COLLUV.(cr-ta)	86	-	23.58	1.90	-	-
COLLUV.(cr-ta)	87	-	-	-	-	-
COLLUV.(cr-ta)	88	-	21.16	1.95	-	-
COLLUV.(cr-ta)	89	-	-	-	-	-
COLLUV.(cr-ta)	90	-	-	-	-	-
COLLUV.(cr-ta)	92	-	-	-	-	-
COLLUV.(cr-ta)	96	-	20.14	1.96	-	-
COLLUV.(cr-ta)	97	-	19.50	1.99	-	-

GLQ UNIT	SAMPLE NUMBER	STATION	LT.2MM BD	NUC WET BD	NUC DRY BD	NUC MOIST PCT
COLLUV.(cr-ta)	-	B-11	1.21	-	1.58	-
COLLUV.(cr-ta)	-	B-15	1.26	-	1.44	-
COLLUV.(cr-ta)	-	B-9	1.28	-	1.43	-
COLLUV.(cr-ta)	-	-	-	1.38	1.33	3.15
COLLUV.(cr-ta)	7	-	-	1.40	1.36	2.98
COLLUV.(cr-ta)	13	-	-	1.34	1.55	2.53
COLLUV.(cr-ta)	15	-	-	1.42	1.39	2.25
COLLUV.(cr-ta)	41	-	-	1.43	1.39	3.38
COLLUV.(cr-ta)	42	-	-	1.45	1.40	3.34
COLLUV.(cr-ta)	43	-	-	1.32	1.26	5.00
COLLUV.(cr-ta)	52	-	-	1.42	1.38	2.87
COLLUV.(cr-ta)	53	-	-	1.48	1.44	2.92
COLLUV.(cr-ta)	54	-	-	1.42	1.38	3.23
COLLUV.(cr-ta)	55	-	-	1.44	1.39	3.32
COLLUV.(cr-ta)	56	-	-	1.38	1.33	3.81
COLLUV.(cr-ta)	72	-	-	1.37	1.33	3.41
COLLUV.(cr-ta)	76	-	-	-	-	-
COLLUV.(cr-ta)	77	-	-	-	-	-
COLLUV.(cr-ta)	78	-	-	1.49	1.47	1.48
COLLUV.(cr-ta)	79	-	-	1.41	1.38	2.66
COLLUV.(cr-ta)	85	-	-	1.43	1.39	2.70
COLLUV.(cr-ta)	86	-	-	1.37	1.33	2.58
COLLUV.(cr-ta)	87	-	-	1.39	1.34	3.79
COLLUV.(cr-ta)	88	-	-	-	-	-
COLLUV.(cr-ta)	89	-	-	1.36	1.33	2.52
COLLUV.(cr-ta)	90	-	-	1.49	1.46	2.36
COLLUV.(cr-ta)	92	-	-	1.25	1.22	2.19
COLLUV.(cr-ta)	96	-	-	1.50	1.45	3.03
COLLUV.(cr-ta)	97	-	-	1.45	1.41	2.79

GLQ UNIT	SAMPLE NUMBER	STATION	SC MOIST PCT	SC WET BD	SC DRY BD	OM
COLLUV.(cr-ta)	-	B-11	15.49	1.87	1.62	0.98
COLLUV.(cr-ta)	-	B-15	13.73	1.75	1.54	0.99
COLLUV.(cr-ta)	-	B-9	17.05	1.75	1.50	1.32
COLLUV.(cr-ta)	2	-	-	-	-	-
COLLUV.(cr-ta)	7	-	-	-	-	-
COLLUV.(cr-ta)	13	-	-	-	-	-
COLLUV.(cr-ta)	15	-	-	-	-	-
COLLUV.(cr-ta)	41	-	-	-	-	-
COLLUV.(cr-ta)	42	-	-	-	-	-
COLLUV.(cr-ta)	43	-	-	-	-	-
COLLUV.(cr-ta)	52	-	-	-	-	-
COLLUV.(cr-ta)	53	-	-	-	-	-
COLLUV.(cr-ta)	54	-	-	-	-	-
COLLUV.(cr-ta)	55	-	-	-	-	-
COLLUV.(cr-ta)	56	-	-	-	-	-
COLLUV.(cr-ta)	72	-	-	-	-	-
COLLUV.(cr-ta)	76	-	-	-	-	-
COLLUV.(cr-ta)	77	-	-	-	-	-
COLLUV.(cr-ta)	78	-	-	-	-	-
COLLUV.(cr-ta)	79	-	-	-	-	-
COLLUV.(cr-ta)	85	-	-	-	-	-
COLLUV.(cr-ta)	86	-	-	-	-	-
COLLUV.(cr-ta)	87	-	-	-	-	-
COLLUV.(cr-ta)	88	-	-	-	-	-
COLLUV.(cr-ta)	89	-	-	-	-	-
COLLUV.(cr-ta)	90	-	-	-	-	-
COLLUV.(cr-ta)	92	-	-	-	-	-
COLLUV.(cr-ta)	96	-	-	-	-	-
COLLUV.(cr-ta)	97	-	-	-	-	-

GLQ UNIT	SAMPLE NUMBER	STATION	ASPECT	SLOPE PERCENT	VERT POSITION	HORIZ POSITION
COLLUV.(cr-ta)	-	B-11	NORTH	33.33	47.06	57.14
COLLUV.(cr-ta)	-	B-15	NORTH	-	-	-
COLLUV.(cr-ta)	-	B-9	NORTH	-	-	-
COLLUV.(cr-ta)	2	-	NORTH	47.11	76.92	89.74
COLLUV.(cr-ta)	7	-	NORTH	42.40	88.24	88.00
COLLUV.(cr-ta)	13	-	WEST	56.53	33.67	60.22
COLLUV.(cr-ta)	15	-	WEST	53.00	23.26	9.13
COLLUV.(cr-ta)	41	-	NORTH	42.40	89.19	92.73
COLLUV.(cr-ta)	42	-	NORTH	42.40	89.19	92.73
COLLUV.(cr-ta)	43	-	NORTH	42.40	89.19	92.73
COLLUV.(cr-ta)	52	-	NORTH	40.38	90.00	93.65
COLLUV.(cr-ta)	53	-	NORTH	42.40	92.86	95.52
COLLUV.(cr-ta)	54	-	NORTH	53.00	82.05	91.43
COLLUV.(cr-ta)	55	-	NORTH	47.11	76.92	89.74
COLLUV.(cr-ta)	56	-	NORTH	47.11	76.92	89.74
COLLUV.(cr-ta)	72	-	NORTH	53.00	60.00	67.74
COLLUV.(cr-ta)	76	-	WEST	53.00	15.33	6.20
COLLUV.(cr-ta)	77	-	WEST	47.11	13.51	6.20
COLLUV.(cr-ta)	78	-	WEST	53.00	23.26	9.13
COLLUV.(cr-ta)	79	-	WEST	53.00	23.26	9.13
COLLUV.(cr-ta)	85	-	WEST	33.92	51.16	24.35
COLLUV.(cr-ta)	86	-	WEST	56.53	33.67	60.22
COLLUV.(cr-ta)	87	-	WEST	56.53	33.67	60.22
COLLUV.(cr-ta)	88	-	WEST	60.57	41.49	45.59
COLLUV.(cr-ta)	89	-	WEST	70.67	62.75	70.59
COLLUV.(cr-ta)	90	-	WEST	70.67	73.47	78.68
COLLUV.(cr-ta)	92	-	NORTH	42.40	85.00	88.33
COLLUV.(cr-ta)	96	-	WEST	47.11	59.09	71.70
COLLUV.(cr-ta)	97	-	WEST	47.11	60.00	79.55

GLQ UNIT	SAMPLE NUMBER	STATION	BEDROCK UNIT
COLLUV.(cr-ta)	-	B-11	CKS
COLLUV.(cr-ta)	-	B-15	CKS
COLLUV.(cr-ta)	-	B-9	CKS
COLLUV.(cr-ta)	2	-	CKS
COLLUV.(cr-ta)	7	-	CKS
COLLUV.(cr-ta)	13	-	-
COLLUV.(cr-ta)	15	-	-
COLLUV.(cr-ta)	41	-	CKS
COLLUV.(cr-ta)	42	-	CKS
COLLUV.(cr-ta)	43	-	CKS
COLLUV.(cr-ta)	52	-	CKS
COLLUV.(cr-ta)	53	-	CKS
COLLUV.(cr-ta)	54	-	CKS
COLLUV.(cr-ta)	55	-	CKS
COLLUV.(cr-ta)	56	-	CKS
COLLUV.(cr-ta)	72	-	CKS
COLLUV.(cr-ta)	76	-	-
COLLUV.(cr-ta)	77	-	-
COLLUV.(cr-ta)	78	-	-
COLLUV.(cr-ta)	79	-	-
COLLUV.(cr-ta)	85	-	-
COLLUV.(cr-ta)	86	-	-
COLLUV.(cr-ta)	87	-	-
COLLUV.(cr-ta)	88	-	-
COLLUV.(cr-ta)	89	-	-
COLLUV.(cr-ta)	90	-	-
COLLUV.(cr-ta)	92	-	CKS
COLLUV.(cr-ta)	96	-	CKS
COLLUV.(cr-ta)	97	-	CKS

---------- GLQ UNIT: RESIDUUM ----------

GLQ UNIT	SAMPLE NUMBER	STATION	COBBLE COUNT	GRAVEL	SAND	SILT
RESIDUUM	-	102-1	-	-	-	-
RESIDUUM	-	102-2	-	-	-	-
RESIDUUM	-	102-3	-	-	-	-
RESIDUUM	-	C-2	-	-	-	-
RESIDUUM	-	B-3	-	-	-	-
RESIDUUM	-	B-5	-	-	-	-
RESIDUUM	-	B-7	-	-	-	-
RESIDUUM	1	-	9.25	24.47	61.85	18.42
RESIDUUM	4	-	7.50	39.03	52.58	26.77
RESIDUUM	5	-	20.50	23.67	66.11	18.04
RESIDUUM	16	-	11.25	31.69	64.91	20.58
RESIDUUM	17	-	8.25	27.59	61.17	18.81
RESIDUUM	18	-	5.75	29.30	66.46	14.18
RESIDUUM	19	-	12.75	47.18	58.96	20.58
RESIDUUM	20	-	6.00	28.54	71.61	13.70
RESIDUUM	45	-	16.75	35.79	60.71	22.63
RESIDUUM	46	-	23.25	36.67	59.59	16.25
RESIDUUM	47	-	12.75	24.35	62.70	21.70
RESIDUUM	48	-	7.25	25.90	60.76	21.70
RESIDUUM	49	-	9.25	35.15	65.16	21.12
RESIDUUM	50	-	10.50	47.19	65.78	23.43
RESIDUUM	51	-	16.50	55.51	62.07	22.42
RESIDUUM	61	-	15.25	37.74	66.03	18.23
RESIDUUM	62	-	6.00	31.24	59.75	22.65
RESIDUUM	63	-	1.50	36.53	65.01	19.71
RESIDUUM	101	101	14.00	26.12	69.95	12.72
RESIDUUM	102	-	12.75	19.91	66.63	17.89

GLQ UNIT	SAMPLE NUMBER	STATION	CLAY	LT.2MM GMGS	LT.2MM GSTDEV	ROCK PART DENS
RESIDUUM	-	102-1	-	-	-	-
RESIDUUM	-	102-2	-	-	-	-
RESIDUUM	-	102-3	-	-	-	-
RESIDUUM	-	C-2	-	-	-	-
RESIDUUM	-	B-3	-	-	-	-
RESIDUUM	-	B-5	-	-	-	-
RESIDUUM	-	B-7	-	-	-	-
RESIDUUM	1	-	19.73	0.05	6.06	-
RESIDUUM	4	-	20.65	0.04	5.48	-
RESIDUUM	5	-	15.85	0.06	5.76	-
RESIDUUM	16	-	14.51	0.06	5.92	2.53
RESIDUUM	17	-	20.02	0.05	6.51	-
RESIDUUM	18	-	19.37	0.06	6.69	2.54
RESIDUUM	19	-	20.46	0.05	6.98	-
RESIDUUM	20	-	14.69	0.07	5.90	-
RESIDUUM	45	-	16.66	0.05	5.13	-
RESIDUUM	46	-	24.16	0.04	6.33	-
RESIDUUM	47	-	15.60	0.05	5.59	-
RESIDUUM	48	-	17.54	0.05	5.93	-
RESIDUUM	49	-	13.72	0.06	5.38	-
RESIDUUM	50	-	10.79	0.07	5.21	2.52
RESIDUUM	51	-	15.51	0.06	5.54	2.50
RESIDUUM	61	-	15.74	0.06	5.27	2.49
RESIDUUM	62	-	17.60	0.05	5.76	2.46
RESIDUUM	63	-	15.28	0.06	5.75	2.49
RESIDUUM	101	101	17.33	0.06	5.75	-
RESIDUUM	102	-	15.48	0.06	5.59	-

GLQ UNIT	SAMPLE NUMBER	STATION	ROCK POROSITY	ROCK BULK DENS	BC TOT BD	GT. 2MM VF
RESIDUUM	-	102-1	-	-	1.43	20.9
RESIDUUM	-	102-2	-	-	1.61	44.3
RESIDUUM	-	102-3	-	-	1.62	33.2
RESIDUUM	-	C-2	-	-	1.63	43.3
RESIDUUM	-	B-3	-	-	1.62	30.8
RESIDUUM	-	B-5	-	-	-	-
RESIDUUM	-	B-7	-	-	1.67	48.2
RESIDUUM	1	-	-	-	-	-
RESIDUUM	4	-	-	-	-	-
RESIDUUM	5	-	-	-	-	-
RESIDUUM	16	-	37.44	1.58	-	-
RESIDUUM	17	-	-	-	-	-
RESIDUUM	18	-	35.93	1.63	-	-
RESIDUUM	19	-	-	-	-	-
RESIDUUM	20	-	-	-	-	-
RESIDUUM	45	-	-	-	-	-
RESIDUUM	46	-	-	-	-	-
RESIDUUM	47	-	-	-	-	-
RESIDUUM	48	-	-	-	-	-
RESIDUUM	49	-	-	-	-	-
RESIDUUM	50	-	32.08	1.71	-	-
RESIDUUM	51	-	26.65	1.83	-	-
RESIDUUM	61	-	23.92	1.89	-	-
RESIDUUM	62	-	23.50	1.89	-	-
RESIDUUM	63	-	22.13	1.94	-	-
RESIDUUM	101	101	-	-	1.45	24.6
RESIDUUM	102	-	-	-	-	32.8

GLQ UNIT	SAMPLE NUMBER	STATION	LT.2MM BD	NUC WET BD	NUC DRY BD	NUC MOIST PCT
RESIDUUM	-	102-1	1.25	-	1.30	-
RESIDUUM	-	102-2	1.22	-	1.30	-
RESIDUUM	-	102-3	1.39	-	1.30	-
RESIDUUM	-	C-2	1.27	-	1.49	-
RESIDUUM	-	B-3	1.41	-	1.32	-
RESIDUUM	-	B-5	-	-	1.40	-
RESIDUUM	-	B-7	1.26	-	1.48	-
RESIDUUM	1	-	-	1.44	1.40	2.29
RESIDUUM	4	-	-	1.49	1.42	4.88
RESIDUUM	5	-	-	1.43	1.39	3.20
RESIDUUM	16	-	-	1.43	1.39	3.34
RESIDUUM	17	-	-	1.35	1.31	3.38
RESIDUUM	18	-	-	1.39	1.35	3.15
RESIDUUM	19	-	-	1.41	1.37	3.28
RESIDUUM	20	-	-	1.44	1.41	2.56
RESIDUUM	45	-	-	1.41	1.37	3.15
RESIDUUM	46	-	-	1.39	1.35	3.12
RESIDUUM	47	-	-	1.40	1.35	3.60
RESIDUUM	48	-	-	1.52	1.46	3.84
RESIDUUM	49	-	-	1.40	1.36	2.96
RESIDUUM	50	-	-	1.43	1.40	2.75
RESIDUUM	51	-	-	1.45	1.41	2.47
RESIDUUM	61	-	-	1.36	1.32	2.80
RESIDUUM	62	-	-	1.36	1.32	2.77
RESIDUUM	63	-	-	1.42	1.38	2.70
RESIDUUM	101	101	1.23	1.42	1.38	2.75
RESIDUUM	102	-	1.29	1.36	-	4.53

GLQ UNIT	SAMPLE NUMBER	STATION	SC MOIST PCT	SC WET BD	SC DRY BD	OM	ASPECT
RESIDUUM	-	102-1	-	-	-	1.[illegible]	-
RESIDUUM	-	102-2	-	-	-	0.96	-
RESIDUUM	-	102-3	-	-	-	0.89	-
RESIDUUM	-	C-2	9.94	1.94	1.76	0.92	SOUTH
RESIDUUM	-	B-3	15.82	1.59	1.37	1.17	NORTH
RESIDUUM	-	B-5	13.01	1.60	1.42	-	NORTH
RESIDUUM	-	B-7	13.06	1.79	1.58	1.15	NORTH
RESIDUUM	1	-	-	-	-	-	NORTH
RESIDUUM	4	-	-	-	-	-	NONE
RESIDUUM	5	-	-	-	-	-	EAST
RESIDUUM	16	-	-	-	-	-	EAST
RESIDUUM	17	-	-	-	-	-	EAST
RESIDUUM	18	-	-	-	-	-	EAST
RESIDUUM	19	-	-	-	-	-	EAST
RESIDUUM	20	-	-	-	-	-	EAST
RESIDUUM	45	-	-	-	-	-	EAST
RESIDUUM	46	-	-	-	-	-	EAST
RESIDUUM	47	-	-	-	-	-	NORTH
RESIDUUM	48	-	-	-	-	-	NORTH
RESIDUUM	49	-	-	-	-	-	NORTH
RESIDUUM	50	-	-	-	-	-	NORTH
RESIDUUM	51	-	-	-	-	-	NORTH
RESIDUUM	61	-	-	-	-	-	EAST
RESIDUUM	62	-	-	-	-	-	EAST
RESIDUUM	63	-	-	-	-	-	EAST
RESIDUUM	101	101	-	-	-	0.94	EAST
RESIDUUM	102	-	-	-	-	-	NONE

GLQ UNIT	SAMPLE NUMBER	STATION	SLOPE PERCENT	VERT POSITION	HORIZ POSITION
RESIDUUM	-	102-1	33.33	72.22	73.77
RESIDUUM	-	102-2	33.33	85.00	82.86
RESIDUUM	-	102-3	40.00	93.33	90.37
RESIDUUM	-	C-2	22.22	10.34	22.73
RESIDUUM	-	B-3	22.22	11.76	25.00
RESIDUUM	-	B-5	25.00	21.21	35.85
RESIDUUM	-	B-7	30.77	36.36	49.02
RESIDUUM	1	-	28.27	25.00	57.14
RESIDUUM	4	-	0.	0.	0.
RESIDUUM	5	-	23.56	14.29	25.00
RESIDUUM	16	-	23.56	14.29	25.00
RESIDUUM	17	-	23.56	14.29	25.00
RESIDUUM	18	-	37.69	42.86	54.55
RESIDUUM	19	-	22.32	58.33	67.00
RESIDUUM	20	-	23.56	16.00	32.50
RESIDUUM	45	-	23.56	0.	0.
RESIDUUM	46	-	19.57	2.50	3.77
RESIDUUM	47	-	28.27	25.00	57.14
RESIDUUM	48	-	28.27	25.00	57.14
RESIDUUM	49	-	47.11	40.00	64.29
RESIDUUM	50	-	31.41	50.00	64.29
RESIDUUM	51	-	32.62	50.00	74.29
RESIDUUM	61	-	33.92	4.17	8.11
RESIDUUM	62	-	33.92	4.17	8.11
RESIDUUM	63	-	33.92	4.17	8.11
RESIDUUM	101	101	14.13	0.	0.
RESIDUUM	102	-	0.	0.	0.

GLQ UNIT	SAMPLE NUMBER	STATION	BEDROCK UNIT
RESIDUUM	-	102-1	CCR
RESIDUUM	-	102-2	CCR
RESIDUUM	-	102-3	CCR
RESIDUUM	-	C-2	CKS
RESIDUUM	-	B-3	CKS
RESIDUUM	-	B-5	CKS
RESIDUUM	-	B-7	CKS
RESIDUUM	1	-	CKS
RESIDUUM	4	-	CKS
RESIDUUM	5	-	CCR
RESIDUUM	16	-	CCR
RESIDUUM	17	-	CCR
RESIDUUM	18	-	CCR
RESIDUUM	19	-	CCR
RESIDUUM	20	-	CUC
RESIDUUM	45	-	CUL
RESIDUUM	46	-	CUL
RESIDUUM	47	-	CKS
RESIDUUM	48	-	CKS
RESIDUUM	49	-	CKS
RESIDUUM	50	-	CKS
RESIDUUM	51	-	CKS
RESIDUUM	61	-	CUC
RESIDUUM	62	-	CUC
RESIDUUM	63	-	CUC
RESIDUUM	101	101	CCR
RESIDUUM	102	-	CCR

APPENDIX B

SUBSURFACE SOIL TEXTURE DATA

EXPLANATION OF SAMPLE LABELS

Sample Label	Explanation
STATION	Trench sample station: C-5 = trench C, station 5 (see Plate 2).

EXPLANATION OF VARIABLE ABBREVIATIONS

Abbreviation	Units	Explanation
SAND	(%)	Gravimetric sand content of <2 mm soil.
SILT	(%)	Gravimetric silt content of <2 mm soil.
CLAY	(%)	Gravimetric clay content of <2 mm soil.
DG	(mm)	Geometric mean grain size of <2 mm soil.
GSTDEV		Geometric standard deviation of <2 mm soil.

STATION	SAND	SILT	CLAY	DG	GSTDEV
A-1	45.710	26.748	27.541	0.028	6.011
A-10	51.485	25.700	22.815	0.035	5.922
A-11	48.817	23.966	27.217	0.031	6.610
A-12	47.598	26.941	25.460	0.031	6.344
A-13A	45.524	20.320	34.156	0.025	6.882
A-13B	38.151	15.549	46.299	0.017	7.204
A-14A	48.707	20.681	30.612	0.029	6.543
A-14B	40.785	19.515	39.700	0.023	8.031
A-15A	59.040	27.887	13.073	0.049	4.625
A-15B	59.423	34.437	6.140	0.058	3.871
A-16B	51.988	39.074	8.938	0.045	4.077
A-17A	64.792	25.946	9.262	0.068	4.950
A-2	46.634	19.662	33.704	0.028	7.829
A-3	52.092	19.994	27.915	0.031	6.256
A-4	51.259	18.473	30.268	0.027	6.354
A-5	28.798	20.847	50.355	0.013	7.228
A-6	35.558	25.959	38.482	0.020	7.130
A-7	41.864	24.841	33.295	0.022	6.335
A-8	41.635	26.065	32.300	0.023	6.226
A-9	37.089	19.823	43.087	0.019	7.852
B-1	54.283	18.098	27.619	0.034	6.480
B-10	62.016	23.403	14.581	0.052	5.398
B-11	54.080	25.822	20.097	0.042	6.052
B-12	40.572	21.829	37.598	0.022	6.967
B-13A	54.323	30.406	15.271	0.047	5.339
B-13B	35.464	27.802	36.735	0.020	6.716
B-14A	57.338	31.418	11.244	0.048	4.417
B-14B	27.284	17.878	54.839	0.012	7.868
B-15A	53.369	28.586	18.045	0.040	5.185
B-15B	49.233	10.227	40.541	0.046	15.219
B-16A	51.331	32.115	16.554	0.039	5.278
B-16B	48.312	32.632	19.057	0.038	6.094
B-17A	49.754	31.270	18.976	0.037	5.486
B-17B	64.266	26.962	8.772	0.070	5.259
B-18A	57.533	31.302	11.165	0.051	4.547
B-18B	65.238	26.630	8.132	0.057	3.705
B-19	65.053	23.214	11.733	0.076	5.947
B-2	64.361	17.653	17.986	0.056	6.172
B-3	52.919	22.199	24.883	0.034	5.927
B-4	64.749	17.850	17.401	0.051	5.599
B-5	51.660	23.850	24.490	0.039	7.104
B-6	59.938	23.878	16.184	0.050	5.435
B-7	55.421	20.242	24.337	0.038	6.677
B-8	53.151	22.367	24.482	0.038	6.521

STATION	SAND	SILT	CLAY	DG	GSTDEV
B-9	58.160	23.331	18.509	0.063	7.273
C-1	46.196	25.151	28.652	0.028	6.699
C-2	64.798	16.674	18.528	0.049	5.747
C-3	33.229	20.782	45.989	0.015	6.989
C-4	61.514	19.288	19.198	0.049	6.179
C-5A	53.079	21.207	25.714	0.037	6.743
C-5B	68.931	19.702	11.368	0.067	4.714
C-6	74.268	15.892	9.840	0.123	6.467
D-1	61.199	14.351	24.450	0.043	6.239
D-10	55.603	29.830	14.566	0.048	5.391
D-11	58.513	26.807	14.680	0.050	5.397
D-12	56.490	28.743	14.767	0.047	5.269
D-13	70.911	21.022	8.067	0.076	4.452
D-2	71.715	17.960	10.325	0.070	4.554
D-3	65.502	17.714	16.783	0.055	5.414
D-4	72.863	18.170	8.967	0.073	4.688
D-5	65.457	21.253	13.289	0.065	5.496
D-6	67.906	20.967	11.128	0.070	5.048
D-7	62.178	21.599	16.223	0.054	5.702
D-8	66.236	19.654	14.110	0.063	5.869
D-9	61.321	23.241	15.438	0.055	5.630

U.S. DEPARTMENT OF ENERGY

OCRWM

YUCCA MOUNTAIN

YUCCA MOUNTAIN SITE CHARACTERIZATION PROJECT

REFERENCES FOR STUDY PLAN 8.3.1.9.2.2

Enclosure 4

8.3.1.9.2.2

References: for STUDY PLAN 8.3.1.9.2.2

DeGabriele, C.D. and C.L. Wu. 1987. Water Requirements, Bechtel National, Inc., for Sandia National Laboratory, 52-9817.

Gibbons, D.C., 1986. The Economic Value of Water, Resources of the Future, Washington, D.C.

Gollnick, C.A., 1988. Irrigation Study. Valley Electric Association, Pahrump, Nev.

copyrighted document. Only the cover page and reference page supplied.

ENCLOSURE 4

8.3.1.9.2.2

Gollnick

IRRIGATION STUDY

VALLEY ELECTRIC ASSOCIATION, INC.
NEVADA 18, VALLEY
HIGHWAY 372
PAHRUMP, NEVADA 89041

Enclosure 4

8.3.1.9.2.2

IRRIGATION STUDY

VALLEY ELECTRIC ASSOCIATION, INC.
PAHRUMP, NEVADA 89041

OFFICERS AND BOARD OF DIRECTORS

President:	I. C. Spears
Vice President:	Harry J. Johnson
Secretary:	Dan J. Peterson
Treasurer:	Kenneth G. Tankersley
General Manager:	Ross L. Dohlen

Prepared by: Chuck Gollnick,
Manager of Engineering & Operations

April 1988